ABSTRACT

Humanized Mice to Test Vaccination against Influenza Virus via Dendritic Cells

Chun-I Yu, Ph.D.

Mentors: A. Karolina Palucka, M.D. Ph.D.
Jacques Banchereau, Ph.D.

Critical to the development of human vaccines is the availability of *in vivo* models of the human immune system that permit testing of vaccine efficacy. Here, we used NOD-SCID-$\beta_2m^{-/-}$ immunodeficient mice which, when engrafted with human $CD34^+$ hematopoietic progenitors, develop all subsets of human dendritic cells (DCs) and B cells. T cells and their subsets were reconstituted by adoptive transfer. We found myeloid DCs, plasmacytoid DCs and monocytes in the bone marrow, spleen, and peripheral tissues including skin and lungs. To test DC biology *in vivo*, we first used live influenza A/PR8/34 (H1N1) virus. Upon intranasal inoculation, all subsets of human antigen presenting cells were activated. Matured DCs were found accumulated in mediastinal lymph nodes. To evaluate the value of these mice for testing human vaccines, humanized mice were immunized with 1) *ex vivo*-generated DCs, 2) seasonal influenza vaccines and 3) protein antigens fused to anti-DC receptor. Upon vaccination with *ex vivo*-generated DCs pulsed with heat-inactivated influenza virus, mice developed influenza-specific immunity, i.e. influenza-specific immunoglobulins (Igs) in the serum

and influenza virus matrix protein 1 (FluM1)-specific $CD8^+$ T cells in the blood, spleen and lungs. Influenza-specific Igs were protective as sera from vaccinated mice inhibited influenza virus-induced hemagglutination *in vitro* and offered passive protection *in vivo*. Upon vaccination with seasonal influenza vaccines, i.e. live attenuated trivalent vaccine (LAIV) or killed trivalent vaccine (TIV), humanized mice developed both humoral and cellular immunity. Plasma cells differentiation and the secretion of specific Igs were dependent on the reconstitution with $CD45RA^-CD27^+CD4^+$ central memory T cells. $CD8^+$ T cells specific to two influenza antigens, i.e. FluM1 and NS1, were detected in mice vaccinated with LAIV. TIV-vaccinated mice showed the expansion of FluM1, but not NS1, specific $CD8^+$ T cells. Antigen-specific $CD8^+$ T cells produced IFN-γ and expressed surface CD107a consistent with the acquisition of effector function. Finally, upon vaccination with anti-DC receptor (DCIR)-FluM1 fusion protein and poly I:C as an adjuvant, DCs efficiently cross-presented FluM1 and expanded antigen-specific $CD8^+$ T cells. Therefore, humanized mice might be valuable model for testing human vaccines against influenza virus.

Humanized Mice to Test Vaccination against Influenza Virus via Dendritic Cells

by

Chun-I Yu, M.S.

A Dissertation

Approved by the Institute of Biomedial Studies

_____
Robert R. Kane, Ph.D., Chairperson

Submitted to the Graduate Faculty of
Baylor University in Partial Fulfillment of the
Requirements for the Degree
of
Doctor of Philosophy

Approved by the Dissertation Committee

_____
A. Karolina Palucka, M.D., Ph.D., Chairperson

_____
Damien Chaussabel, Ph.D.

_____
William D. Hillis, M.D.

_____
Christopher J. Kearney, Ph.D.

_____
Gerard Zurawski, Ph.D.

_____
SangKon Oh, Ph.D.

Accepted by the Graduate School
May 2008

_____
J. Larry Lyon, Ph.D., Dean

Page bearing signatures is kept on file in the Graduate School.

TABLE OF CONTENTS

TABLE OF CONTENTS iii

LIST OF FIGURES vi

LIST OF TABLES viii

LIST OF ABBREVIATIONS ix

ACKNOWLEDGMENTS xiv

CHAPTER ONE 1

Introduction 1

Dendritic Cells 1

Influenza Virus Infection: A Medical Need 13

Humanized Mouse Models 23

CHAPTER TWO 32

Objectives 32

Aim 1: The Interaction of Human DCs with Influenza Virus in Humanized Mice 33

Aim 2: Humoral Responses against Influenza Virus 33

Aim 3: Role of $CD4^+$ T cells in Humoral Responses against Influenza Virus 34

Aim 4: $CD8^+$ T cell Responses against Influenza Virus 34

CHAPTER THREE 35

Materials and Methods 35

Antibodies and Reagents 35

Humanized Mice 36

T Cell Isolation 37

Monocyte-Derived DCs 37

Vaccination 38

Humanized Mouse Analysis 39

Flow Cytometry 39

Immunohistofluorescence Staining 41

ELISA 41

Hemagglutination Inhibition Assay 43

IgM Depletion 43

In vitro Neutralization Assay 44

Influenza Virus Infection and Passive Protection 45

$TCID_{50}$ 45

Thymidine Incorporation 46

Chromium Release Assay 46

CHAPTER FOUR 48

Results 48

Mobilization and Activation of Human Dendritic Cells in the Lung upon Influenza Virus Infection 48

Mice Vaccinated with *Ex vivo*-Generated DC Generate Influenza Virus-Specific Humoral Immunity 58

Mice Vaccinated with Influenza Vaccine Generate Influenza Virus-Specific Humoral Immunity 67

Mice Vaccinated with *Ex vivo*-Generated DCs Expand Antigen-Specific $CD8^+$ T Cells 70

Cross-presentation of Seasonal Influenza Virus Vaccine Antigens to $CD8^+$ T Cells 76

In vivo Targeting of Human Dendritic Cells to Generate Influenza Virus-Specific Immune Responses 87

CHAPTER FIVE 91

Discussion 91

CHAPTER SIX 99
Conclusions 99
APPENDIX 101
APPENDIX 102
List of Current and Future Publications 102
Original Publications 102
Review 102
BIBLIOGRAPHY 103

LIST OF FIGURES

Figure 1. Subsets of human DCs.....2

Figure 2. DCs sense microbes and initiate immune responses.. 4

Figure 3. Antigen presentation by DCs.. 7

Figure 4. The structure of influenza A virus.....15

Figure 5. Stepwise approach to establish humanized mice as a model for testing human vaccines 33

Figure 6. The construction of humanized mice.. 49

Figure 7. Identification of human DCs in humanized mice 51

Figure 8. Clinical symptoms of influenza A virus infection in humanized mice. 52

Figure 9. Antigen presenting cells in the lungs of humanized mice 54

Figure 10. Lung DCs undergo maturation upon influenza virus infection.....55

Figure 11. Mature DCs accumulate in mediastinal lymph nodes upon influenza virus infection 57

Figure 12. *Ex vivo*-generated DCs pulsed with heat-inactivated influenza virus 59

Figure 13. Humanized mice vaccinated with heat-inactivated influenza virus-pulsed DCs generate specific antibody response 60

Figure 14. Plasma cell differentiation in the spleen of humanized mice upon vaccination 62

Figure 15. Influenza virus-specific neutralizing antibody in the serum of vaccinated mice 63

Figure 16. T cell-dependent neutralizing IgM 65

Figure 17. Serum of vaccinated mice prevents infection *in vivo* in passive protection experiments 66

Figure 18. Mice vaccinated with LAIV generate influenza virus-specific IgM in the serum.....68

Figure 19. The generation of influenza virus-specific IgM in LAIV vaccinated mice is dependent on central memory $CD4^+$ T cells..... 68

Figure 20. Plasma cell differentiation in LAIV vaccinated mice is dependent on central memory $CD4^+$ T cells..... 69

Figure 21. Mice vaccinated with peptide-pulsed *ex vivo*-generated DCs can mount primary and recall $CD8^+$ T cells immunity..... 71

Figure 22. Expanded antigen-specific $CD8^+$ T cells can be found in lymphoid and peripheral tissues..... 72

Figure 23. Antigen-specific $CD8^+$ T cell responses elicited by *ex-vivo* DCs loaded with HI-PR8 virus..... 74

Figure 24. Antigen-specific $CD8^+$ T cells elicited by *ex-vivo* DCs loaded with HI-PR8 virus *in vivo* acquired cytotoxic function..... 74

Figure 25. The kinetics of $CD8^+$ T cells response elicited by vaccination with *ex-vivo* DCs..... 75

Figure 26. Mice vaccinated with trivalent live attenuated influenza vaccine (LAIV) expand FluM1-specific $CD8^+$ T cells..... 77

Figure 27. Mice vaccinated with trivalent split influenza vaccine (TIV) expand FluM1-specific $CD8^+$ T cells..... 79

Figure 28. Cross-presentation of FluM1 to $CD8^+$ T cells by myeloid APCs in humanized mice..... 81

Figure 29. The breadth of $CD8^+$ T cells in mice vaccinated with influenza vaccines..... 84

Figure 30. Cytokine production and effector cell differentiation of $CD8^+$ T cells after vaccination. 86

Figure 31. *In vivo* DC targeting..... 89

Figure 32. Mice vaccinated with DCIR-FluM1 fusion protein expand FluM1-specific effector $CD8^+$ T cells..... 90

Figure 33. DCs play a central role in vaccination..... 100

LIST OF TABLES

Table 1. Major humanized mouse models with hematopoietic stem cell transplantation. 26

Table 2. Antibody titers in the serum of humanized mice vaccinated with *ex vivo*-generated DCs. 60

Table 3. The frequency of FluM1-specific $CD8^+$ T cells in humanized mice vaccinated with LAIV..... 78

Table 4. The frequency of FluM1-specific $CD8^+$ T cells in mice vaccinated with TIV... 80

LIST OF ABBREVIATIONS

APC	allophycocyanin
APCs	antigen presenting cells
APRIL	a proliferation-inducing ligand
ASGPR	asialoglycoprotein receptor
AU	arbitrary unit
β_2m	β_2 microglobulin
BCR	B cell receptor
BlyS	B lymphocyte stimulator
BM	bone marrow
BSA	bovine serum albumin
CCL19	C-C chemokine ligand 19
CCR7	C-C chemokine receptor 7
CLRs	C-type lectin receptors
CpG	unmethylated CG dinucleotides
CRBCs	chicken red blood cells
CRD	carbohydrate recognition domain
CTL	cytotoxic T lymphocyte
CTLA-4	cytotoxic T lymphocyte antigen 4
CXCL8	C-X-C chemokine ligand 8
DCIR	DC immunoreceptor
DCs	dendritic cells
DC-SIGN	DC-specific ICAM3-grabbing nonintegrin

DEC-205	dendritic and epithelial cells, 205 kDa
dectin	DC-associated C-type lectin
DMEM	Dulbecco's Modified Eagle's Medium
DNA	deoxyribonucleic acid
E: T	effector: target
EBV	Epstein-Barr virus
ELISA	enzyme-linked immunosorbent assay
ER	endoplasmic reticulum
ERAAP	ER-associated aminopeptidase
ERAD	ER-associated degradation
FCS	fetal calf serum
FDCs	follicular dendritic cells
Flt-3L	fms-like tyrosine kinase ligand
FluM1	influenza virus matrix protein 1
GM-CSF	granulocyte/macrophage colony stimulating factor
HA	hemagglutinin
HAI	hemagglutinin inhibition
HI	heat-inactivated
HIV	human immunodeficiency virus
HLA	human leukocyte antigen
HPCs	hematopoietic progenitor cells
HRP	horseradish peroxidase
ICOS-L	inducible costimulatory ligand
IFNα	interferon α
Ig	immunoglobulin

i.h.	intra-hepatic
Ii	invariant chain
IL	interleukin
i.p.	intraperitoneal (ly)
IPAF	ICE-protease activating factor
i.v.	intravenous (ly)
LAIV	live attenuated influenza vaccine
LNs	lymph nodes
LOX-1	lectin-like oxidized low-density lipoprotein receptor 1
LPS	lipopolysaccharide
MDA-5	melanoma differentiation-associated gene-5
mDCs	myeloid dendritic cells
MDDCs	monocyte-derived dendritic cells
MHC	major histocompatibility complex
MIIC	MHC II compartment
MLR	mixed lymphocyte reaction
MR	mannose receptor
NA	neuraminidase
NAIPs	neuronal apoptosis inhibitor proteins
NALPs	NACHT-, leucine-rich repeat-, and pyrin-domain-containing proteins
NK	natural killer
NLRs	nucleotide oligomerization domain-like receptors
NOD1	nucleotide-binding oligomerization domain 1
NOD-SCID	non-obese diabetic, sever combined immunodeficiency
NP	nucleoprotein

PALS	periarteriolar lymphoid sheaths
PAMPs	pathogen-associated molecular patterns
PBMCs	peripheral blood mononuclear cells
PBS	phosphate buffered saline
pDCs	plasmacytoid dendritic cells
PD-L	programmed death ligand
PE	phycoerythrin
PerCP	peridinin chlorophyll protein
pfu	plaque forming unit
PR8	influenza A/PR8/34
Prkdc ^{scid}	protein kinase, DNA activated, catalytic polypeptide; sever combined immunodeficiency
PRRs	pattern recognition receptors
Rag	recombination-activating gene
γ_c	common cytokine receptor γ chain
RIG-I	retinoic acid-inducible protein I
RNPs	ribonucleoproteins
s.c.	subcutaneous (ly)
SCID	severe combined immunodeficiency
SEB	Staphylococcal enterotoxin B
SP	spleen
SRC	SCID repopulating cells
ssRNA	single strand ribonucleic acid
TAP	transporter associated with antigen processing
$TCID_{50}$	50% tissue culture infectious dose
T_{CM}	central memory T cells

TCR	T cell receptor
T_{EM}	effector memory T cells
T_{FH}	follicular B helper T cells
TGF-β	tumor growth factor β
Th	T helper
TIV	trivalent inactivated influenza vaccine
TLRs	toll-like receptors
TNF-α	tumor necrosis factor α
TPO	thrombopoietin
Tr1	T regulatory type 1
TREC	TCR-rearrangement excision circles
Tregs	regulatory T cells
TSLP	thymic stromal lymphopoietin
TT	tetanus toxoid

ACKNOWLEDGMENTS

The journey of pursuing the doctoral degree takes great effort on the part of many people. It would not be possible to present this work without all the people contributing either directly or indirectly.

First, I would like to acknowledge my mentor, Dr. Karolina Palucka, who has guided me throughout my graduate studies.

Second, I would like to say "thank you" to all the people contributing to this work. Florentina Marches was involved in a great deal of the study regarding to humanized mouse construction and many other aspects. Mike Gallegos helped me in the vaccination and analysis of humanized mice. Alexander Pedroza-Gonzales helped me setting up the cytotoxicity assay. Jenny Smith, Mark Michnevitz, and Sasha Tindle helped me to process tissue samples.

Third, I would like to thank my collaborators: Dr. Aldofo Garcia-Sastre for providing strains of influenza virus and for his expert advice; Dr. Mark Jenkins for whole-body analysis and imaging of humanized mice; Dr. Octavio Ramilo for providing influenza vaccines; and Dr. Gerard Zurawski for providing the fusion protein and targeting antibodies.

I would also like to give special thanks to special members of Baylor Institute for Immunology Research: Cindy Samuelsen for the assistance in purchasing and other administrative issues; Carson Harrod for the assistance in scientific writing; Nicolas Taquet for technical supports; Albert Barnes and Kristin Prescott for taking good care of our mice on weekdays and weekends; Lynnette Walters for processing and freezing

donor stem cells; Sandra S. Clayton for the assistance in immunofluorescence staining and operating the confocol microscope; Elizabeth Kawalski and Sebastin Coquery for the assistance in operating the flow cytometer; Sandy Zurawski and her team for providing monoclonal antibodies; Jennifer Shay for Luminex analysis; and Casey Glaser for microarray analysis.

My appreciation also goes to all of the faculty members who are always ready to discuss science including Dr. Damien Chaussabel, Dr. John Connolly, Dr. William Hillis, Dr. Christopher Kearney, Dr. SangKon Oh, Dr. Virginia Pascual, Dr. Ann Rushing, Dr. Douglas W. Smith, Dr. Alex Tong and Dr. Hideki Ueno.

I am grateful for all the wonderful colleagues and friends who have always been there including: Adam, Amanda, Amy, Angela, Anne Laure, Asun, Caroline, David, Davor, Dorcus, Eiji, Erica, Eynav, Gerlinde, Gloria, Greg, Jason, Jean Philippe, Jingtao, Luis, Matthew, Melissa, Nathalie, Nicolas, Pinakeen, Rimpei, Olivier, Quynh, Susan, Xiao-Hua, Yaming and many others.

Last but not least, I would like to say ‘thank you for the support’ to Dr. Jacques Banchereau, the director of Baylor Institute for Immunology Research, and Dr. Bob Kane, the chairman of Biomedical Studies at Baylor University.

This work was supported by National Institutes of Health (U19 AIO57234) for translational research on human immunology and biodefense.

CHAPTER ONE

Introduction

Dendritic Cells

Dendritic cells (DCs) are the most important antigen presenting cells (APCs) in the initiation of adaptive immune responses. DCs sense danger signals derived from pathogens, acquire and present antigens to T cells and B cells, and consequently turn on adaptive immune responses. To complete these tasks, the DC system evolved multiple subsets and the capacity to perform distinct functions at different maturation stages (Banchereau and Steinman 1998; Palucka and Banchereau 2002; Pulendran and others 2001).

DC Subsets

DCs originate from $CD34^+$ hematopoietic progenitor cells (HPCs) in the bone marrow. In humans, two pathways of DC differentiation have been identified: one, the myeloid pathway, which gives rise to myeloid DCs (mDCs) in the blood, Langerhans cells in the epidermis, and interstitial DCs in the dermis and other tissues; the other, the plasmacytoid pathway, which gives rise to plasmacytoid DCs (pDCs), also known as interferon producing cells (Fig. 1) (Palucka and others 2005b; Pulendran and others 2001; Rissoan and others 1999). *In vitro* culture of $CD34^+$ HPCs with granulocyte/macrophage colony stimulating factor (GM-CSF) and tumor necrosis factor (TNF)-α gives rise to $CD1a^+$ Langerhans cell-like DCs and $CD14^+$ interstitial DCs (Caux and others 1996). $CD34^+$ HPCs can also give rise to both mDCs and pDCs in the presence of fms-like

tyrosine kinase-3 ligand (Flt-3L) and thrombopoietin (TPO) (Chen and others 2004; Palucka and others 2005a). The role of Flt-3L on DC homeostasis is further supported by the increase of circulating mDCs and pDCs after the administration of Flt-3L *in vivo* in mice and humans (Karsunky and others 2003; Maraskovsky and others 1996; Pulendran and others 2000).

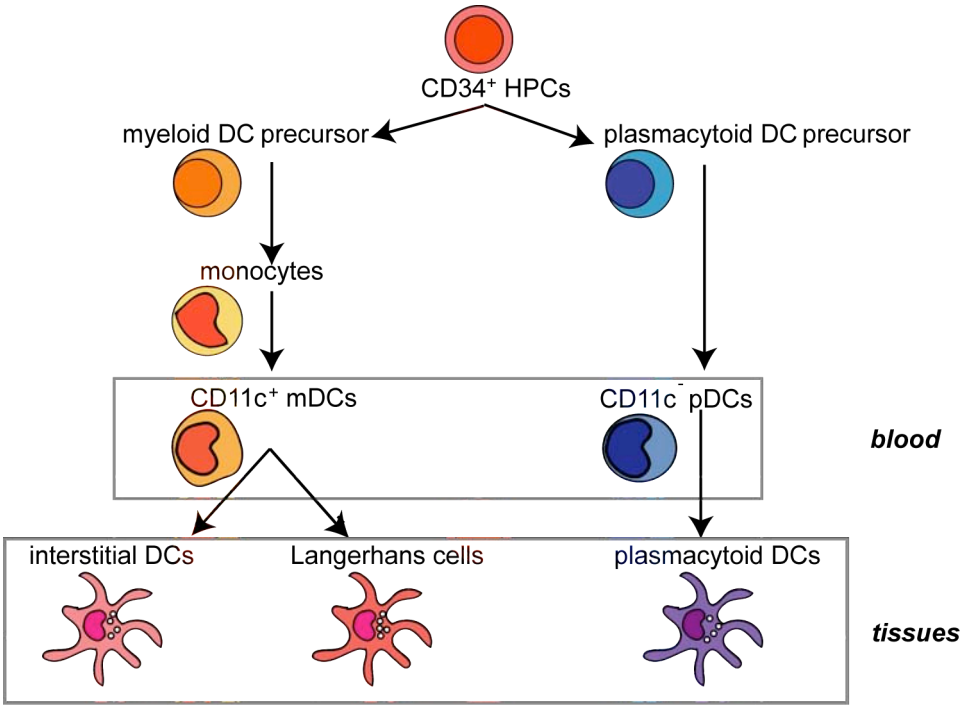

Figure 1. Subsets of human DCs. $CD34^+$ HPCs can differentiate into subsets of DCs in two pathways. The myeloid pathway gives rise to myeloid DCs, Langerhans cells, and interstitial DCs, while the plasmacytoid pathway gives rise to plasmacytoid DCs.

DC subsets display functional plasticity. mDCs derived from $CD34^+$ HPCs exhibit different specialization in tuning the immune response (Caux and others 1997). While $CD1a^+$ Langerhans cells activate cytotoxic $CD8^+$ T cells efficiently (Klechevsky unpublished observation), $CD14^+$ interstitial DCs have the unique capacity to prime follicular B helper T cells (T_{FH}) and naïve B cells into antibody-secreting plasma cells *in vitro* (Morita unpublished observation). DCs derived from monocytes also have different

functional phenotypes depending on the cytokine encountered, i.e. interleukin (IL)-4, TNF-α, interferon (IFN)-α, IL-15 or thymic stromal lymphopoietin (TSLP). For example, *in vitro* culture of monocyte-derived DCs (MDDCs) with IL-15 derives a subset of DCs that is specialized in priming $CD8^+$ T cells (Dubsky and others 2007). $CD11c^+$ mDCs activated with TSLP prime naïve $CD4^+$ T cells into T helper (Th) 2-type T cells to secrete high amounts of proallergic cytokines like IL-13, IL-5, and TNF-α (Soumelis and others 2002; Watanabe and others 2005). pDCs secrete high amounts of IFN-α as a mediator of the innate immune response and thereafter acquire the ability to initiate adaptive immune responses (Cella and others 2000; Fonteneau and others 2003; Kadowaki and others 2000).

Sensing Microbes

Underneath the epithelial layer, DCs align as a dense network of cells that monitors the infectious status by continuously probing the environment through phagocytosis, pinocytosis, and endocytosis (Fig. 2). In the steady state, DCs remain immature and are thought to maintain tolerance toward self-antigen (Steinman and others 2003). When the body is invaded by pathogens, DCs are activated via the recognition of pathogen-associated molecular patterns (PAMPs), conserved molecular patterns uniquely belonging to pathogens, through pattern recognition receptors (PRRs). PRRs include toll-like receptors (TLRs), C-type lectin receptors (CLRs), nucleotide oligomerization domain-like receptors (NLRs) and others (Geijtenbeek and others 2004; Mariathasan and Monack 2007; Medzhitov and others 1997). TLR family members are composed of an extracellular leucine-rich repeat domain, a transmembrane domain, and an intracellular toll/IL-1 receptor domain (Takeda and others 2003). By the nature of TLR ligands,

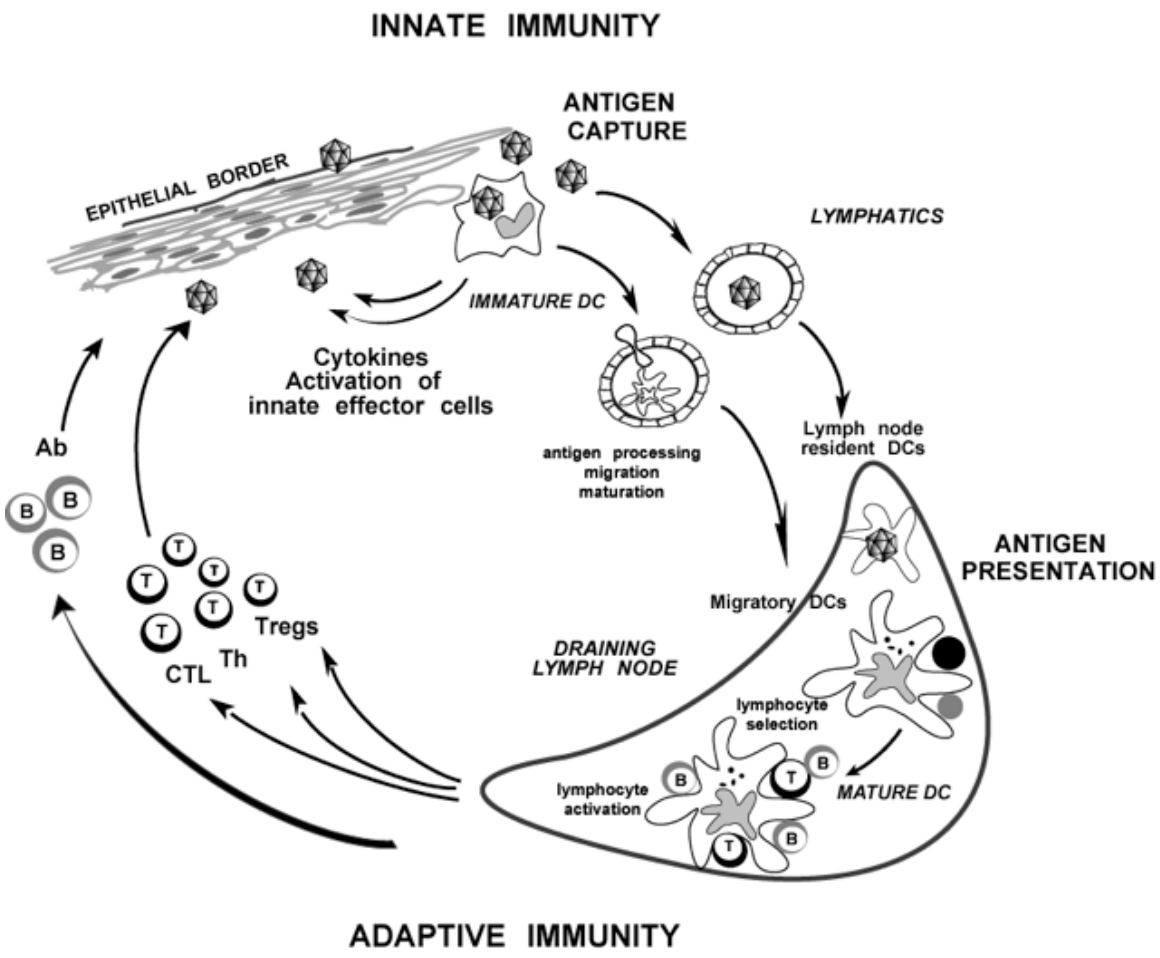

Figure 2. DCs sense microbes and initiate immune responses. Circulating DC precursors enter tissues as immature DCs. There, they encounter pathogens and secrete inflammatory cytokines, which then activate effector cells of innate immunity. Following the antigen capture, DCs migrate to lymphoid organs, where they encounter and present antigens to specific B and T cells. With the help from activated T cells, DCs undergo further maturation and can expand B and T cells into effector cells. Activated T cells migrate to the inflamed tissue to eliminate microbes and microbe-infected cells. Activated B cells migrate to various locations and differentiate into plasma cells, which produce antibodies to neutralize microbes. Antigen can also reach draining lymph nodes without involvement of peripheral tissue DCs and be captured by lymph node resident DCs.

they are classified into different subfamilies: TLR1, -2, -4, and -6 recognize lipid and lipopeptides unique to bacteria and fungi and are localized to the plasma membrane; TLR3, -7, -8, and -9 recognize bacterial and viral nucleic acid and are localized to the intracellular compartment (Gay and Gangloff 2007). The intracellular localization of

TLR9 is suggested to prevent the recognition of self deoxyribonucleic acid (DNA), but facilitate the access to viral DNA (Barton and others 2006). The binding of TLR on DCs activates signaling pathways for the secretion of proinflammatory cytokines (e.g. IL-1, TNF-α, IL-6, and IL-12) or the transcription of type I interferon and interferon-inducible genes (McGettrick and O'Neill 2004; Takeda and others 2003). CLRs are a group of structurally related membrane proteins composed of calcium-dependent carbohydrate recognition domains (CRD) for antigen recognition and capturing. In general, CLRs are classified into two families. The mannose receptor family is composed of a type I transmembrane protein with multiple CRD domains including mannose receptor (MR, CD206) and 'dendritic and epithelial cells, 205kDa' (DEC-205, CD205). The asialoglycoprotein receptor (ASGPR) family is composed of a type II transmembrane protein with a single CRD domain including Langerin (CD207), DC-specific ICAM3-grabbing nonintegrin (DC-SIGN, CD209), DC immunoreceptor (DCIR), DC-associated C-type lectin (dectin)-1, and lectin-like oxidized low-density lipoprotein receptor 1 (LOX-1) (Geijtenbeek and others 2004). NLRs recognize intracellular microbial components and trigger a signaling pathway for proinflammatory cytokine production (such as IL-1β and IL-18). NLRs include proteins such as NOD1 (nucleotide-binding oligomerization domain 1), NOD2, NALPs (NACHT-, leucine-rich repeat-, and pyrin-domain-containing proteins), IPAF (ICE-protease activating factor) and NAIPs (neuronal apoptosis inhibitor proteins) (Mariathasan and Monack 2007; Ting and others 2006). In addition, viral RNA can be recognized by cytoplasmic RNA helicases including retinoic acid-inducible protein I (RIG-I) (Kato and others 2005) and melanoma differentiation-associated gene-5 (MDA-5) (Gitlin and others 2006; Kang and others 2002). Different

DC subsets are equipped with different combinations of PRRs for sensing microbes. For example, blood pDCs express TLR7 and -9, which recognize single stranded RNA (ssRNA) and unmethylated CG dinucleotides (CpG) motifs (Jarrossay and others 2001; Kadowaki and others 2001). Blood mDCs express the rest of the TLRs including TLR2, -3, -4, -5, -6 and -8 for pathogen recognition (Jarrossay and others 2001). Langerhans cells express Langerin (Valladeau and others 2000) while pDCs express BDCA-2 and DCIR (Meyer-Wentrup and others 2008).

DC Maturation and Antigen Presentation

Immature DCs present antigens to T cells in a tolerogenic fashion (Steinman and others 2003), while mature DCs do so in an immunogenic fashion. Thus, upon pathogen encounter, DCs experience physiological and morphological changes commonly described as maturation. DCs become less phagocytic and gain the expression of C-C chemokine receptor (CCR) 7, a receptor of C-C chemokine ligand (CCL) 19 and CCL21. This allows them to migrate from peripheral tissues to draining lymph nodes. DCs also upregulate a number of costimulatory molecules (CD80, CD86, etc.) and upregulate the secretion of cytokines (IFN-α, IL-12, etc.), all of which contribute to their next task, which is to present the antigen to T cells and to prime antigen-specific T cells. It is a matter of debate whether migrating DCs present antigens directly to T cells in the draining lymph node or whether they transfer antigens to resident DCs for presentation to activate naïve or memory T cells. Possibly both mechanisms can operate under different conditions (Fig. 2) (Fonteneau and others 2003; MartIn-Fontecha and others 2003; Martln-Fontecha and others 2003; Saeki and others 1999; Sallusto and others 1999; Yanagihara and others 1998).

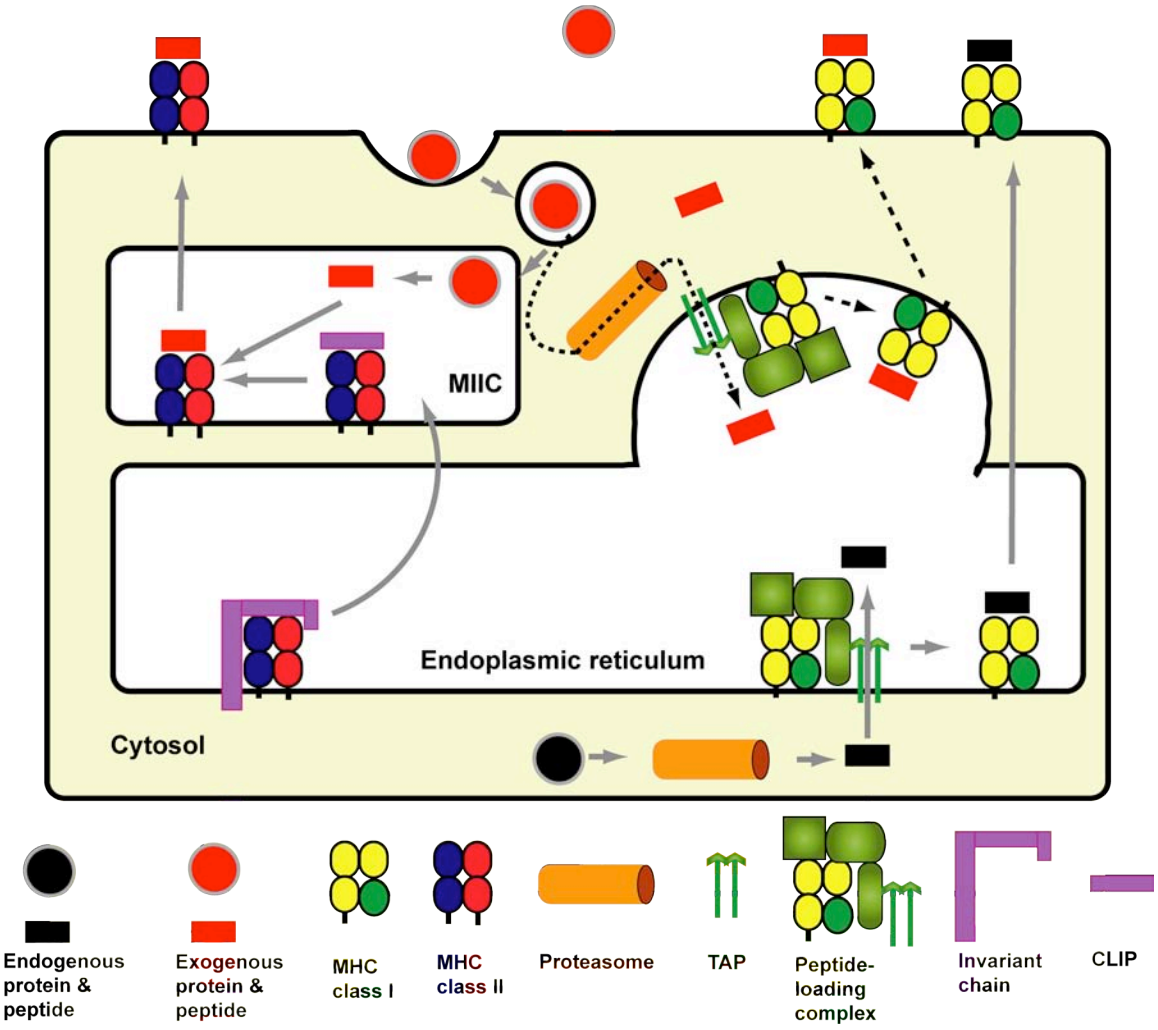

Figure 3. Antigen presentation by DCs. There are two classical antigen processing and presentation pathways. Exogenous protein are internalized, fragmented into peptides, and loaded onto the peptide-binding groove of MHC class II molecules, which are then transported to the cell surface for the recognition by $CD4^+$ T cells. Endogenous peptides, generated in cytosol by proteasomes, are transported into ER, loaded onto MHC class I molecules with the help of peptide-loading complex. Peptide-MHC class I complexes are then transported to cell surface for $CD8^+$ T cell recognition. Exogenous protein can gain access to the cytosol and be cross-presented by MHC class I molecules to $CD8^+$ T cells in DCs (dashed line).

There are two classical antigen-presentation pathways, major histocompatibility complex (MHC) class I and class II presentation (Fig. 3). In general, exogenous antigens are presented by MHC class II molecules to $CD4^+$ T cells, and endogenous antigens are presented by MHC class I molecules to $CD8^+$ T cells. Cross-presentation occurs in DCs

when presenting extracellular antigens and it enables DCs to regulate the activation of cytotoxic $CD8^+$ T cells (Cresswell and others 2005; Jensen 2007).

MHC class II presentation. DCs are efficient at capturing exogenous antigens, processing them, and presenting the processed antigens on MHC class II molecules to $CD4^+$ T cells. MHC class II molecules are heterodimeric proteins composed of α and β chains that combine to form peptide-binding grooves. MHC class II heterodimers are formed and stabilized in the endoplasmic reticulum (ER) with the help of the invariant chain (Ii) and then transported to the MHC II compartment (MIIC), where Ii is cleaved and a short peptide, CLIP, is left in the peptide-binding groove (Fig. 3). In the MIIC, HLA-DM, a chaperone protein, helps the release of CLIP and the loading of exogenous peptides to MHC class II molecules. Upon peptide loading, the MHC class II molecules are released to cell surface (Jensen 2007; Li and others 2005). The turnover of MHC class II molecules is governed by the ubiquitination of the cytoplasmic domain. Upon maturation, ubiquitination of MHC class II molecules ceases resulting in the accumulation of surface expression of MHC class II molecules (Ohmura-Hoshino and others 2006; Shin and others 2006; van Niel and others 2006). The colocalization of TLR ligands with antigens in the phagosome can enhance antigen processing and presentation (Blander and Medzhitov 2006). Apart from exogenous antigens, endogenous proteins gain MHC class II presentation via autophagy, a cellular mechanism to remove damaged organelles. In DCs, autophagosomes frequently merge with MIIC resulting in peptides from endogenous proteins being presented on MHC class II molecules (Schmid and others 2007).

MHC class I presentation. The assembling and loading of MHC class I molecules with peptides occurs in the ER (Fig. 3). Upon synthesis, MHC class I heavy chain binds to β_2 microglobulin (β_2m) and forms a heterodimer with the assistance of the ER chaperone, calnexin. The MHC class I heterodimer forms the peptide-loading complex together with two subunits of 'the transporter associated with antigen processing' (TAP1 and TAP2); the transmembrane glycoprotein, tapasin; the soluble ER chaperone, calreticulin; and the soluble thiol oxidoreductase, ERp57. Cytosolic endogenous proteins or antigens are cleaved by proteasomes and other enzymes to form short peptides. Peptides are then transported into the ER lumen by TAP and trimmed by an ER-associated aminopeptidase (ERAAP) to 8-10 amino acids in length. If the peptide has the appropriate sequence, it binds to the peptide-binding groove of the MHC class I molecule. MHC class I molecules are then released from the peptide-binding complex and transported through the Golgi apparatus to the cell surface where they are recognized by $CD8^+$ T cells (Cresswell and others 2005; Jensen 2007).

Cross-presentation. Apart from the classical pathway of MHC class I antigen presentation, DCs specialize in cross-presentation, which enables them to present exogenous antigen to $CD8^+$ T cells (Fig. 3) (Albert and others 1998; Allan and others 2006; Belz and others 2002; Bennett and others 1997; Kurts and others 1997) . There are several possible ways for exogenous antigens to gain access to the MHC class I presentation pathway including: 1) phagocytosis (for example, capture of virally infected cells) and 2) receptor-mediated endocytosis (for example, targeting a DC receptor). After antigen internalization via phagocytosis, early phagosomes recruit ER membrane proteins for the export of antigen into the cytosol using the ER-associated degradation (ERAD)

system, which allows misfolded endogenous proteins to gain access to the cytosol for degradation. In the cytosol, translocated antigens are processed and then transported into either the ER or ER-phagosome for MHC class I presentation by TAP (Ackerman and others 2003; Ackerman and others 2005; Guermonprez and others 2003; Houde and others 2003). Soluble antigens can also be captured by receptor-mediated endocytosis (for example, via DC targeting using anti-DC antibodies fused with antigen). This can result in antigen delivery to distinct compartments (for example, antigens taken up through mannose receptor traffic into endosomes but not lysosomes) (Burgdorf and others 2007). Studies from the group of R. Steinman and M. Nussenzweig demonstrate that DEC-205 targeting delivers antigens at least 400 times more efficiently to $CD8^+$ T cells than soluble antigen (Bonifaz and others 2002; Bonifaz and others 2004). Another DC receptor is LOX-1, which has also been shown to mediate cross-presentation of antigen (Delneste 2004; Delneste and others 2002).

Tuning the Response

DCs activate T cells through peptide-MHC and T cell receptor (TCR) recognition, the costimulatory ligand and receptor ligation, and cytokines stimulation (such as IL-12). $CD4^+$ T cells display a broad spectrum of phenotypes, which are likely to depend on the priming APCs. DCs regulate $CD4^+$ T cell differentiation through a variety of molecules that belong to three major families: B7, TNF and IL-12. The affinity of the immunological synapses, the presence of costimulatory molecules and the cytokine microenvironment may decide the polarization of $CD4^+$ T cells into Th1, Th2, Th17 or regulatory T cells (Tregs) (Steinman and Banchereau 2007). Indeed, DCs regulate naïve $CD4^+$ T cell differentiation through IL-12 family including: i) IL-12 p70, which controls

Th1 response and the secretion of IFN-γ (Heufler and others 1996; Macatonia and others 1995); ii) IL-23, which contributes to the expansion of inflammatory $CD4^+$ T cells secreting IL-17 (Th17) (Bettelli and others 2007; Uhlig and others 2006; Weaver and Murphy 2007); and iii) IL-27, which appears to control IL-17 (Kastelein and others 2007; Smits and others 2004). Another type of $CD4^+$ T cells, i.e. Tregs, can inhibit the effector function of $CD8^+$ T cells (Roncarolo and Battaglia 2007; Sakaguchi 2006; Shevach 2006). Tregs can be divided into two major subsets: thymus-derived naturally occurring $CD4^+CD25^{high}$ Tregs (Itoh and others 1999; Thornton and Shevach 1998), and periphery-induced Tregs. Periphery-induced Tregs are thought to be derived from naïve $CD4^+$ T cells, and include T regulatory cell 1 (Tr1), which mainly produce IL-10 (Groux and others 1997), and Th3 cells, which mainly produce TGF-β (Fukaura and others 1996). The presence of IL-10 favors the Tr1 development and TGF-β favors the Th3 development (Dhodapkar and Steinman 2002; Kapsenberg 2003; Lanzavecchia and Sallusto 2001).

Besides cytokines, costimulatory molecules from B7 and TNF families are essential to generate the response. B7 family members are the major costimulatory molecules on DCs. There are 7 members that have been identified so far: CD80 (B7.1), CD86 (B7.2), inducible costimulatory ligand (ICOS-L), programmed death ligand (PD-L)-1 (B7-H1), PD-L2 (B7-DC), B7-H3, and B7-H4 (Greenwald and others 2005). CD80 and CD86 are expressed in mature DCs and the engagement with CD28 potently activates T cells while the engagement with cytotoxic T lymphocyte antigen 4 (CTLA-4) dampens the T cells response. In mice, low avidity binding of MHC-peptide-TCR recognition induces the anergy and increases the expression of CTLA-4 on T cells

(Mirshahidi and others 2001). ICOS-L interacts with ICOS on a subset of T cells that express CD28 and CD45RO in germinal centers of tonsils. This engagement activates T cell proliferation and cytokine secretion (like IL-10), and helps the B cells in antibody secretion (Hutloff and others 1999). Activated pDCs express high level of ICOS-L and prime naïve $CD4^+$ T cells into regulatory T cells with high IL-10 production (Ito and others 2007). The ligation of ICOS-L with ICOS has been shown to be critical in the generation of regulatory T cells for the control of airway hypersensitivity in the murine model (Akbari and others 2002). PD-L1 and PD-L2 engage with inhibitory receptor, PD-1, on activated $CD4^+$ or $CD8^+$ T cells and function as a negative regulator of immune activation presumably involving tolerance (Freeman and others 2000). However, high expression of PD-1 can also be found on exhausted HIV-specific T cells in HIV patients with disease progression (Day and others 2006; Trautmann and others 2006).

TNF and TNF receptor family are critical in the induction of the adaptive immune response. DCs require CD40 activation to upregulate CD80 and CD86 (Caux and others 1994). After CD40 ligation, pDCs secrete high level of IFN-α and IL-12 and drive a potent Th1 response (Cella and others 2000). After the engagement with $CD4^+$ T cells through CD40-CD40L ligation, DCs are licensed to prime $CD8^+$ T cells (Smith and others 2004). In the priming of $CD8^+$ T cells, CD40-licenced DCs activate $CD8^+$ T cells through another TNF family member, CD70. In murine model, CD70-CD27 interaction maintains the survival of antigen specific $CD8^+$ T cells and establishes long-term memory (Hendriks and others 2000; Taraban and others 2004). Similar to CD70-CD27 interaction, the engagement of 4-1BB-L and 4-1BB is important in maintaining the survival of human $CD8^+$ T cells against Epstein-Barr virus (EBV) or influenza virus *in*

vitro (Bukczynski and others 2004). Under the influence of TSLP, an epithelial cell cytokine, DCs express high level of OX40L. The OX40L-OX40-mediated signaling can maintain Th2 differentiation with strong IL-4 and IL-13 secretion and block the induction of regulatory T cells (Ito and others 2006; Wang and others 2006). In addition, TNF family members play a central role in the induction of the humoral response. DCs express several TNF family members, such as B lymphocyte stimulator (BlyS) and a proliferation-inducing ligand (APRIL), which help the survival and the differentiation of B cells (Litinskiy and others 2002; Schneider and others 1999). Independent of CD40L-mediated activation on B cells, human DCs activated by IFN-α, IFN-γ, or CD40L upregulate their expression of BlyS and APRIL. BlyS and APRIL induce immunoglobulin (Ig)-class switch in B cells in the presence of IL-10 or tumor growth factor β (TGF-β) and plasma differentiation upon BCR stimulation or the addition of IL-15 *in vitro* (Litinskiy and others 2002). Taken together, DCs play the central role in the coordination of immune responses.

Influenza Virus Infection: A Medical Need

Despite the availability of influenza vaccines, an epidemic of influenza virus infection occurs every year with 36,000 deaths and many hospitalizations in United States (Thompson and others 2004; Thompson and others 2003). The importance of studying influenza vaccines is further emphasized by the potential pandemic threat due to the infection of avian influenza virus in humans. Although avian influenza A viruses could experimentally infect volunteers but failed to generate a large-scale virion production, direct transmissions from avian to human have been identified in 1997 by avian H5N1 subtype (Subbarao and others 1998), in 1999 by avian H9N2 subtypes

(Peiris and others 1999), and in 2004 by avian H5N1 subtype (de Jong and others 2005; Ungchusak and others 2005). Due to possible human-to-human transmission in the future and high mortality rates (Beigel and others 2005; Ungchusak and others 2005), H5N1 virus has attracted the global attention for a potential pandemic threat. Therefore, studies of influenza viruses and vaccines against influenza are necessary.

Influenza Virology

There are three types of influenza virus, A, B, and C, of which influenza A virus causes the most threat to the public health. Influenza A virus is a negative-strand, segmented RNA virus that belongs to the family of *Orthomyxoviridae*. The influenza A virion is a pleomorphic-enveloped virion with the size of 80-120 nm in diameter (Fig. 4). The lipid envelope is derived from the host cell membrane integrated with three different kinds of proteins including hemagglutinin (HA), neuraminidase (NA), and small amount of M2 ion channel protein. The virion matrix protein is located underneath the lipid envelope. Within the lipid envelope are eight-segmented helical ribonucleoproteins (RNPs) containing RNA encoding for PB2, PB1, PA, HA, NP, NA, M1, M2, NS1 and NS2. Except for the seventh and eighth segments, each RNA segment only codes for one protein (Steinhauer 2002).

Influenza virus is the respiratory pathogen. Influenza viruses infect respiratory epithelium cells through aerosol infection. The replication begins at the recognition of sialic acid residues of glycoprotein or glycolipid on the cell membrane by HA. The viruses are then engulfed by the cells through a receptor-mediated endocytosis. The acidic pH in endosomes facilitates the uncoating of the virion and RNPs are then released to the cytosol (Lamb and Krug 1996). Soon after, the RNPs are transferred into the

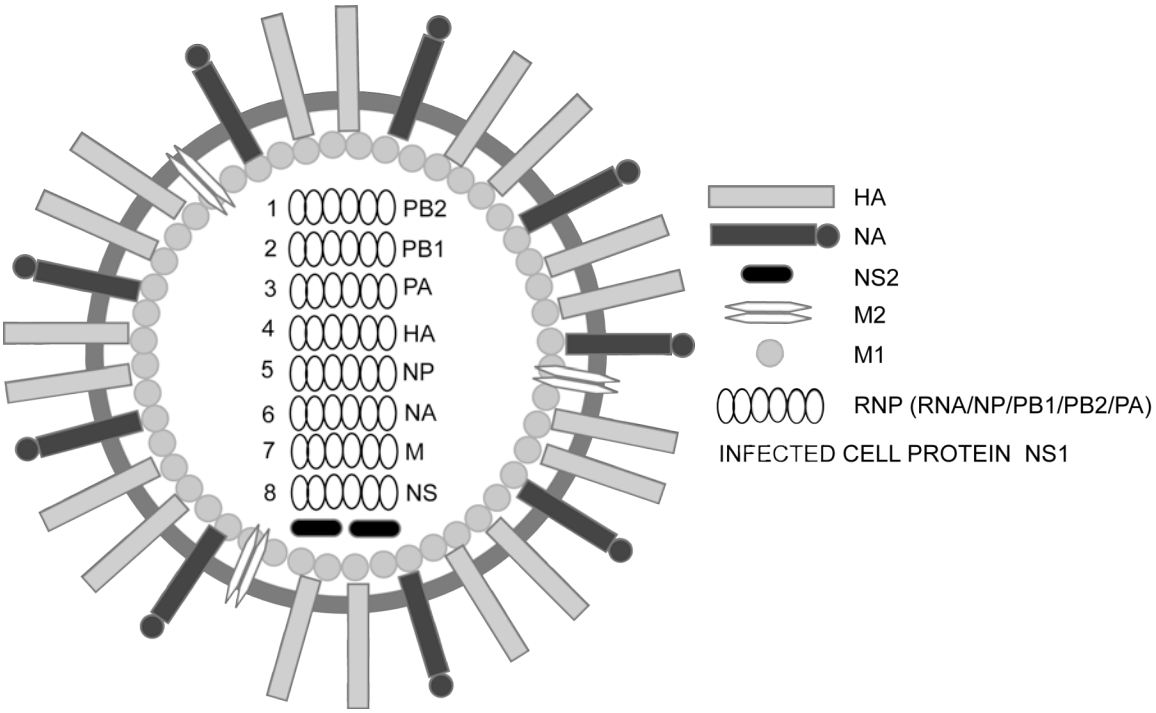

Figure 4. The structure of influenza A virus. The influenza A virion has a membrane envelope integrated with three different kinds of proteins including HA, NA, and small amount of M2. The virion matrix protein is located underneath the lipid envelope. Within the lipid envelope are eight-segmented RNPs containing RNA encoding for PB2, PB1, PA, HA, NP, NA, M, and NS.

nucleus and the viral RNA is used to generate the positive-sense template RNA for viral RNA amplification and mRNA for the viral protein synthesis using the polymerase complex, composed of PA, PB1 and PB2. Newly assembled RNPs are exported to the cytoplasm. Influenza viruses bud out and released from host cell with the absolute requirement of M1 (Gomez-Puertas and others 2000) and the assistance of NA to facilitate the yield (Gomez-Puertas and others 2000; Liu and others 1995; Palese and others 1974).

Influenza Pathology

Influenza A viruses are host-specific pathogens. There are 15 HA and 9 NA subtypes. Influenza A viruses have been isolated from human, horse, swine, and several

different kinds of avian species. Among them, most of the subtypes were identified from wild birds, which have been considered as the biggest reservoirs of influenza A viruses (Lamb and Krug 1996; Steinhauer 2002). H1N1, H2N2, and H3N2 have been shown to infect human which caused the pandemics in the last century.

The emerging of new subtype of influenza A virus in human population is one of the best characteristics of influenza A virus called "antigenic shift" (Gething and others 1980; Verhoeyen and others 1980). New subtype that causes pandemic in human is thought to be derived from the reassortment of avian and human influenza viruses. Nucleotide sequencing shows that the PB1 genes of human H2N2 and H3N2, the successor of H1N1, are more closely related to the avian virus than H1N1 virus (Kawaoka and others 1989). Avian influenza A virus preferentially recognizes α (2, 3)-linked sialic acid on the trachea of birds, but not α (2, 6)-linked sialic acid on the trachea (Palese and Schulman 1976). Because of the poor adaptation of avian influenza A virus in humans and its segmental genome, a third host is needed to play a bridge between birds and human. Swine is considered as the "mixing vessel" for the double infection by both avian and human influenza A viruses, which allows the reassortment of human influenza A virus with the avian origin (Palese and Schulman 1976; Steinhauer 2002). The PB1 genes of H1N1, H3N2 and H3N2 isolated from swine during 1957, 1968, and 1977 pandemic seasons in China contain majority of human origin and a minor fraction of avian origin (Shu and others 1994). The difference in sialic acid in swine's tracheas may explain why they can be infected by both avian and human influenza A viruses. The trachea of swine contains both types of sialic acid and therefore supports the infection of both avian and human influenza viruses (Palese and Schulman 1976). Thus, the swine

could be actively infected by influenza A viruses of human and avian origins as the intermediate host for the reassortment of influenza A viruses. Recently, a study showed that humans could be the vessel as well since the lower respiratory tract contains α (2, 3)-linked sialic acid for avian strains and the upper respiratory tract contains α (2,6)-linked sialic acid for human strains (Kogure and others 2006).

The influenza A virus is a reoccurring pathogen because of another property called "antigenic drift" (Gething and others 1980; Verhoeyen and others 1980). Each subtype of influenza A viruses has different variant strains responsible for influenza season each year. The HA and NA are two glycoprotein protruding out of the virion and are used to identify different strains. These two proteins are highly variable not only because of the high mutation rate of the RNA polymerase but also because of the positive selection involved. Influenza A viruses replicate using the viral encoded RNA polymerase, PB1, PB2, and PA. Due to the lack of the 3' to 5' exonuclease to proofread the newly synthesized RNA sequence, the replication is usually full of mutation (Lamb and Krug 1996; Palese and Schulman 1976). Upon all the mutation, the NA and HA are highly selectable as targets of host immune system. The neutralizing antibodies usually target HA and NA and favor the one that is mutated. Lambkin and others (1994) used monoclonal antibodies against different antigenic sites on the hemagglutinin to demonstrate that neutralizing antibodies positively selected the escape mutants. Among the full sequence of HA, 18 codons are highly variable and under the positive selection. Based on the result of retrospective studies, the positive pressure for the selection for the fittest variant is associated with the antibody-binding site and the sialic acid receptor-binding site, where the 18 codons are. Only the one that has the most changes in these 18

codons can become the ancestor of the future epidemic (Bush and others 1999). The ability of human cross-immunity diminishes accordingly to the increase of the antigenic distances and the time post exposure. This short life of human cross-immunity against variant strains explains the emergence of one dominant strain at a time and the restricted viral diversity in the host (Ferguson and others 2003).

Innate Immunity against Influenza Virus

Interferon provides the first wave of innate immunity against influenza viruses. Virus-carried ssRNA can activate TLR7 and -8 (Diebold and others 2004) while dsRNA is recognized by TLR3 and RIG-I (Le Goffic and others 2007). Upon infection, viral genomic RNA bearing 5'-phosphates triggered RIG-I pathway for interferon production (Pichlmair and others 2006). IFN-α and TNF-α can upregulate the transcription of RIG-I and subsequently increase IFN-α production in lung epithelium cells (Veckman and others 2006). However, viral protein NS1 can bind to RIG-I and RNA complex to inhibit interferon production and promote viral growth (Pichlmair and others 2006). pDCs are also thought to be very important in the production of IFN-α by the recognition of viral ssRNA through TLR7 (Diebold and others 2004).

Type I interferon induces the expression of Mx protein in infected cells and prevents viral replication. Mouse Mx1 blocks the synthesis of viral mRNA in the nucleus of infected cell presumably through the interaction with viral polymerase subunit PB2 because overexpression of PB2 can titrate out the antiviral effect of Mx1. Different from murine Mx1, human MxA does not inhibit mRNA synthesis of influenza virus; it inhibits a subsequent cytoplasmic viral multiplication step (Pavlovic and others 1992). The resistance to influenza virus infection in Mx1 transgenic mice (Kolb and others 1992)

and pig with mouse Mx1 cDNA (Muller and others 1992) demonstrates the anti-viral capacity of mouse Mx1 proteins. In humans, patients with Down's syndrome have an increased expression of MxA proteins because of gene dosage effects. Comparing to normal individuals, they are more susceptible to upper respiratory infection (Horisberger 1995). Therefore, the induction of MxA in humans does not seem sufficiently to prevent influenza virus spreading in contrast to the murine Mx system.

Influenza virus-infected epithelium cells and mononuclear leukocytes produce pro-inflammatory chemokines and cytokines. Influenza virus infection of primary human lung epithelial cells triggers exclusively the release of C-X-C chemokine ligand 8 (CXCL8) (Arndt and others 2002). CXCL8 rapidly recruits neutrophils to remove necrotic debris in infected site. Macrophages die of apoptosis within 24-36 hours after influenza virus infection, but DCs do not (Bender and others 1998). Upon infection, macrophages initiate the transcription and subsequently release chemokines including CCL2, CCL3, and CCL5 for mononuclear cell recruitment (Sprenger and others 1996). In contrast, DCs produce a variety of chemokines. At early time points (2 to 4 hours), chemokines potentially attract effector cells such as neutrophils, cytotoxic T cells, and natural killer (NK) cells (CXCL16, CXCL1, CXCL2, and CXCL3); at 8 to 12 hours, chemokines attract effector memory T cells (CXCL8, CCL3, CCL4, CCL5, CXCL9, CXCL10, and CXCL11) (Piqueras and others 2006). Therefore, these immediate innate responses limit the infection and ignite the viral-specific adaptive immune response.

Adaptive Immunity against Influenza Virus

DCs play a central role in presenting influenza viral antigens for the induction of adaptive immune response. Despite the fact that DCs can be infected by influenza virus,

the infection in DCs is less toxic with the expression of viral antigens but little production of infectious virions (Bender and others 1998). When mice are infected with influenza viruses, pulmonary DCs rapidly migrate through the lymph to regional lymph nodes like mediastinal or peribronchial lymph nodes and through the blood to the spleen in the first six hours (Legge and Braciale 2003). At day three post infection, viral HA can transiently be detected in the mediastinal lymph node because of infected migratory DCs (Sealy and others 2003). Viral antigens are presented either through direct presentation by migratory DCs or through cross-presentation by resident DCs in the lymphoid tissue (Belz and others 2004a; Belz and others 2004b; Crowe and others 2003).

Antibody response provides immediate protection from influenza virus infection. The action of protective antibodies comes from the recognition of HA from infecting cells or the recognition of NA or M2 from budding out viral progenies (Gerhard 2001). While B cells effectively recognize unprocessed antigens directly or through antigen-bearing DCs, $CD4^+$ T cells recognize peptide fragments on MHC class II molecules presented by DCs. $CD4^+$ T cells offer cognate help to B cells for the induction of antibody responses against influenza virus (Mozdzanowska and others 2005). When comparing to naïve mice, more specific plasma cells are generated in the presence of memory $CD4^+$ T cells (Marshall and others 1999). Although viral neutralizing activity is required for protection, passive transfer of HA-specific antibody with very low neutralizing activity cures influenza virus infection in severe combined immunodeficiency (SCID) mice (Mozdzanowska and others 1997). Different isotypes including IgM, IgG, and IgA can all contribute to the clearance of influenza virus (Harada and others 2003; Kopf and others 2002; Renegar and others 2004). While IgA

offers protection in upper respiratory tract, IgG is the dominant isotype in the lung protecting mice from infection (Renegar and others 2004).

$CD8^+$ T cell-mediated responses might be beneficial through eliminating viral infected cells. The significance of $CD8^+$ T cells responses can be illustrated by the shortened disease course (Flynn and others 1998). Specific $CD8^+$ T cells are generated in mediastinal lymph nodes in both primary and secondary immune responses (Flynn and others 1998; Tripp and others 1995). In the primary response, specific $CD8^+$ T cells are present in the lung as early as 7 days and peak at 10-13 days post infection. In secondary response, specific $CD8^+$ T cells still take 4-5 days to localize to the infected site (Flynn and others 1998). The $CD8^+$ T cells generated toward influenza virus are diverse in epitope recognition and cytokine profile (Belz and others 2001). There are no differences in the effector phenotypes like granzymes and perforin between $CD8^+$ T cells isolated from lungs and mediastinal lymph nodes (Johnson and others 2003). However, in murine model using TCR-transgenic T cells specific to influenza HA to control influenza infection, *in vitro*-primed $CD8^+$ T cells with low expression of CD62L, a lymph node-homing receptor, can rapidly migrate to the pulmonary infected site and reduce the viral titer when compared to naïve or $CD62L^{high}CD8^+$ T cells (Cerwenka and others 1999a; Cerwenka and others 1999b). Thus, the protective value of a $CD8^+$ cell population against influenza virus infection is strongly correlated with the ability to perform its effector function at the site of infection.

Current and Future Influenza Vaccine

Seasonal influenza virus escapes existing adaptive immune responses due to the antigenic drift in circulating strains. As a result, influenza vaccine is suggested to be

administered annually with strains recommended from the prediction of the World Health Organization Global Influenza Network. Currently, influenza vaccine is trivalent vaccine composed of H3N2 and H1N1 of influenza A virus and one influenza B virus. Traditional influenza vaccine is an inactivated split trivalent influenza vaccine (TIV) produced from virus propagated in the allantoic cavity of embryonated eggs. Recently, cold adaptive live-attenuated influenza vaccine (LAIV) is available. Through intranasal delivery, this LAIV replicates in the nasal passage but not in the lung and generates better mucosal immune response than traditional TIV which is given intramuscularly (Beyer and others 2002; Brokstad and others 2002).

Despite the existing influenza vaccines, the potential pandemic threat poses the need for new influenza vaccine. Currently, the vaccine manufactures cannot meet the production requirement and time constraint for the global immunization. The new technologies are being developed. The use of reverse genetics by transfecting Vero cells with plasmid encoding for viral RNA enable rapidly production of virus preparation containing the HA and NA of circulating strains (Fodor and others 1999; Neumann and others 1999). Other ongoing efforts include exploring the use of adjuvant to improve the immune response (Boyle and others 2007; Leroux-Roels and others 2007). The effort on using attenuate influenza virus with altered NS1 gene to induce a more balance humoral and cellular responses is underway (Ferko and others 2004). Finally, the concept of distinct DC subsets generating quantitatively and qualitatively distinct immune responses (Pulendran and others 1999) may be the key for rational design of new vaccines.

Humanized Mouse Models

Mouse models have been used extensively to study human diseases *in vivo* to circumvent the complexicity dealing with human patients. However, one should keep in mind the important differences between mouse and human immune systems (Mestas and Hughes 2004). For example, TLR9, which binds CpG in pathogens, is expressed on all myeloid cells, pDCs and B cells in mice but expressed on pDCs, B cells and neutrophils in human. Such differences may mean an effective therapy in mouse but a failure in a human trial. Because of the need for the *in vivo* model of a human immune system, various humanized mouse models have been developed. Humanized mice are defined as mice transgenically expressing human genes or immunodeficient mice engrafted with human cells or tissues. The discovery of the $Prkdc^{scid}$ (protein kinase, DNA activated, catalytic polypeptide; severe combined immunodeficiency) mutation in CB17 mice (Bosma and others 1983) was followed by attempts of constructing human/mice chimeras using human peripheral blood mononuclear cells (PBMCs) (Mosier and others 1988), fetal hematopoietic tissues (McCune and others 1988), or HPCs (Kamel-Reid and Dick 1988), which resulted in successful transfer of a functional human immune system in mice.

HuPBL-SCID chimera is generated by injecting human peripheral blood lymphocytes into the peritoneal cavity of an immunodeficient mouse (Ifversen and Borrebaeck 1996; Mosier and others 1988). Transplantation of mature human lymphocytes into immunodeficient mice results in a spontaneous production of human Ig in the serum and offers an easy way of reconstituting a human immune system in mice. However, the significant xenogeneic host-versus-graft and graft-versus-host reactions

(Tary-Lehmann and others 1994) and the rapid disappearance of naïve T cells and myeloid cells like monocytes and DCs poses a significant fault in examining primary responses and restricts the model for studying secondary immune responses (Murphy and others 1996).

SCID-hu model distinguishes itself from other humanized mouse model by grafting the immunodeficient mice with intact human haematoid-lymphoid tissues rather than dispersed cells suspension. Since the model was first described in late 1980s (McCune and others 1988), there are many variations that have been developed (McCune 1996). The SCID-hu Thy/Liv is constructed by implanting fetal liver and thymus into the kidney capsule, which allows the differentiation of thymocytes into mature circulating T cells (McCune and others 1988; Namikawa and others 1990). SCID-hu BM is generated by transplanting a piece of fetal femur or tibia under the skin. The incorporation of bone into the chimera is essential for B cells development (Kyoizumi and others 1992). The implanting of fetal bone and fetal thymus (SCID-hu BM/Thy) or in combination with fetal spleen (SCID-hu BM/Thy/Sp) ultimately leads to multilineage development of lymphoid and myeloid cells (Carballido and others 1995; Fraser and others 1995). However, SCID-hu chimera still needs a peripheral tissue like the skin in addition to haematoid-lymphoid tissues to be able to mount a specific immune response (Carballido and others 2000).

SCID-hu chimera permits a long-term engraftment and renewal of the human immune system. The bone and thymus are microscopically indistinguishable from age-matched human tissues and are composed of 90-95% human cells, of which contains 50-75% of thymocytes including double-negative, double-positive, and single positive

thymocytes, 8-20% of B cells, and 3-6 % of $CD14^+$ and $HLA\text{-}DR^+$ myeloid cells. Majority of T cells and B cells are immature in the graft; however, mature T cells and B cells can be found in circulation (Carballido and others 1995). Human T cells are restricted to human MHC but are tolerized toward murine MHC due to the presence of thymic epithelium cells and bone marrow derived cells (Vandekerckhove and others 1992). Circulating T cells have a naïve phenotype with CD45RA expression and acquire CD45RO upon exposure to alloantigens (Rouleau and others 1996). All classes of Ig including IgM, IgG and its subclass, IgA and IgE are detected in the serum indicating a normal class-switch (Carballido and others 1995; Vandekerckhove and others 1993).

The SCID-hu model has immediate limitations that restrict its application. First, SCID-hu model requires implanting of multiple fetal tissues simultaneously, which inadvertently gives rise to the ethical concern and limits its availability. Second, SCID-hu requires 3-4 months to have sufficient mature lymphocytes circulating in the blood and the engraftment is generally variable. Finally, the presence of human cells in the periphery is very limited and requires co-transplant of human skin to mount an immune response (Carballido and others 2000).

Humanized Mouse Model with Hematopoietic Stem Cell Transplantation

With all the limitations with humanized mice engrafted with either fetal tissues or PBMCs, a better model is necessary for studying human immunology. Mice constructed by Kamel-Reid (Kamel-Reid and Dick 1988) shed the light for this new generation of humanized mice. This chimera employs the idea that human HPCs will differentiate into multiple lineages of human cells and repopulate in the immunodeficient mice. Table 1 summarized the major humanized mouse models with stem cell transplantation.

Table 1. Major humanized mouse models with hematopoietic stem cell transplantation.

Strain	Modalities of Engraftment			Human immune cells	Reference
	Age	HPCs	Route		
NOD-SCID-$\beta_2m^{-/-}$	Adult	Mobilized blood	i.v.	B cells, myeloid cells, pDCs	(Palucka and others 2003)
NOD-SCID-$\gamma c^{-/-}$	Adult	Cord blood	i.v.	Multilineage differentiation including T cells	(Hiramatsu and others 2003; Yahata and others 2002)
NOD-SCID-$\gamma c^{-/-}$	Adult	Mobilized blood	i.v.	B cells, myeloid, pDCs, and T cells (+ IL-7)	(Shultz and others 2005)
NOD-SCID-$\gamma c^{-/-}$	Newborn	Cord blood	i.v.	B cells, T cells, myeloid cells, pDCs	(Ishikawa and others 2005)
BALB/c-Rag2$^{-/-}$-$\gamma c^{-/-}$	Newborn	Cord blood	i.h.	B cells, T cells, myeloid cells, pDCs	(Traggiai and others 2004)
BALB/c-Rag2$^{-/-}$-$\gamma c^{-/-}$	Newborn	Fetal liver	i.p.	B cells, T cells, myeloid cells, pDCs	(Gimeno and others 2004)
NOD-SCID	Adult	HPCs+ fetal thymus/ liver	i.v.	B cells, T cells, myeloid cells, pDCs, lymphoid organs	(Lan and others 2006; Melkus and others 2006)

The development of immunodeficient hosts. There are few breakthroughs along with the optimization of immunodeficient mice. The discovery of SCID mice is the most important event (Bosma and others 1983). The *scid* mutation results in defective DNA repair and high radiosensitivity. Mice bearing the *scid* mutation are immunodeficient due to the lack of mature B cells and T cells. Targeted mutation at the recombination-activating gene (Rag) 1 and Rag 2 loci can also prevent the development of mature B and T cells (Mombaerts and others 1992; Shinkai and others 1992). In early attempts with SCID mice engrafted with human bone marrow cells, the engraftment in the bone marrow only happened at a very low level with up to 1% of human cells. Only human cells with myeloid lineage are found in these mice (Kamel-Reid and Dick 1988; Lapidot and others 1992). After treating with human growth factor, hematopoietic stem cells can have multi-lineage differentiation, including immature and mature myeloid cells, granulocytes as well as B cells bearing CD19. $CD2^+$ T cells are not detectable in these mice (Lapidot and others 1992).

The engraftment of human cells in the mice has dramatically improved when SCID mice with non-obese diabetic (NOD) background referred to as NOD-SCID are used. NOD-SCID mice have multiple defects in the innate immunity including the decrease of NK cell activity, macrophage dysfunction and the absence of hemolytic complement activity (Shultz and others 1995). When NOD-SCID mice are engrafted with human cord blood stem cells, results are more consistent with higher level of engraftments (Lowry and others 1996). However, the limitations of NOD-SCID mice are related to the residual NK activity and the limited life span due to spontaneous thymogenesis (Prochazka and others 1992). Attempts in eliminating residual NK activity include pre-treatment with anti-asialo GM1 antiserum (Yoshino and others 2000) or further modificaiton of the genetic background on host mice including the null mutations of perforin 1 (Shultz and others 2003) or β_2m (Kollet and others 2000). With the improvement of engraftment, multiple lineages of human cells are identified in the mice with occasional development of T cells.

The most recent breakthrough comes from the humanization of immunodeficient mice with mutation at the common cytokine receptor γ chain (γ_c). The γ_c is the component of high-affinity receptors for IL-2, IL-4, IL-7, IL-9, IL-15, and IL-21, and the absence of it completely impairs the function and the development of T cells, B cells and NK cells (Cao and others 1995; Habib and others 2002). Mice bearing the γ_c mutation including NOD-SCID-IL2$\gamma_c^{-/-}$, or BALB/c-Rag2$^{-/-}$-$\gamma_c^{-/-}$ demonstrate even better engraftment by human HPCs and multi-lineage human cells development including T cells (Matsumura and others 2003; Traggiai and others 2004).

Human hematopoiesis. The knowledge of hematopoietic development accumulates along with the development of humanized mice transplanted with human HPCs. Transplanting HPCs from fetal liver, cord blood or G-CSF mobilized peripheral blood into NOD-SCID mice permits the development of multilineage human immune cells. Through transferring subsets of HPCs into NOD-SCID mice, it allows the identification of primitive hematopoietic cells called SCID repopulating cells (SRC) (Bhatia and others 1998). Lineage $(LIN)^{-}CD34^{-}CD133^{+}$ cells isolated from either cord blood or G-CSF mobilized peripheral blood are identified to be more primitive than $CD34^{+}$ HPCs and can give higher multilineage engraftment in NOD-SCID mice (Gordon and others 2003; Kuci and others 2003). Human HPCs migrate to murine bone marrow through the interaction of CXCR4 with murine chemokine CXCL12 secreted by damaged bone marrow stromal cells after sublethal total body irradiation, a procedure commonly performed prior to the HPC transfusion (Lapidot and Kollet 2002; Peled and others 1999). Human cells possess $CD34^{+}CD38^{-}$ phenotype and are capable of initiating hematopoiesis in secondary irradiated NOD-SCID mice demonstrates the renewal capacity of HPCs in murine microenvironment (Bhatia and others 1997; Cashman and others 1997a).

Distinct populations of functional human DCs are found in various tissues. Human HPCs differentiate into different subsets of DCs in bone marrow of NOD-SCID (Palucka and others 2003), BALB/c-$Rag2^{-/-}$-$\gamma_c^{-/-}$ (Traggiai and others 2004), or NOD-SCID-$IL2\gamma_c^{-/-}$ mice (Shultz and others 2005). Two subsets of DCs that resemble human blood DCs with LIN^{-}HLA-$DR^{+}CD11c^{+}$ mDCs and LIN^{-}HLA-$DR^{+}CD123^{+}$ pDCs can be identified in the bone marrow, spleen, and liver (Palucka and others 2003; Traggiai and

others 2004). Human mDCs from bone marrow induce strong mixed lymphocyte reaction (MLR) upon coculturing with allogeneic T cells and specific proliferation of autologous T cells upon loading of recall antigen, TT, *in vitro* (Palucka and others 2003). Human pDCs from bone marrow secrete large amount of IFN-α *in vitro* upon exposure to influenza A viruses (Palucka and others 2003; Traggiai and others 2004). The function of human pDCs is also confirmed by elevated serum IFN-α after influenza A virus exposure (Palucka and others 2003). DCs are also found in various peripheral tissues like $CD207^+$ Langerhans cells in the skin, $CD11c^+$ interstitial DCs in the liver and lung parenchyma (Palucka and others 2003).

Human B cells differentiated become functionally mature in humanized mice with HPCs transfer. Kinetic studies of B cells in the bone marrow and spleen suggest the differentiation of B cells occurs in the bone marrow (Cashman and others 1997b). While majority of B cells in the bone marrow display $CD19^+CD10^+IgM^{+/-}$ immature B cell phenotypes, mature human B cells with $IgD^+IgM^+CD20^+CD19^+$ are found in the spleen and lymph nodes of NOD-SCID (Cashman and others 1997b), BALB/c-$Rag2^{-/-}$-$\gamma_c^{-/-}$ (Traggiai and others 2004), or NOD-SCID-IL2$\gamma_c^{-/-}$ (Shultz and others 2005) mice engrafted with various sources of HPCs. A minor population of human B cells with $CD5^+$ phenotype resembling B-1 cells is also found in the spleen of NOD-SCID-$\gamma_c^{-/-}$ (Matsumura and others 2003). Even though mature human B cells are located in large quantity in the spleen of NOD-SCID mice, no distinct B cells follicles are found (Shultz and others 2005). B cell follicles similar to periarteriolar lymphoid sheaths (PALS) in human spleen can be seen in BALB/c-$Rag2^{-/-}$-$\gamma_c^{-/-}$ (Traggiai and others 2004), or NOD-SCID-IL2$\gamma_c^{-/-}$ (Shultz and others 2005) mice. The function of B cells can be illustrated

with human IgM and IgG, which correlate with $CD19^{+}CD27^{+}CD138^{+}$ plasma cell differentiation in the bone marrow and spleen (Traggiai and others 2004).

Among all hematopoietic lineage cells, human T cell development presents itself to be the most challenging. *De novo* T cell genesis is finally achieved in mice without γ_c chain including NOD-SCID-IL2$\gamma_c^{-/-}$ (Shultz and others 2005) and BALB/c-Rag2$^{-/-}$-$\gamma_c^{-/-}$ (Traggiai and others 2004). First, the *de novo* development of human T cells is supported by the increase cellularity of thymus and the presence of human thymocytes in different differentiation stages including double-negative, double-positive, single-positive CD4 and single-positive CD8 thymocytes (Ishikawa and others 2005; Shultz and others 2005; Traggiai and others 2004). Second, TCR-rearrangement excision circles (TREC), a byproduct form during the TCR rearrangement and the quantity decrease upon the increase of cell division (Hazenberg and others 2003), are detected with highest amount in the thymus but less in the spleen and lymph nodes (Shultz and others 2005; Traggiai and others 2004). Third, the analysis of TCR Vβ repertoire demonstrates a variety of Vβ usages in T cells (Shultz and others 2005; Traggiai and others 2004). Overall, recent data on the analysis of T cells in γ_c null mice is suggesting a *de novo* genesis of human T cells in murine thymus.

A functional human adaptive immune system is demonstrated by the development of specific T cells and B cells. When human T cells are isolated from EBV-infected BALB/c-Rag2$^{-/-}$-$\gamma_c^{-/-}$ mice, they proliferate in response to autologous EBV-transformed B cells but not un-infected B cells. This observation suggests the recognition of EBV epitopes presented by B cells in the context of human MHC by human T cells (Traggiai and others 2004). When BALB/c-Rag2$^{-/-}$-$\gamma_c^{-/-}$ mice are vaccinated with TT vaccine at 12

weeks post $CD34^+$ HPC transplant, mice generate specific human IgM as well as IgG in the serum. B cell follicles with murine follicular dendritic cells (FDC) are also observed in the spleen and lymph nodes of vaccinated mice, demonstrating a germinal center reaction (Traggiai and others 2004). The functional B cell response can also illustrated by the generation of HIV gp120 and gp24-specific antibodies in HIV infected humanized NOD-SCID-$\gamma_c^{-/-}$ mice (Watanabe and others 2007). Overall, recent studies suggest a functional adaptive immune system in humanized mice engrafted with $CD34^+$ HPCs.

Despite successful development of human T cell in humanized γ_c null mice, human adaptive immune responses are still suboptimal in these mice. First, endogenous T cells proliferate in response to autologous EBV-transformed B cells illustrate the recognition of human MHC by TCR (Traggiai and others 2004). However, the TCR repertoire maybe selected biased toward murine MHC in the periphery since virus-specific T cells only recognize epitope presented by murine MHC in influenza virus infected humanized BALB/c-$Rag2^{-/-}$-$\gamma_c^{-/-}$ mice (Legrand and others 2006). Second, the lack of T cell responses and very limited B cell responses are detected against HIV in infected humanized BALB/c-$Rag2^{-/-}$-$\gamma_c^{-/-}$ mice (Baenziger and others 2006). The lack of proper human immune responses is mainly due to the improper T cells repertoire. Third, the limited antibody responses other than IgM are generated after immunization illustrating the lack of efficient germinal center reaction that would permit isotype switch and affinity maturation (Ishikawa and others 2005; Kuruvilla and others 2007; Traggiai and others 2004). Therefore, the reconstitution of T cells with broad TCR repertoire against human MHC and the reconstitution of germinal center structure remain the key challenges for these models.

CHAPTER TWO

Objectives

DCs are the most important antigen presenting cells. The role of DCs is to capture, transport, process, and present antigens to T cells. Once DCs migrate into the draining lymph node, they mature and become potent T cell and B cell activators through their costimulatory signals, such as CD80 and CD86, and cytokines like IL-12 and IFN-α. The essential role of DCs in the induction of innate and adaptive immunity has been studied intensively *in vitro* and *in vivo* mouse models. However, murine DCs are quite different from human DCs in the aspect of TLR expression and CD1 antigen presentation system. To understand more about human DCs *in vivo*, we proposed the utilization of humanized mouse model, NOD-SCID-$\beta_2m^{-/-}$ mice engrafted with human $CD34^+$ HPCs, to study *in vivo* interaction of human DCs with influenza viruses and influenza vaccines. Influenza viruses have been studied intensively *in vitro* and are excellent immunostimulator *in vitro* in activating DCs to induce a Th1 response, which is very effective in clearing the viral infection; however, influenza infection is still a major disease burden in public health. Therefore, we were very interested in studying the influenza viral infection *in vivo* in humanized mice. We postulated that human DCs in humanized mice were similar to DCs in human body in inducing an immune response *in vivo*. The proposed experiments would allow us to understand the behavior of human DCs in response to influenza virus and to further evaluate the potential of humanized mice as an *in vivo* model of human immune system for testing human vaccines (Fig. 5).

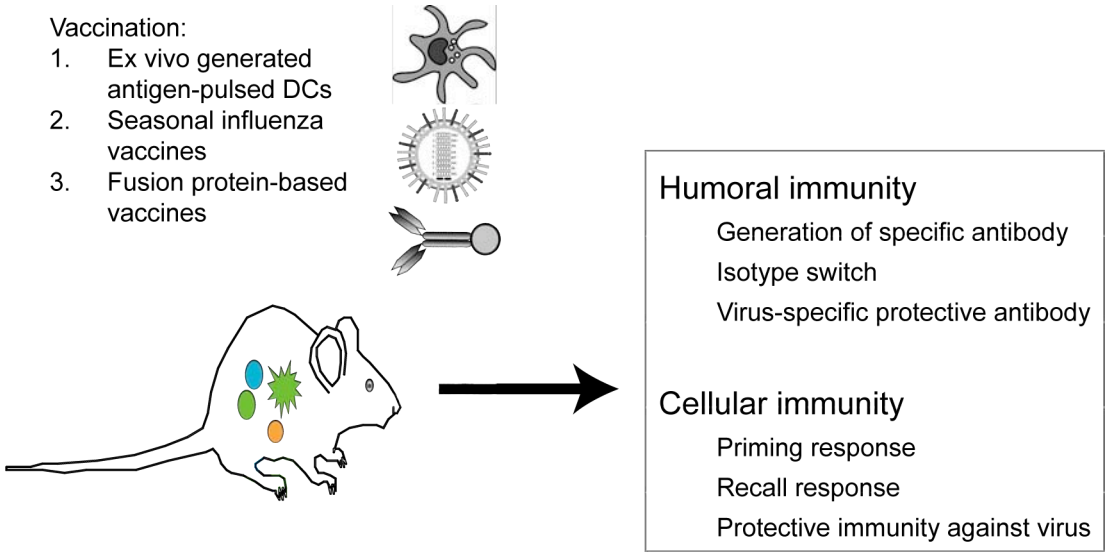

Figure 5. Stepwise approach to establish humanized mice as a model for testing human vaccines. Humanized mice are vaccinated with *ex vivo*-generated antigen-pulsed DCs, seasonal influenza vaccines and fusion protein-based vaccines in sequence. The adaptive immune responses are then evaluated.

Aim 1: The Interaction of Human DCs with Influenza Virus in Humanized Mice

We hypothesized that two subsets of human DCs, mDCs and pDCs, respond differently to influenza viruses *in vivo*. To address that, we analyzed the maturation of two DC subsets by analyzing 1) the phenotype and 2) the ability of DC trafficking into the draining lymph node.

Aim 2: Humoral Responses against Influenza Virus

We hypothesized that humoral immune responses could be generated upon vaccination with antigen-pulsed *ex vivo*-generated DCs in humanized mice. Here, we assayed humoral immune responses against influenza viruses by analyzing 1) plasma cell differentiation and 2) influenza-specific antibodies in the serum and their neutralizing capacity. This approach permitted us to test the B cell compartment in humanized mice.

Aim 3: Role of $CD4^+$ T cells in Humoral Responses against Influenza Virus

We hypothesized that a subset of $CD4^+$ T cells was important in generating humoral responses in humanized mice. Here, we assayed humoral immune responses induced by vaccination upon adoptive transferring of different $CD4^+$ T cell subsets by analyzing 1) plasma cell differentiation and 2) influenza-specific antibodies in the serum.

Aim 4: $CD8^+$ T cell Responses against Influenza Virus

We hypothesized that cellular immune responses could be generated in humanized mice upon vaccination. Here, we assayed antigen-specific $CD8^+$ T cell responses induced via vaccination by measuring 1) the frequency of influenza virus-specific $CD8^+$ T cells using influenza-specific tetramer staining and 2) functional differentiation of antigen-specific $CD8^+$ T cells, such as IFN-γ secretion and cytotoxicity.

CHAPTER THREE

Materials and Methods

Antibodies and Reagents

Antibodies

Antibodies to human CD2 (S5.2), CD3 (SK7), CD4 (SK3), CD8 (SK1), CD11c (S-HCL-3), CD19 (HIB19), CD20 (2H7), CD28 (L293), CD34 (8G12), CD45 (HI30), CD45RA (clone), CD49d (9F10), CD56 (B159), CD57 (NHK-1), CD80 (L307.4), CD83 (HB15e), CD86 (IT2.2), CD107a (H4A3), CD123 (9F5), HLA-DR (L243), IFN-γ (25723.11), IL2 (5344), Lineage cocktail and TNFα (6401.1111) were from BD (Franklin Lakes, NJ). Antibodies to human CD3 (UCHT1), CD138 (B-B4), CD207 (DCGM4) and DC Lamp (104.G4) were from Beckman Coulter (Fullerton, CA); human CD14 (TuK4), CD27 (CLB-27/1) and CD38 (HIT2) were from Invitrogen (Carlsbad, CA); human CD1a (NA1/34) and HLA-ABC (W6/32) antibodies were from Dako (Denmark); human IgD, IgM, IgG were from Southern Biotech (Birmingham, AL).

Peptides and Tetramers

All peptides used here were HLA-A*0201-restricted and synthesized by Bio-Synthesis (Lewisville, TX) with purity higher than 95% including: influenza A virus M1 58-66 (GILGFVFTL), NP 383-391 (SRYWAIRTR) and NS1 122-130 (AIMDKNIIL); HIV gag 77-85 (SLYNTVATL) and pol 476-484 (ILKEPVHGV); and melan A/MART-1 27-35 (AAGIGILTV). The HLA-A*0201 tetramers loaded with influenza A virus M1

58-66 (GILGFVFTL), NS1 122-130 (AIMDKNIIL), HIV gag 77-85 (SLYNTVATL), and melan A/MART-1 27-35 (AAGIGILTV) were from Beckman Coulter.

Viruses and Vaccines

Live influenza virus A/PR8/34 (PR8) in allantoic fluids was kindly provided by Aldofo Garcia-Sastre (Mount Siani Medical School, New York, NY) and purified virus was from Charles River Laboratories (Wilmington, MA). Influenza trivalent live-attenuated vaccine, FluMist® (LAIV; 2006-7 season; MedImmune, Gaithersburg, MD), inactivated vaccine, Fluzone® (TIV; 2006-7 season; Sanofi Pasteur, Swiftwater, PA), alum-precipitated tetanus toxoid, Tetanus Toxoid Adsorbed USP (TT; Aventis Pasteur, Swiftwater, PA) were all obtained from Baylor hospital pharmacy. Recombinant FluM1 protein and anti-DCIR antibody and FluM1 protein conjugate were provided by Gerard Zurawski (Baylor Institute for Immunology Research, Dallas, TX).

Humanized Mice

Humanized mice were generated as previously described (Palucka and others 2003). Briefly, NOD-SCID-$\beta_2m^{-/-}$ mice (Jackson Laboratories, Bar Harbor, ME) at the age of four to five weeks were sub-lethally irradiated (12 cGy per gram of body weight) using ^{137}Cs gamma irradiator (MDS Nordion, Ottawa, Canada) at twenty-four hours before the transplant. $3x10^6$ of $CD34^+$ HPCs from normal donor G-CSF mobilized peripheral blood aphaeresis were resuspended into 200 μl in phosphate buffered saline (PBS, and given intravenously into previously irradiated mice through tail-vein injection. Mice were used between four to fifteen weeks post HPCs transplant. All the protocols

were reviewed and approved by institutional review board and institutional animal care and use committee at Baylor Research Institute.

T Cell Isolation

T cells were isolated from PBMCs in $CD34^-$ fraction using magnetic beads (Miltenyi Biotec, Auburn, CA) following the manufactures protocol. Briefly, thawed PBMCs were incubated with magnetic beads recognizing CD14, CD16, CD19, CD56 and HLA-DR at 4-8 °C for 15 minutes. After wash, PBMCs were passed through the column in the magnetic field and the negative fraction containing total T cells was collected. Isolated total T cells had purity >95% with <0.5% of B cells. $CD4^+$ T cells were isolated with the same protocol with addition of CD8 beads in the beads cocktail. Isolated $CD4^+$ T cells had purity >95% with <0.5% of B cells. In experiments with subsets of $CD4^+$ T cells, $CD4^+$ T cells were further stained with CD45RA-FITC, CD27-PE, and CD4-APC antibody. $CD45RA^-CD27^+CD4^+$ central memory T cells and $CD45RA^-CD27^-CD4^+$ effector memory T cells were sorted by FACSAria or FACSVantage (BD) with purity >99%.

Monocyte-Derived DCs

Monocytes were enriched from PBMCs by plastic adherence and cultured in complete RPMI with 10% FCS, 100 ng/ml of GM-CSF (Immunex, Seattle, WA) and 10 ng/ml of IL-4 (R&D Systems, Minneapolis, MN) at 37°C in 5% CO_2 incubator for five days. Cells were feed with the same amount of cytokines every two days. Immature DCs were loaded with 10^5 HA units of heat-inactivated influenza A/PR8/34 (56°C for thirty minutes) per $1x10^6$ cells for 2 hours and matured with 200 ng/ml of CD40L (R&D

Systems) and 20ng/mL of TNF-α (R&D Systems) for 16 hours. Routinely, the recovery of DCs was 71.1±4.1%. In some experiments, adherent monocytes were cultured in CellGenix DC medium (CellGenix, Germany) with 100ng/ml of GM-CSF and 500U/ml of IFN-α2b (IntronA; Schering Corporation, Kenilworth, NJ) or 100ng/ml of IL-15 (R&D Systems) at 37°C 5% CO_2 incubator for three days and matured with 10ng/ml of LPS (Sigma-Aldrich, St Louis, MO) for 30 hours and loaded with peptides for the last 14 hours before harvest.

Vaccination

Vaccination with Ex Vivo-Generated DCs

Humanized mice were first reconstituted with autologus T cells by giving $10x10^6$ of $CD4^+$ T cells or $20x10^6$ of total T cells via i.p. or s.c. injection. Mice were vaccinated with $2x10^6$ of *ex vivo*-generated DCs i.p. or s.c. and boosted at day 7. Mice were bled at different time points prior and post DCs vaccination to monitor the immune response and harvested according to individual experimental design.

Vaccination with Human Vaccines

Post T cell transfer, influenza virus vaccines either LAIV (one fifth of human dose, $2x10^6$ $TCID_{50}$ of each strain) or TIV (one fifth of human dose; 3 μg HA of each strains) were given to the mice through i.p. and i.v. injections. PBS or TT (one tenth of human dose were used as the control. Mice were bled at different time points prior and post vaccination to monitor the immune response, and harvested according to individual experimental design.

Humanized Mouse Analysis

Humanized mice were first euthanized and the blood was collected with or without heparin. Plasma or serum was collected for antibody and cytokine measurements. Lymph nodes, lungs, and spleen were frozen for tissue analysis. After flushing out blood from the lungs by incising the left atrium and injecting 10 mL of PBS into right ventricle, lungs were harvested for the preparation of a single cell suspension. Lymph nodes and lungs were digested with 2 mg/mL of collagenase D (Roche Diagnostics, Indianapolis, IN) for 30 minutes at 37°C. The single cell suspension was made with two frosted slides and the debris was removed by filtering through 70 μm cell strainer (BD). Spleen was digested for 10 minutes using the same method. Bone marrow was harvested from femur, pelvis and tibia by flushing out the marrow. The single cells suspension was furthered ficolled or purified for *in vitro* experiments.

Flow Cytometry

Surface Phenotype

For phenotypic analysis, cells were was first treated with purified antibody against murine CD16/32 (2.4G2; to block nonspecific FcR interactions) and then stained on ice with FITC, phycoerythrin (PE), peridinin chlorophyll protein (PerCP), and allophycocyanin (APC) conjugated specific antibody, or appropriate isotype control. After washing twice with PBS, cells were fixed with FACSlysis solution (BD) or 1% paraformaldehyde and analyzed up to six parameters on FACSCalibeur (BD) using CellQuest software (BD) or FlowJo software (Tree Star, Ashland, OR).

Tetramer Analysis

Heparinized blood or single cell suspension from different tissues were resuspended with PBS-2% FCS. Each sample was stained with FITC, PE, PerCP or APC conjugated antibody to CD8 and CD3 for surface marker and PE or APC conjugated FluM1-HLA-A*0201 tetramer for FluM1-specific $CD8^+$ T cells and HIVgag-HLA-A*0201 tetramer for the negative control, incubated at room temperature for 30 minutes and washed twice with PBS. The sample was resuspended with FACSlysis buffer and incubated at room temperature for 10 minutes for red cells to lyse. FACSlysis buffer was washed away, sample was resuspended with 1% paraformaldehyde, and analyzed for FluM1-HLA-A201 tetramer positive $CD8^+$ T cells.

Intracellular Cytokine Staining

Intracellular cytokine and degranulation of $CD8^+$ T cells was examined using a modified protocol as described (Betts and others 2003). Briefly, total cells from vaccinated mice were stimulated with 2.5 μM of specific peptide in the presence of anti-CD28 and anti-CD49d antibodies. Monesin and FITC-conjugated anti-CD107a were included during the culture period. Following T cell stimulation, cells were surface labeled with surface antibodies, and then intracellularly labeled with antibodies specific for IFN-γ, IL-2 and TNF-α using BD Pharmingen Cytofix/Cytoperm and perm/wash reagents. Samples were analyzed up to six parameters on FACSCalibeur and up to twelve parameters on FACSaria.

Immunohistofluorescence Staining

Tissues were harvested and embedded in OCT (Sakura Finetek U.S.A., Torrance, CA) and snap frozen in liquid nitrogen. Frozen sections were cut at 6 μm and air dried on Superfrost slides (CardinalHealth, Dublin, Oh). Frozen sections were fixed with cold acetone for five minutes and air dried. Frozen sections were blocked with 5% BSA in PBS containing 0.1% saponin for twenty minutes and stained with primary mouse monoclonal antibodies specific to DC-LAMP or CD3 for one hour at room temperature and then goat anti-mouse IgG Alexa 568 conjugated (Invitrogen). After washing off excess antibody, sections were further stained with FITC-conjugated antibody to HLA-DR or human IgG for one hour at room temperature. Mouse IgG1 was used as isotype control. Finally, sections were counterstained with 1 μg/ml of DAPI (Invitrogen) and mounted with coverslips. Fluorescence staining was visualized using fluorescence microscope (Olympus, Japan) and recorded using MetaMorph software (Molecular Devices).

ELISA

Total Immunoglobulin

Total human immunoglobulins including IgM, IgG and IgA were determined by quantitative ELISA kits (Bethyl, Montgomery, TX) following manufacture's protocols. Briefly, 96-well ELISA plate (Nunc, Roskilde, Denmark) was first coated with10 μg/ml of anti-human immunoglobulin capture antibody in 0.05 M sodium carbonate solution (pH=9.6) at 4-8 °C for overnight. After washing with washing solution (50 mM Tris, 0.14 M NaCl, 0.05% Tween 20, pH=8.0), blocking solution (50 mM Tris, 0.14 M NaCl,

1% BSA, pH=8.0) was added to each well and the plate was incubated at room temperature for one hour. Then, samples and standards diluted with sample diluent (50 mM Tris, 0.14 M NaCl, 1% BSA, 0.05% Tween 20, pH=8.0) were added to each well and incubated for one hour at room temperature. After incubation, samples were removed and wells were washed five times with washing solution. Then, goat anti-human immunoglobulin antibody HRP conjugated was transferred into each well for one hour at room temperature. After incubation, HRP conjugate was removed and plate was washed five times with washing solution. Then, 100 μl TMB substrate reagent (BD) was added into each well at room temperature in the dark. After five minutes of incubation, 100 μl of 1 M H_3PO_4 was added subsequently to stop the reaction and the plate was read at 450 nm with the ELISA reader (Molecular Devices, Sunnyvale, CA). The standard curve was generated and the amount of total human immunoglobulin was further calculated.

Specific Immunoglobulin

ELISA plate was first coated with10 μg/ml of purified FluA/PR8/34 virus in 0.05 M sodium carbonate solution (pH=9.6) at 4-8°C for overnight. After washing, blocking solution was added to each well and the plate was incubated at room temperature for one hour. Then, sample and standard diluted with sample diluent were added to each well and incubated for two hours at room temperature. Here, reference human serum was used as the standard which contained 1,000 AU (arbitrary unit) of specific IgM and 100,000 AU of specific IgG. After incubation, samples were removed and wells were washed five times with washing solution. Then, goat anti-human IgM or IgG antibody HRP conjugated was transferred into each well for one hour at room temperature. After

incubation, HRP conjugate was removed and plate was washed five times with washing solution. Then, 100 μl TMB substrate was added into each well at room temperature in the dark. After twenty minutes of incubation, 100 μl of 1 M H_3PO_4 was added subsequently to stop the reaction and the plate was read at 450 nm with ELISA reader. Standard curve was generated and the amount of virus-specific IgM or IgG was further calculated.

Hemagglutination Inhibition Assay

The hemagglutination inhibition (HAI) assay was performed to detect and quantitate antiviral antibodies in the serum. Aliquots of 50 μl of serum (including all the test sera and reference human serum as positive control) were first treated with receptor destroying enzyme (Sigma) for 16-18 hours at 37°C. Sera were then heated to 56 °C for thirty minutes to remove the enzyme activity and incubated with 200 μl of 1% chicken red blood cells (CRBCs) at room temperature for thirty minutes to remove non-specific hemagglutination activity in the serum. Diluted samples (1/5 dilution) were recovered by centrifuging at 1200 rpm for ten minutes. Mixture of 50 μl of influenza virus containing 4 HA unit and 50 μl of 2-fold serial diluted serum were incubate at room temperature for thirty minutes in duplicate on 96-well U bottom plates. Then, 50 μl of 1% CRBCs were added into each well and incubated at room temperature for forty-five minutes. The HAI titer was defined as the reciprocal of the final dilution that did not give hemagglutination.

IgM Depletion

Aliquots of 50 μl of serum were treated with 50 μl of anti-human IgM-biotin antibody (2mg/ml; Jackson ImmunoResearch Laboratories, West Grove, PA) in 1.5 mL

tube for overnight at 4 °C and then further treated with 25 µl of streptavidin-agarose (Invitrogen) for one hour at room temperature. The IgM depleted serum was recovered from the supernatant after spinning 12,000 rpm for 10 minutes. More than 99% of IgM were depleted as determined by ELISA.

In vitro Neutralization Assay

A preparation of influenza virus containing 200 pfu (plaque forming unit) in 100 µl was mixed with 100 µl of serum diluted 5-fold in ACL-4 medium composed of D-MEM/F-12 (Invitrogen), 0.02 mg/ml insulin, 0.01 mg/ml transferrin, 25 nM sodium selenite, 50 nM hydrocortisone, 0.01 mM ethanolamine, 0.01 mM O-phosphorylethanolamine, 0.1 nM 3, 3', 5-triiodo-L-thyroine, 2 mg/ml bovine serum albumin, 0.5 mM sodium pyruvate, 10 mM HEPES, 2 mM L-glutamine and 1 ng/ml EGF (BD). After thirty minutes' incubation at room temperature, the mixture of virus and serum were added into 50,000 human lung epithelial cells, NCI-H2405 (ATCC, Manassas, VA), in 4-well chamber slides (BD). After two hours of incubation, virus-serum samples were washed away and cells were cultured in ACL-4 medium at 37 °C for twenty-four hours. At the end of culture, slides were fixed with 4% paraformaldehyde for thirty minutes at room temperature. Slides were treated with 5% BSA in PBS containing 0.1% saponin for twenty minutes and further stained with primary mouse monoclonal antibody against influenza virus NP (IA52.9; ARGENE, North Massapequa, NY), and then goat anti-mouse IgG Alexa 568 conjugated. Cells were counterstained with 1 µg/ml of DAPI and mounted with coverslips. Fluorescence staining was visualized using fluorescence microscope and recorded using MetaMorph software. The

neutralization is defined as the sera able to inhibit viral infection detected by viral nucleoprotein staining.

Influenza Virus Infection and Passive Protection

NOD-SCID-$\beta_2m^{-/-}$ mice were anesthetized with ketamine hydrochloride (120 mg/Kg, Fort Dodge Animal Health, Fort Dodge, IA) and xylazine (6 mg/Kg, Phoenix Scientific, St Joseph, MO). Mice were then inoculated intranasally with 50 μl of 10^2 pfu of influenza virus that was treated with serum from vaccinated humanized mice (with or without T cells). The lungs were harvested at eight days post inoculation to measure total viral load by $TCID_{50}$ using NCI-H2405. In the serum transfer experiment, NOD-SCID-$\beta 2m^{-/-}$ mice were transferred intranasally with 50 μl of serum from vaccinated humanized mice (with or without T cells). After thirty minutes, mice were then inoculated intranasally with 50 μl of 10^2 pfu of influenza virus. The body weights were taken daily.

$TCID_{50}$

The $TCID_{50}$ (50% tissue culture infectious dose) was performed as described with some modification (Cottey and others 2001). Samples were serially diluted (10-fold) in ACL-4 medium. Eight replicates of 100 μl samples of each dilution were placed into 96-well round-bottom tissue culture plates. 100 μl of 2.5 x 10^5 cells/ml suspension of NCI-H2405 cells in ACL-4 medium was added to each well. The plates were incubated at 37°C in 5% CO2 incubator for overnight. The culture fluid was removed and replaced with 200 μl of ACL-4 medium containing 1 μg/ml trypsin. The plates were incubated for 3 days at 37°C in 5% CO_2 incubator. Assay for viral growth was measured by

hemagglutination. For that, 50 μl of a 1% suspension of CRBCs was added to each well. Hemagglutination was read after one hour at 4°C. Viral titers were then calculated.

Thymidine Incorporation

$CD4^+$ T cells, $1x10^5$ cells per well in 96-well U-bottom plate (BD, Franklin Lakes, NJ) were stimulated with different amounts of autologus DCs or 1 μg/ml of SEB (Sigma-Aldrich) in a final volume of 200 μl. After five days of coculture, cells were pulsed with 1 μCi of ^{3}H-thymidine (Amersham Biosciences, Pittsburgh, PA) for sixteen to eighteen hours. The incorporation of ^{3}H-thymidine was measured for triplicate cultures with the liquid scintillation counter (PerkinElmer, Waltham, MA).

Chromium Release Assay

Cytotoxic T lymphocyte (CTL) activity was measured using standard chromium-releasing assay. Briefly, single cells suspensions of lymphocytes from various tissues were used as the effector cells. Effector cells were cultured along with 1,000 ^{51}Cr-labeled target cells at several different effector: target (E: T) ratios in a 96-well U-bottom microtiter plate in a total of 200 μl volume per well. Target cells including PR8 virus-infected lung epithelium cell, NCI-H2405, and K562 were labeled with ^{51}Cr for one hour. The plate was centrifuged at 1200 rpm for 30 sec before incubating at 37°C for 4 hours. At the end of incubation, the plate was first centrifuged at 1200 rpm for 7 minutes. Fifty μl of supernatant from each well was harvested and mixed with 150 μl of scintillation fluid (Perkin Elmer) and then measured on a beta counter (Perkin Elmer). The spontaneous release was determined from targeting cells incubating with medium alone and the maximum release was obtained by substituting the effector cells with 1% Triton

X-100. Cytotoxicity was determined by the amount of ^{51}Cr released by the target cells, and the specific lysis was calculated as: [(experimental cpm)-(spontaneous release cpm)]/[(maximum release cpm)-(spontaneous release cpm)] x100 percentage.

CHAPTER FOUR

Results

Mobilization and Activation of Human Dendritic Cells in the Lung upon Influenza Virus Infection

To understand the immune response in humanized mice to influenza viruses, we first analyzed influenza infectivity in humanized mice and the innate immune response to influenza virus infection. Since DCs are the key players in antigen presentation to T cells, we studied the activation and migration of DCs in response to influenza virus infection.

Construction of Humanized Mice

Humanized mice were generated by transplanting NOD-SCID-$\beta_2m^{-/-}$ mice with G-CSF mobilized adult $CD34^+$ HPCs (Fig. 6a). To reconstitute the mice with human T cells, we first analyzed the distribution of human T cells upon adoptive T cells transfer through different routes of injection. Humanized mice were given $30x10^6$ of total T cells intravenously (i.v.), intraperitoneally (i.p.) or subcutaneously (s.c.). T cells were labeled with 1 μM of CFSE, a fluorescence dye diluted along with cell division. After three days, the distribution of human T cells was analyzed in the bone marrow, spleen, and lymph nodes by flow cytometry (Fig. 6b). Human T cells were found in the spleen with either i.v. or i.p. injection. With i.v. or s.c. injection, human T cells could migrate efficiently to lymph nodes. When we looked at the CFSE intensity of T cells in the spleen and lymph node with i.v. injection of T cells, only a minor fraction of cells lost CFSE intensity, indicating cell division (Fig. 6c). Overall, this demonstrated that human

T cells could travel via blood and lymphatic systems in humanized mice and extravasate through high endothelial cells into lymph nodes.

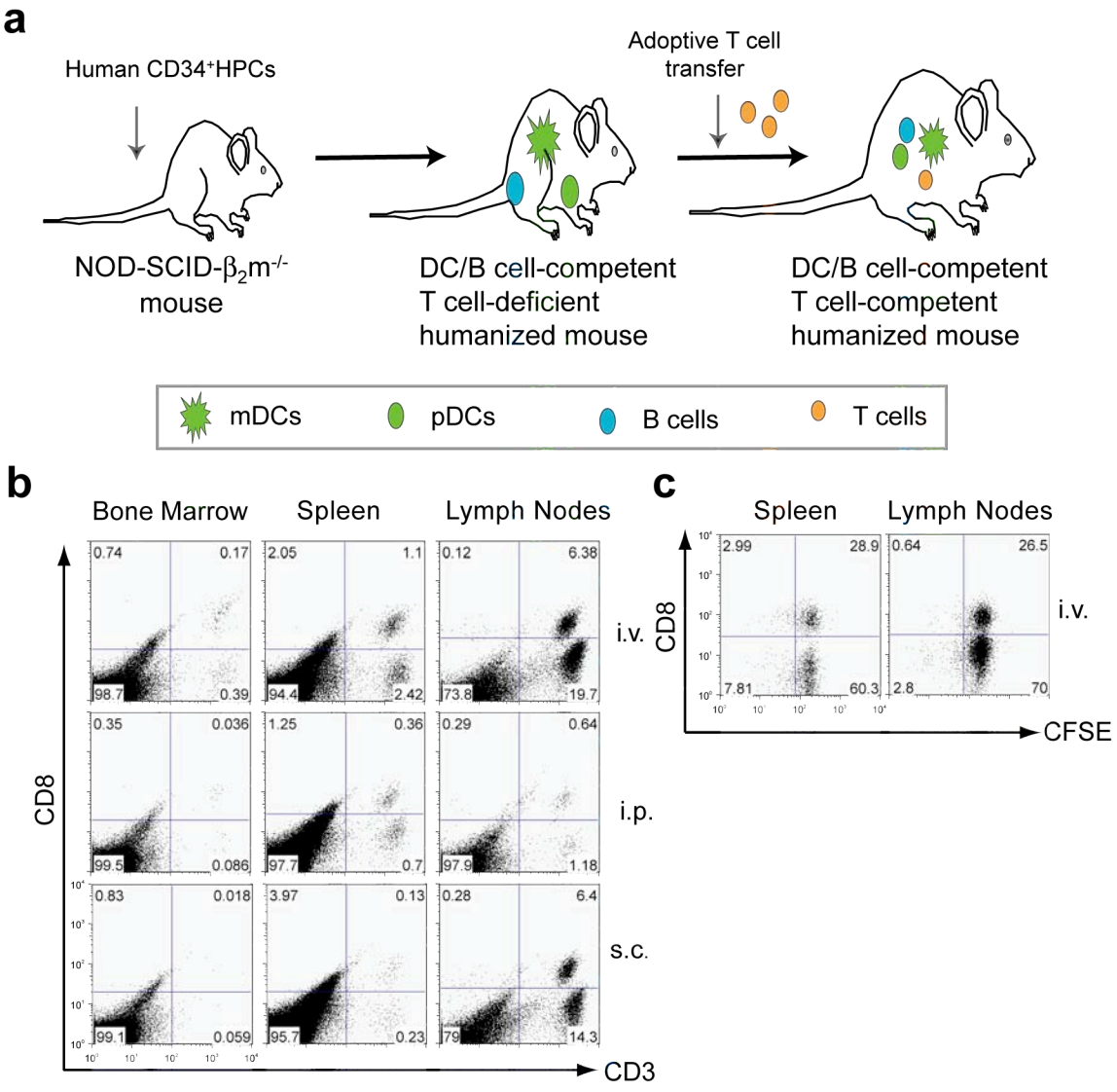

Figure 6. The construction of humanized mice. (a) The process of making the humanized mouse. (b) Total human T cells from PBMCs of $CD34^-$ fraction were isolated, labeled with 1 μM of CFSE, and given to humanized mice at 8 weeks post $CD34^+$ HPCs transplant. After three days, mice were analyzed for the distribution of human T cells in lymphoid organs including bone marrow, spleen and lymph nodes. (b) Intravenously injected T cells were analyzed for CFSE intensity.

Human Dendritic Cells in Humanized Mice

From 4 weeks on, human DCs were repopulated various tissues. Human APCs identified by HLA-DR expression were detected throughout the whole body of mouse (Fig. 7a). In the bone marrow and spleen, HLA-DR^+ cells without κ or λ light chain (B cell marker) expression were identified with dendritic morphology thus considering as human DCs (Fig. 7b and c). pDCs with HLA-DR and CD123 expression were found in the spleen (Fig. 7d). Flow cytometry analysis confirmed the presence of LIN^-HLA-DR^+CD11c^+ mDCs and LIN^-HLA-DR^+CD123^+ pDCs in the bone marrow and spleen (data not shown). Thus, human DCs could be detected in the bone marrow and in the peripheral lymphoid tissues. DCs were also identified in peripheral non-lymphoid tissues. For example, Langerhans cells with the expression of HLA-DR and CD207 were identified in the skin (Fig. 7e). Overall, human DCs repopulated in lymphoid organs and peripheral tissues of humanized mice.

Influenza A Virus Infection in Humanized Mice

Humanized mice were inoculated with influenza A virus (PR8 virus) at 8 weeks post HPCs transplant. Mice were given intranasally (i.n.) different amounts of PR8 virus, or allantoic fluid as control, and analyzed at 20 hours post inoculation (Fig 8a). The respiratory tract including the nose, trachea, and lungs were collected and the infection was determined using immunofluorescence staining for influenza virus NP. When compared to both untreated and allantoic fluid-treated mice, intracellular NP staining was observed in the lung of humanized mice administered as low as 10^4 pfu of PR8 virus (Fig. 8b). At this early time point, influenza virus infection was restricted to respiratory tract with limited infection in the lung alveoli. Mice challenged with 10^4 pfu of PR8

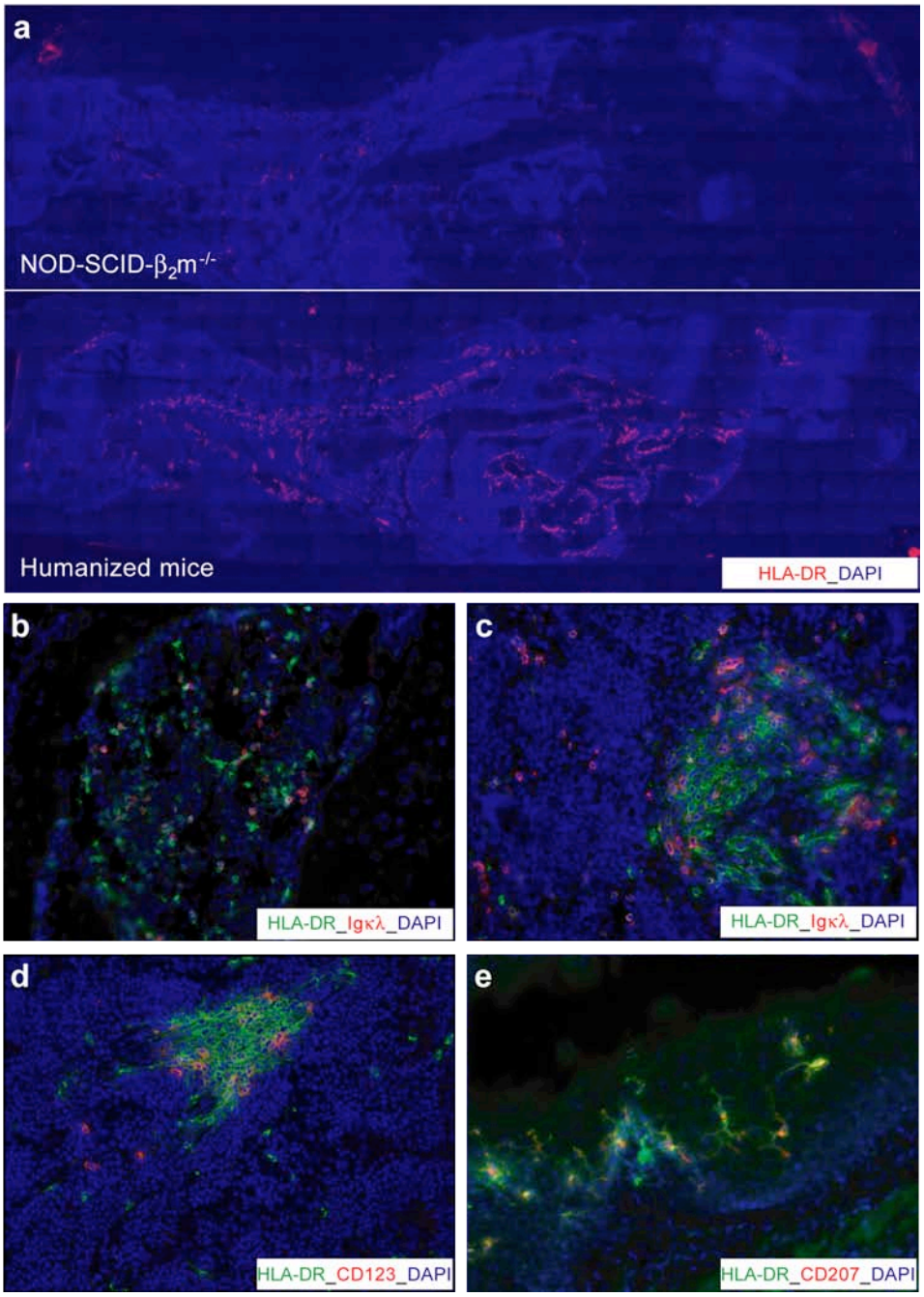

Figure 7. Identification of human DCs in humanized mice. (a) Human DCs were analyzed by immunofluorescence staining. Longitudinal whole body sections of humanized mouse and NOD-SCID-$\beta_2m^{-/-}$ mouse were stained for HLA-DR (red) and DAPI (blue). (b) Bone marrow and (c) spleen section were stained for HLA-DR (green), Ig κ and λ light chains (red) and DAPI (blue). (d) Human pDCs in the spleen were identified by anti-HLA-DR (green), anti-CD123 (red) and DAPI (blue). (e) Langerhans cells were identified in the skin by anti-HLA-DR (green), anti-CD207 (red) and DAPI (blue). Images were originally obtained at 10x magnification.

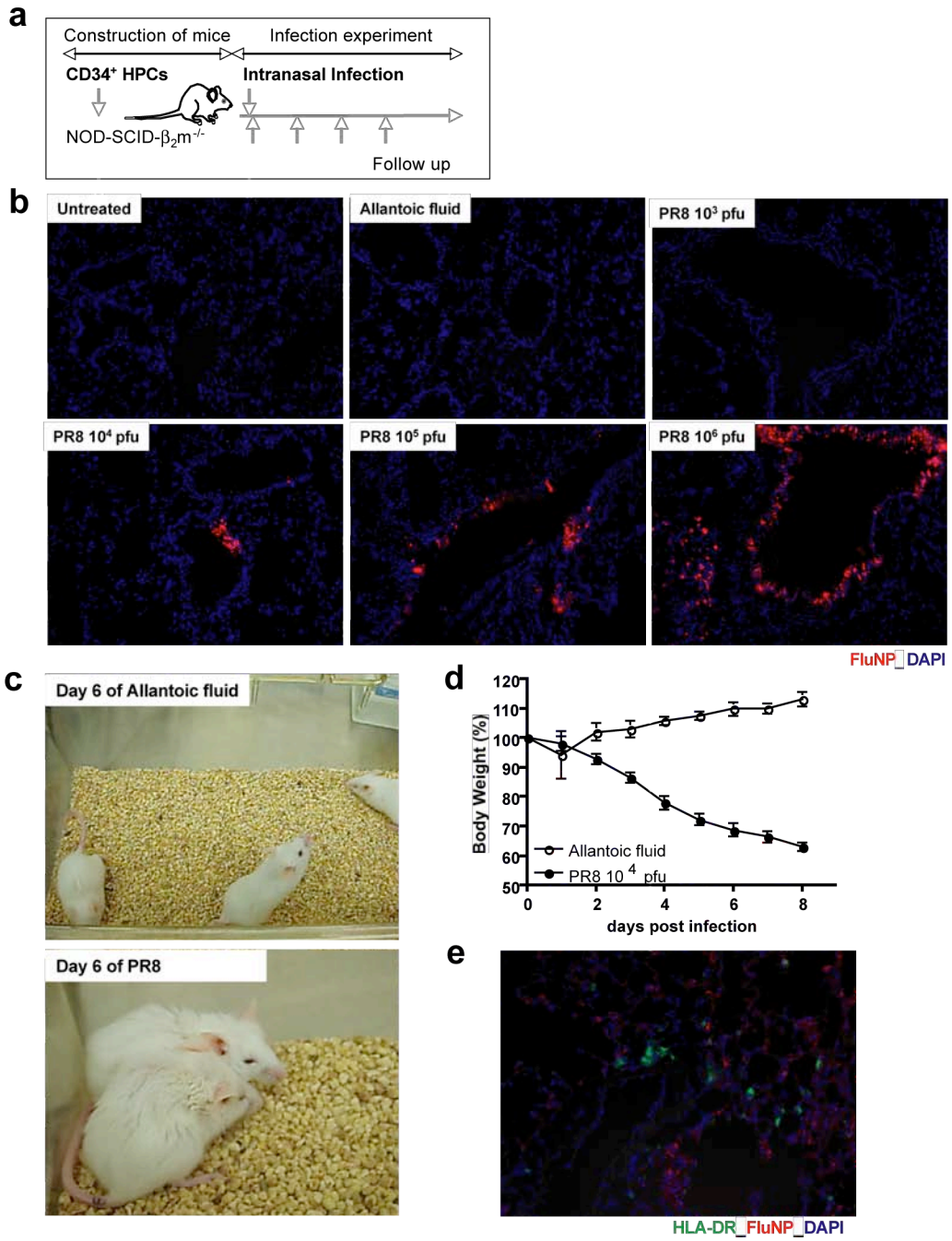

Figure 8. Clinical symptoms of influenza A virus infection in humanized mice. (a) Humanized mice were inoculated with influenza A PR8 virus intranasally. (b) After 20 hours post inoculation, lungs were analyzed for viral infection by immunofluorescence staining. Infected cells were identified by anti-FluNP (red) and DAPI (blue) (c) Humanized mice inoculated with 10^4 pfu of PR8 virus demonstrated symptoms of infection, such as lethargy and (d) body weight loss, and (e) viral replication in the lungs. Cells were identified with anti-HLA-DR (green), anti-FluNP (red) and DAPI (blue). Images were originally obtained at 10x magnification.

virus demonstrated clinical symptoms of infection such as lethargy, loss of body weight, and a widespread infection in lung alveoli (Fig. 8c, d and e). Therefore, an active infection occurs in humanized mice administered influenza virus.

Human Dendritic Cells in the Lung

We found human $CD14^+$ cells, mDCs, and pDCs in the lungs. Lungs from humanized mice at 4 to 12 weeks post HPCs transplant were digested with collagenase D to make single cell suspensions and analyzed by flow cytometry. We found that 5.07±0.58% of cells in the total lung single cell suspension were HLA-ABC^+ human cells. Three types of APCs were identified including $CD14^+$ cell (2.08±0.33%), Lin^- HLA-DR^+CD11c^+ mDCs (1.23±0.14%), and Lin^-HLA-DR^+CD123^+ pDCs (0.22±0.04%; Fig9 a and b). To determine the activation status of human DCs in the lung under steady state, pDCs and mDCs were analyzed for the expression of costimulatory molecules CD80 and CD86. mDCs had low level of CD86 expression and no expression of CD80 whereas pDCs had neither CD80 nor CD86 expression (Fig. 9c). This was consistent with the observation of little or no expression of DC-LAMP in HLA-DR^+ cells in the lung using immunofluorescence staining (data not shown). Thus, in steady state human DCs display immature phenotype.

Activation of Human Dendritic Cells in the Lung upon Influenza Virus Infection

Next, we determined the effect of influenza virus infection on individual human cell subsets in the lung. We compared humanized mice treated with allantoic fluid, 10^4 pfu of PR8 virus, or 10^4pfu of PR8 virus after adoptive T cell transfer. The percentage

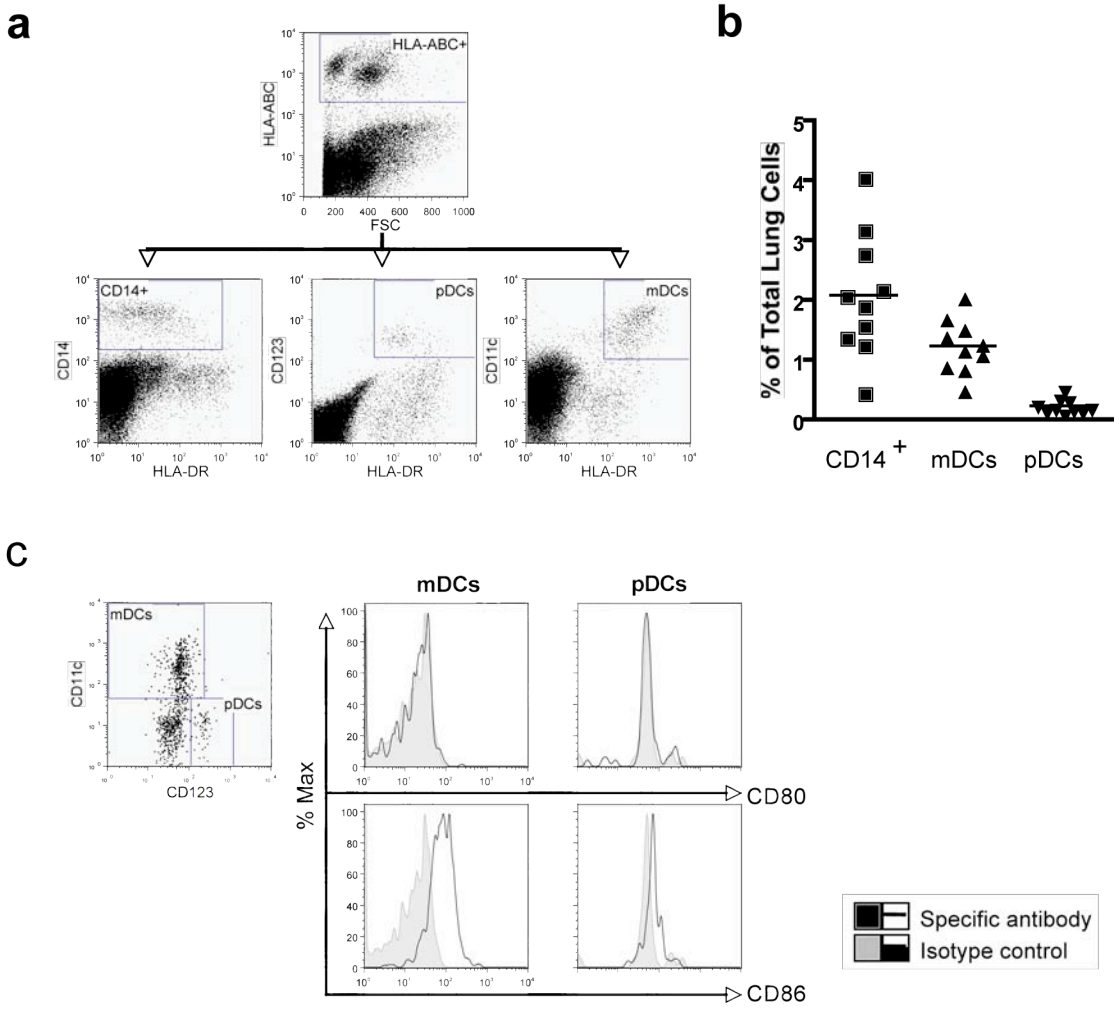

Figure 9. Antigen presenting cells in the lungs of humanized mice. (a) Lung single cell suspensions were analyzed by flow cytometry. Three types of antigen presenting cells including $CD14^+$ cells, $Lin^-HLA\text{-}DR^+CD123^+$ pDCs, and $Lin^-HLA\text{-}DR^+CD11c^+$ mDCs were identified in the lungs of humanized mice. (b) Mean percentage of different cell types in total single cell suspension from lungs (n=10). (c) Human pDCs and mDCs were analyzed for CD80 and CD86 expression. Filled histograms represent isotype controls and open histograms show staining by indicated specific antibodies.

of $CD14^+$ cells was increased after PR8 infection and further increased in mice with human T cells (Fig. 10a). The same trend was also observed in the up-regulation of surface MHC molecules including HLA-ABC and HLA-DR (Fig. 10a). $CD14^+$ cells were not considered as DCs as $CD14^+$ cells isolated from lungs didn't induce allogeneic

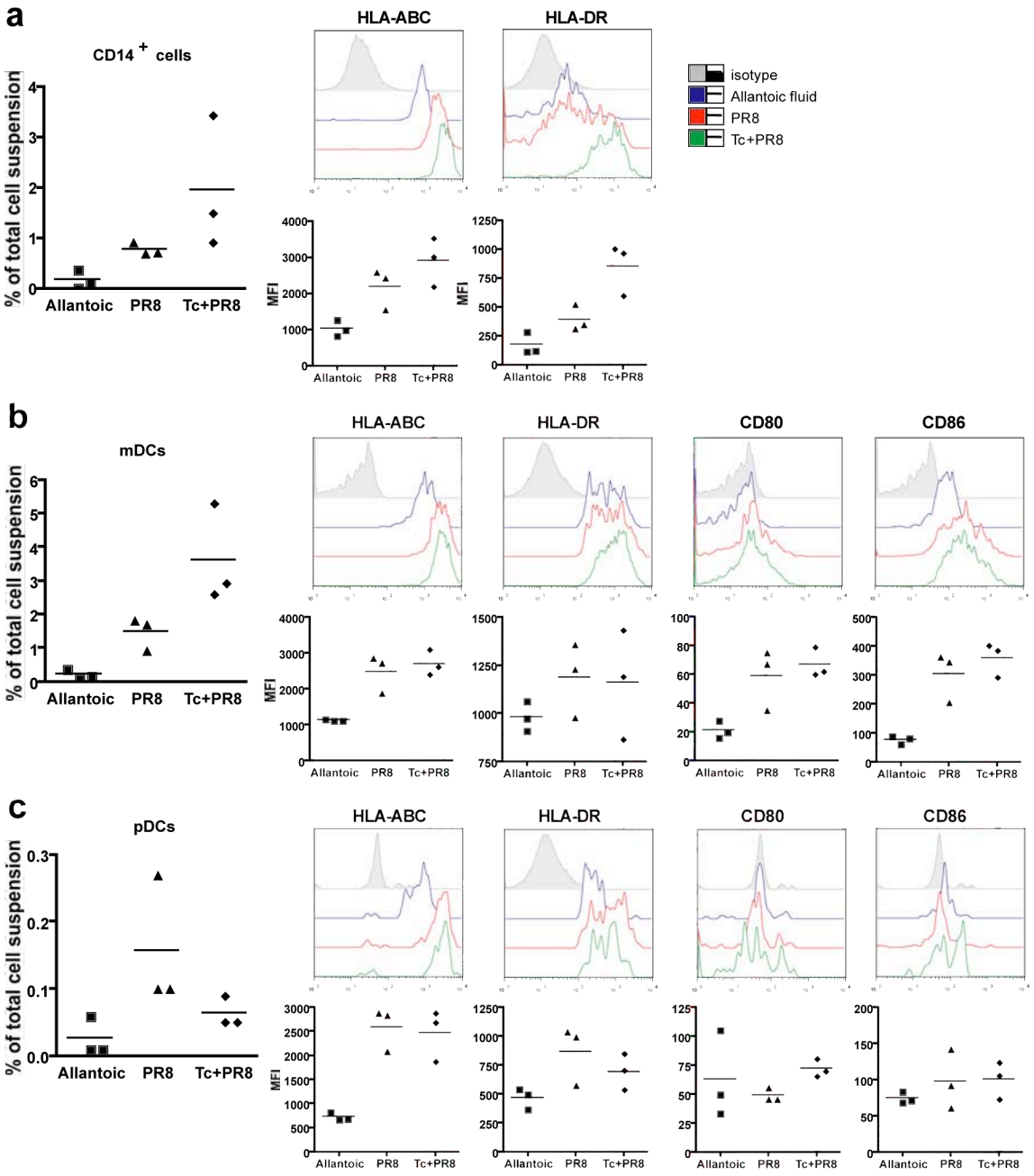

Figure 10. Lung DCs undergo maturation upon influenza virus infection. (a) Humanized mice were treated with allantoic fluid, 10^4 pfu of PR8 virus, or 10^4pfu of PR8 virus after adoptive T cell transfer. At day 8 post infection, single cell suspensions of lungs were analyzed by flow cytometry for the percentage of $CD14^+$ cells in total cell suspension. Human $CD14^+$ cells were analyzed for HLA-ABC and HLA-DR expression. Filled histograms represent isotype controls (grey) and open histograms show staining by indicated specific antibodies in treatment with allantoic fluid (blue), PR8 virus (red), and PR8 virus after adoptive T cell transfer (green). Mean fluorescence intensity (MFI) from three humanized mice per treatment. (b) Human mDCs and (c) pDC were analyzed for the percentage in total lung cell suspension and MFI of specific staining.

lymphocyte proliferation after activation by PR8 virus (data not shown). The percentage of mDCs also increased after PR8 infection and further increased in mice with human T cells. A consistent increase of surface HLA-ABC, CD80 and CD86 was observed on mDCs upon PR8 infection and the up-regulation on HLA-DR to a less extent. The presence of T cells had minimum effect on the maturation of mDCs in the lung (Fig. 10b). The percentage of pDCs also increased after PR8 infection. The expression of HLA-ABC, but not HLA-DR, CD80 and CD86, on pDCs was upregulated in response to PR8 infection (Fig. 10c). Therefore, human DCs in the lung were activated upon influenza virus infection.

Mobilization of Human Dendritic Cells in the Lung upon Influenza Virus Infection

An important characteristic of DCs is their capacity to traffic to local lymph nodes, where adaptive immune responses are initiated. To understand the mobility of human DCs in response to influenza virus infection, we analyzed the mediastinal lymph nodes of mice at different time points post PR8 virus infection including 6 hours, 20 hours, 3 days, and 8 days. Matured DCs were identified by co-localization of HLA-DR and DC-LAMP by immunofluorescence staining (Fig. 11a). At early time points, 6 hours and 20 hours post infection, there were no differences between mice treated with allantoic fluid and PR8 virus. The increased numbers of matured DCs in mediastinal lymph nodes were observed at day 3 and day 8 post PR8 virus inoculation (Fig. 11b and c). The presence or absence of T cells did not affect the influx of matured DCs in mediastinal lymph nodes at 8 days post infection.

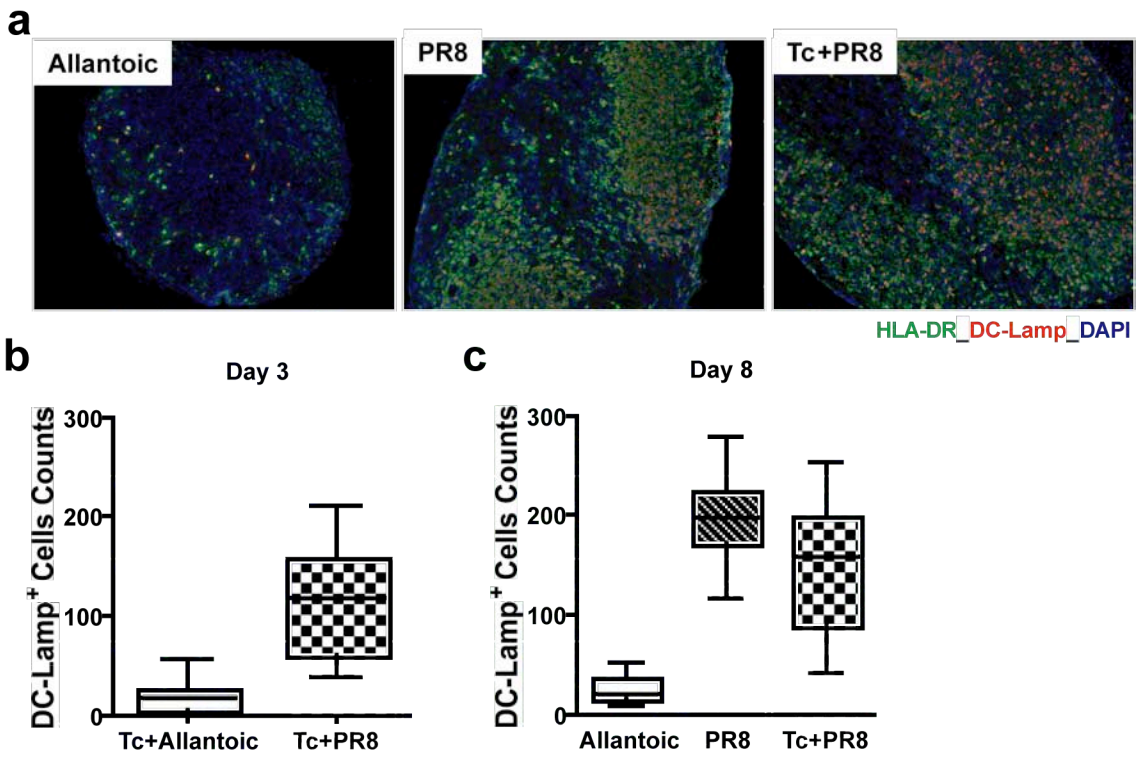

Figure 11. Mature DCs accumulate in mediastinal lymph nodes upon influenza virus infection. (a) Mice were treated with allanotic fluid, 10^4 pfu of PR8 virus, or 10^4pfu of PR8 virus after adoptive T cell transfer. At day 8 post infection, mediastinal lymph nodes were analyzed by immunofluorescence staining for the distribution of human DCs. Mature human DCs were identified by anti-HLA-DR (green), anti-DC-LAMP (red) and DAPI (blue). Images were originally obtained at 10x magnification. (b) At day 3 and (c) day 8 post infection, mediastinal lymph nodes were analyzed by immunofluorescence staining for the quantification of human DCs. Mature human DCs (DC-LAMP$^+$) were counted from a field of 20x magnification. Ten fields of each mediastinal lymph nodes and three mice per condition were analyzed.

In conclusion, humanized mice demonstrated clinical symptoms upon influenza infection. Human cells secreted high amounts of type I interferon in response to influenza virus infection (data not shown). During the infection, there was an increase in the numbers of DCs in the lung. Human DCs in the lung were activated. Concomitantly, an increase amount of human mature DCs were found in the draining mediastinal lymph nodes.

Mice Vaccinated with Ex Vivo-Generated DC Generate Influenza Virus-Specific Humoral Immunity

Humanized Mice Vaccinated with Ex Vivo-Generated DCs Loaded with Influenza Virus Generate Virus Binding Igs

To probe the functionality of the B cell compartment in humanized mice, we first analyzed whether humanized mice could generate influenza-specific antibodies upon vaccination with *ex vivo*-generated DCs. Humanized mice were reconstituted at 8-12 weeks post $CD34^+$ HPCs transplant with $10x10^6$ purified (>95%) autologous total $CD4^+$ T cells (i.p.). Then, mice were vaccinated twice at weekly interval by i.p. injection of $2x10^6$ *ex vivo*-generated DCs that were loaded with heat-inactivated (HI) PR8 virus and activated with TNF-α and CD40L (Fig. 12a). The same DCs pulsed with HI-PR8 virus were able to induce autologous $CD4^+$ T cells proliferation *in vitro* (Fig. 12 b). Vaccinated mice were bled at baseline and multiple time points post vaccination to determine influenza-specific responses (Fig. 13a). Influenza virus-specific antibodies were measured by ELISA coated with HI-PR8 virus and the amounts of PR8-specific antibody were represented as arbitrary units (AU) relative to the detection level in a pool of human AB serum. At baseline, PR8-specific IgM and IgG levels were below detection threshold (Fig. 13b and e). At day 7 post DC vaccination, influenza-specific IgM could be detected and increased considerably after boosting vaccination (Fig. 13b and c, n=3 mice from the same cohort). Elicited IgM could be detected in the serum for at least 3 weeks post vaccination (Fig. 13b). Specific IgM titers could be generated in several mice from different cohorts (mean AU ± SEM= 115 ± 39 at day 7, 4181 ± 1022 at day 14-17, and 3738 ± 1470 at day 19-21; Fig. 13d and Table 2).

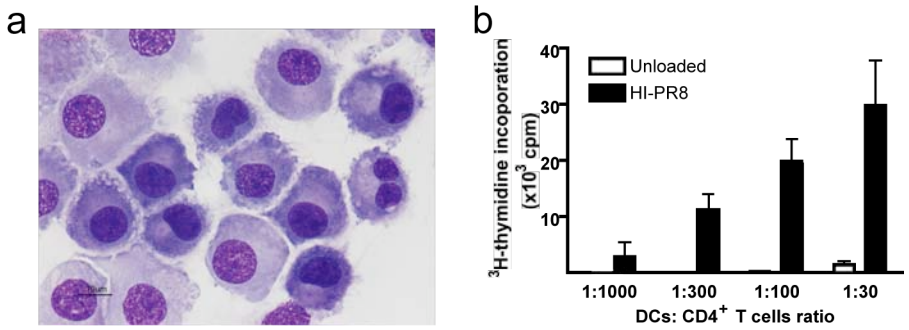

Figure 12. *Ex vivo*-generated DCs pulsed with heat-inactivated influenza virus. (a) DCs were derived from monocyte culture with GM-CSF and IL-4 for 5 days and pulsed with heat-inactivated PR8 virus. The dendritic morphology was revealed by Giemsa staining. (b) Different numbers of DCs were cocultured with autologous $CD4^+$ T cells for 5 days and the cultures were pulsed with ^{3}H-thymidine for the last 16 hours to measure T cell proliferation.

An important question was whether humanized mice were able to mount responses in other Ig subclasses. At day 14 post vaccination, mice generated PR8-specfic IgG which was enhanced with time (Fig. 13e and f). These results were reproducible using mice from different cohorts generated with cells from different donors (mean AU ± SEM= 1.5 ± 0.5 at day 7, 58 ± 16 at day 14-17, and 90 ± 42 at day 19-21; Fig. 13d and Table 2). Serum levels of influenza-binding Igs increased parallel to the increased amount of total human Igs (Table 2). We did not detect influenza-specific IgA at the indicated time points despite the presence of total IgA in the serum (data not shown). Thus, humanized mice vaccinated with *ex vivo*-generated DCs loaded with HI-PR8 virus can generate virus binding IgM and IgG.

Humanized Mice Vaccinated with Ex Vivo-Generated DCs Loaded with Influenza Virus Show Plasma Cell Differentiation

Specific antibody production was associated with the presence of human immune cell clusters in the spleen. Immunofluorescence staining on frozen tissue sections permitted us to detect infiltrates of human cells composed of large clusters of $HLA\text{-}DR^+$

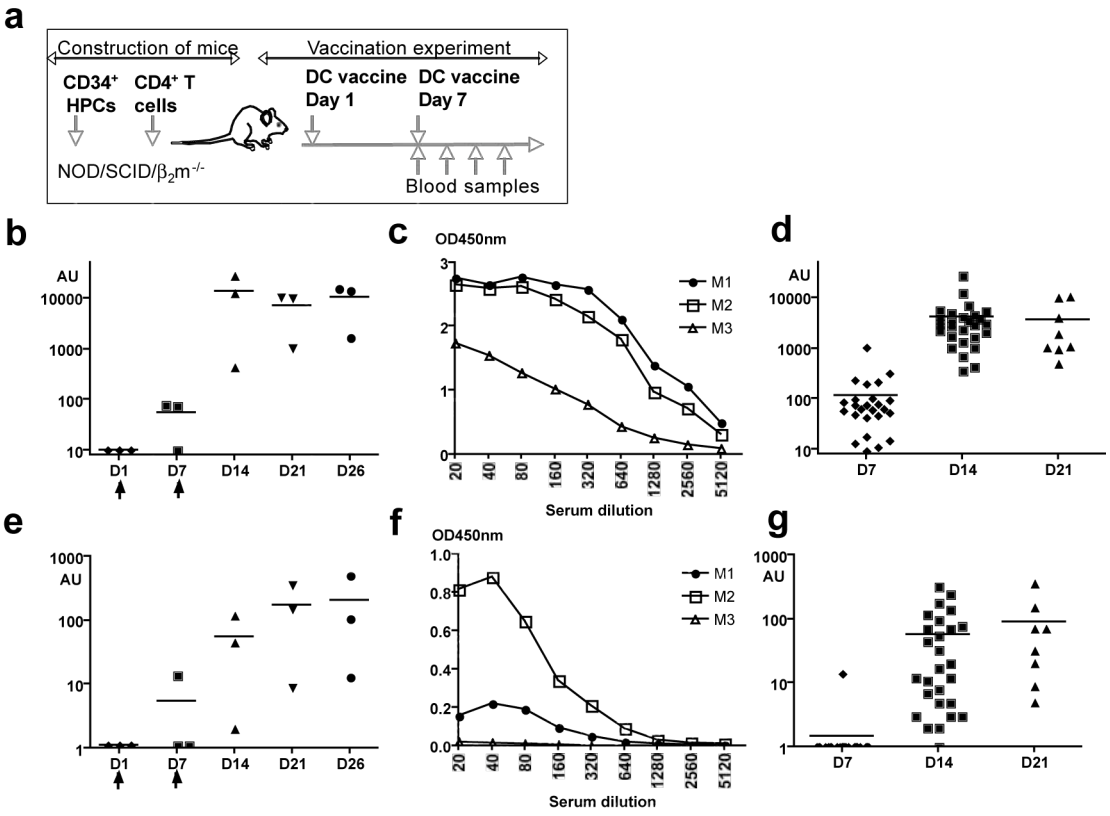

Figure 13. Humanized mice vaccinated with heat-inactivated influenza virus-pulsed DCs generate specific antibody response. (a) Vaccination and assessment scheme. Humanized mice were reconstituted with $CD4^+$ T cells and then vaccinated with HI-PR8 virus-pulsed DCs i.p. at day 1 and day 7. Blood samples were taken prior and post vaccination. (b) PR8 virus-specific IgM in the serum was measured by ELISA and enumerated with arbitrary units. (c) Influenza virus-specific IgM in the serum was titrated by ELISA. (d) Data from six experiments and two different donors. (e) Influenza virus-specific IgG in the serum was measured by ELISA. (f) PR8 virus-specific IgG in the serum was titrated by ELISA. (g) Data from six experiments and two different donors. Each point represents one measurement in vaccinated mouse at indicated time point.

Table 2. Antibody titers in the serum of humanized mice vaccinated with *ex vivo*-generated DCs.

		Reference human serum	Serum (days post vaccination)			
			D0	D7	D14	D21
PR8-binding antibody (AU)	IgM	1000	20±3 (n=3)	116±39 (n=27)	4181±1022 (n=27)	3738±1470 (n=8)
	IgG	100000	1 (n=3)	1.5±0.5 (n=27)	58±16 (n=27)	90±42 (n=8)
Total antibody (μg/ml)	IgM	136	14.84±2.06 (n=8)	22.88±4.67 (n=10)	446.3±12.5 (n=10)	389.6±36.2 (n=10)
	IgG	2643	0 (n-8)	0 (n=10)	15.76±2.45 (n=10)	44.98±9.53 (n=10)

cells surrounded by and partially intertwined with $CD3^+$ T cells (Fig. 14a). The clusters contained DC-LAMP expressing DCs and cells with high intensity IgG staining. While most of B cells in the spleen of non-vaccinated mice were naïve with the phenotype of $IgD^+CD20^+CD27^-$ (Fig. 14b), single cell suspensions prepared from spleens at day 14 after vaccination showed the presence of $CD19^{low}CD138^+$ cells by flow cytometry (Fig. 14c). Plasma cell differentiation was further confirmed by the presence of $CD27^+CD20^{low}$ cells (Fig. 14c). These results demonstrated that humanized mice permit "ménage a trios", i.e., gathering of the three key cells needed for generation of humoral immunity, i.e., DCs, T cells and B cells.

Humanized Mice Vaccinated with Ex Vivo-Generated DCs Loaded with Influenza Virus Generate Specific Neutralizing Antibodies

To determine whether generated antibodies were protective, we have first used hemagglutination inhibition (HAI) assay. There, HAI titer for each sample is reciprocal of the greatest dilution which completely inhibits the agglutination of chicken red blood cells. HAI titer was present in 20/26 mice, from six independent experiments, tested at day 14-17 and 8/10 mice tested at day 19-21 (Fig. 15a). Next, we tested whether sera of vaccinated humanized mice could actually prevent the infection of lung epithelial cells. NCI-H2405 cells were grown to confluence and exposed to live PR8 virus. Influenza virus infection and replication were determined by immunofluorescence staining of influenza virus NP at 24 hours post viral exposure (Fig. 15b). To determine the protection, the presence of influenza NP staining was analyzed in lung epithelial cells exposed to PR8 virus, which were pre-incubated for 30 minutes with sera from vaccinated mice at 1/5 dilution. This resulted in the total absence of influenza NP

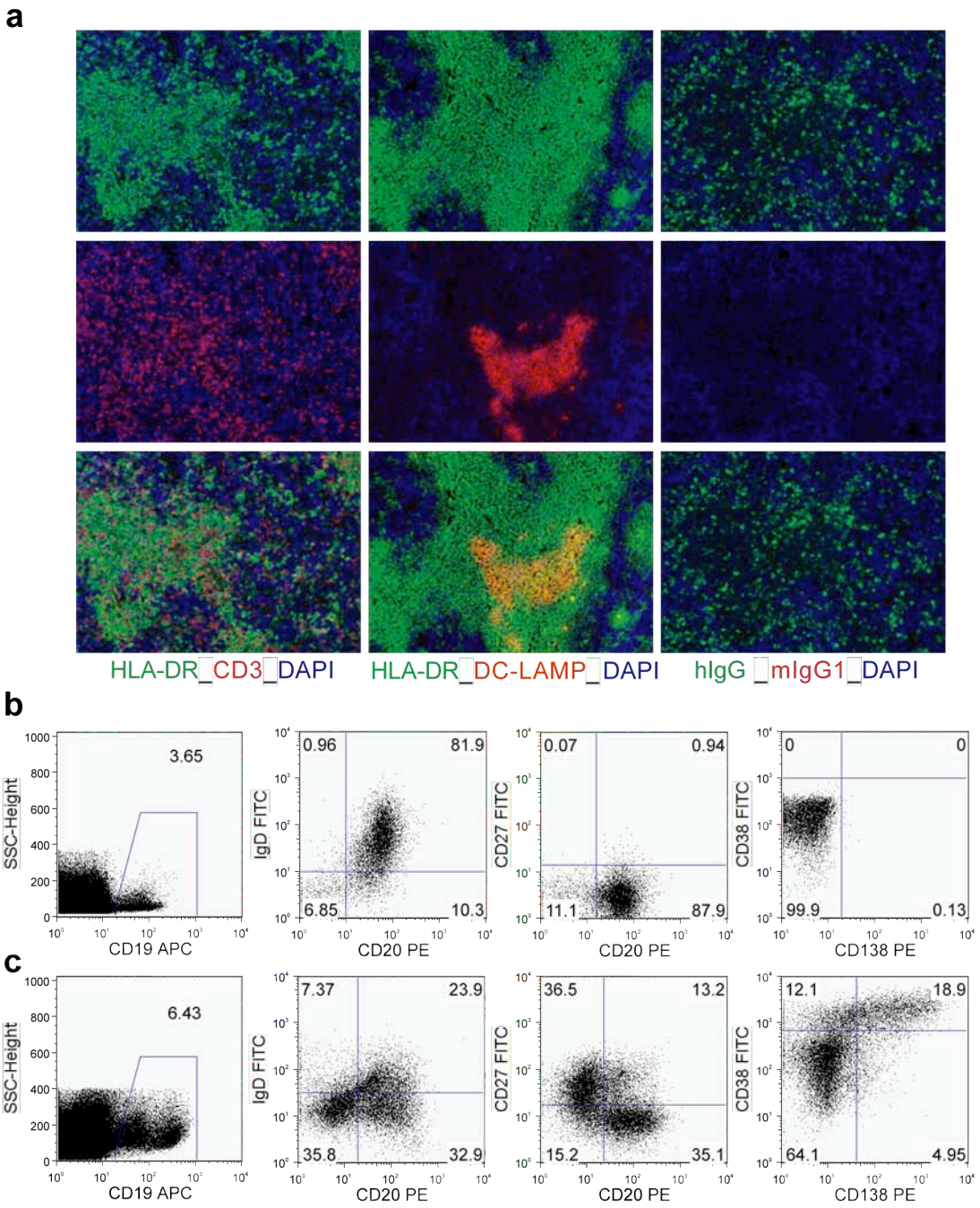

Figure 14. Plasma cell differentiation in the spleen of humanized mice upon vaccination. (a) Humanized mice were vaccinated with *ex vivo*-generated DCs pulsed with HI-PR8 virus. Human lymphoid structures in the spleen were analyzed by immunofluorescence staining. Human cells were identified by anti-HLA-DR (green; left and middle), anti-CD3 (red; left), anti-DC-LAMP (red; middle), anti-human IgG (greed; right), mouse IgG1 isotype control (red; right) and DAPI (blue). Images were originally obtained at 10x magnification. (c) Single cell suspensions from spleen of unvaccinated mice and (d) vaccinated mice were analyzed by flow cytometry. $CD19^{+}$ human B cells were gated and the expression of CD20, CD27, CD38, CD138 and IgD were analyzed.

staining in lung cells suggesting the lack of productive infection (Fig. 15b). After incubating the virus with vaccinated serum, the virus lost the capability to infect NCI-H2405 demonstrating the presence of neutralizing antibody in the serum from vaccinated mice. Thus, vaccination with *ex vivo*-generated DCs led to the generation of specific antibody capable of neutralizing influenza virus *in vitro*.

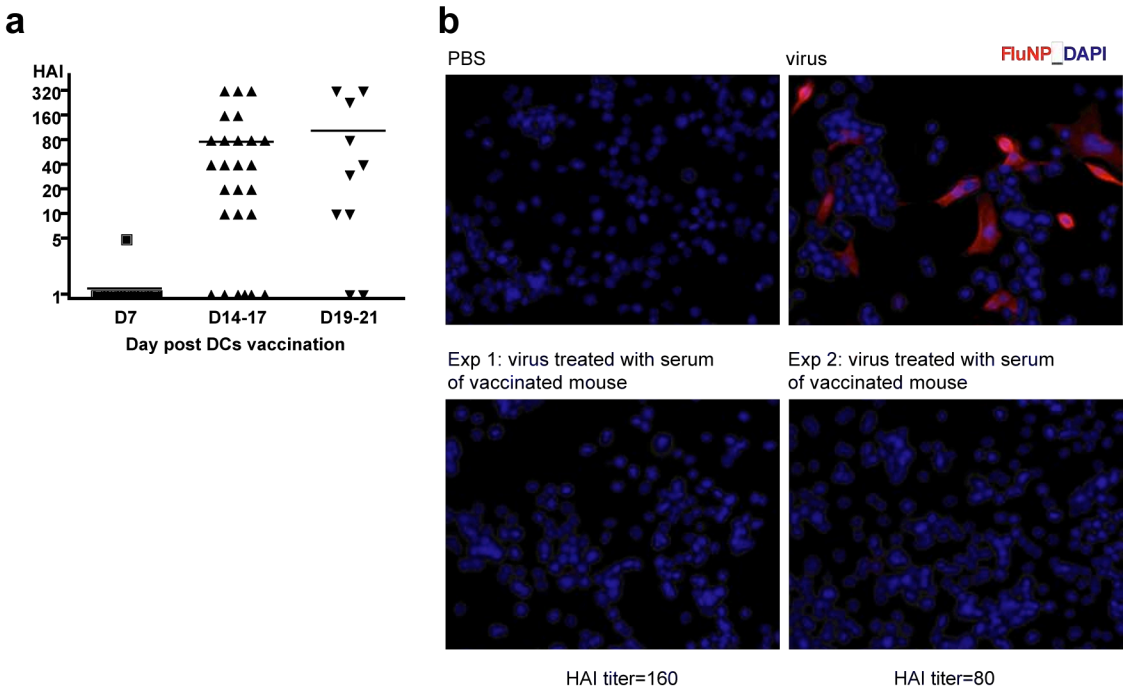

Figure 15. Influenza virus-specific neutralizing antibody in the serum of vaccinated mice. (a) Specific antibodies capable of inhibiting virus-mediated hemagglutination of CRBC were measured in the serum of vaccinated mice at indicated time points post vaccination. Scatter plot showed mean HAI titer in logarithmic scale from 6 different experiments and two independent donors. (b) *In vitro* inhibition of infection assay. Vaccinated serum (1/5 dilution) was mixed with 200 pfu of PR8 virus for 30 minutes before adding to NCI-H2405, a human lung cell line sensitive to influenza virus infection. After 24 hours of culture, influenza virus infection was identified by anti-FluNP (red) and DAPI (blue). NCI-H2405 treated with PBS showed no FluNP staining. NCI-H2405 treated with influenza virus showed FluNP staining. NCI-H2405 treated with the mixture of influenza virus and diluted serum with HAI titer of 160 showed no FluNP staining. In another experiment, NCI-H2405 treated with the mixture of influenza virus and diluted serum with HAI titer of 80 showed no FluNP staining. Images were originally obtained at 20x magnification.

T Cell-Dependent Neutralizing IgM

To understand the nature of specific antibody generated in humanized mice vaccinated with *ex vivo*-generated DCs pulsed with HI-PR8 virus, we first asked the question if specific antibody was dependent on T cells. Humanized mice were vaccinated in the presence or absence of human $CD4^+$ T cells. We found that the generation of specific antibody was dependent on the reconstitution of $CD4^+$ T cells and sera from humanized mice vaccinated in the absence of $CD4^+$ T cells (T-cell deficient humanized mice) did not show HAI activity (Fig. 16a and b). To test which subclasses of human Ig were contributing to the HAI activity, human IgM was depleted from vaccinated serum. In 5/6 tested humanized mice, the depletion of human IgM resulted in the disappearance of HAI activity (Fig. 16c). Thus, we conclude that humanized mice vaccinated via DCs can generate a T-cell dependent IgM capable of neutralizing influenza virus *in vitro*.

Serum from Vaccinated Humanized Mice Confers Passive Protection in vivo

The ultimate test for the efficacy of generated antibody was its capacity to protect mice *in vivo* from infection and from influenza virus induced death. To assess that, we used as parameters i) clinical symptoms such as body weight and survival of NOD-SCID $-\beta_2m^{-/-}$ mice inoculated with live PR8 virus through intranasal delivery, and ii) viral titers in the lung. We tested serum from vaccinated humanized mice without T cells (T cell-deficient, no HAI titer) and serum from vaccinated humanized mice with T cells (T cell-competent, positive HAI titer). First, live PR8 virus was pre-incubated with respective serum and used to inoculate NOD-SCID-$\beta_2m^{-/-}$ mice (Fig. 17a). When serum from vaccinated T cell-deficient humanized mice was used, NOD-SCID-$\beta_2m^{-/-}$ mice become progressively sick, lost weight and succumbed to influenza virus infection. In contrary,

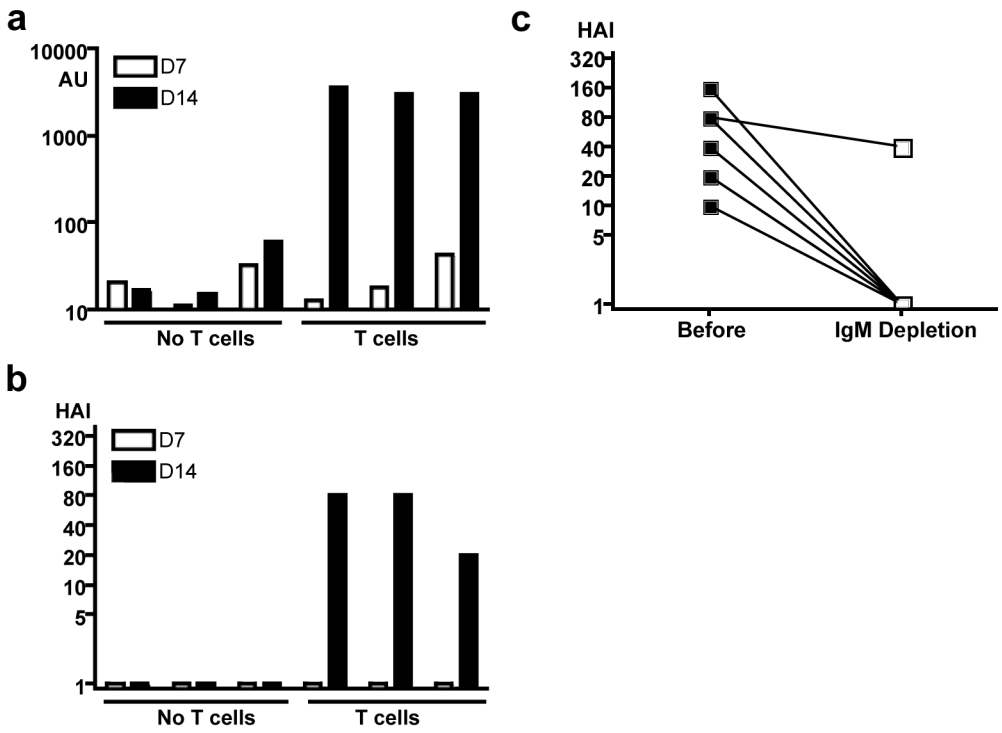

Figure 16. T cell-dependent neutralizing IgM. (a) Mice were vaccinated with *ex vivo*-generated DCs loaded with HI-PR8 virus. To test the dependence of $CD4^+$ T cells in the generation of specific antibody, DC vaccines were given to mice with or without T cell transfer prior to the vaccination. The specific IgM was measured in ELISA using PR8 virus. Each bar represents specific-IgM (AU) at indicated time point post vaccination from one mouse. (b) The neutralizing antibody titers were measured in the serum using HAI assay. Each bar represents HAI titer at indicated time point post vaccination from one mouse. (c) To test if human IgM contributing to the HAI activity, human IgM was depleted from vaccinated serum. HAI titer was measured in the same serum before and after IgM depletion. Each line represents HAI titer in the serum from one mouse before and after IgM depletion (n=6).

when serum from vaccinated T cell-competent humanized mice was used, NOD-SCID-$\beta_2m^{-/-}$ mice did not lose weight and remained healthy (Fig. 17b). Accordingly, there was no detectable titer of influenza virus in lung homogenate (Fig. 17c). Thus, pre-treatment of virus prevented infection. Next, we pre-treated NOD-SCID-$\beta_2m^{-/-}$ mice by intranasal delivery of serum followed by the inoculation of live PR8 virus (Fig. 17d). NOD-SCID-$\beta_2m^{-/-}$ mice pre-treated with serum from vaccinated T cell-competent humanized mice were completely protected from infection as measured by the lack of body weight loss

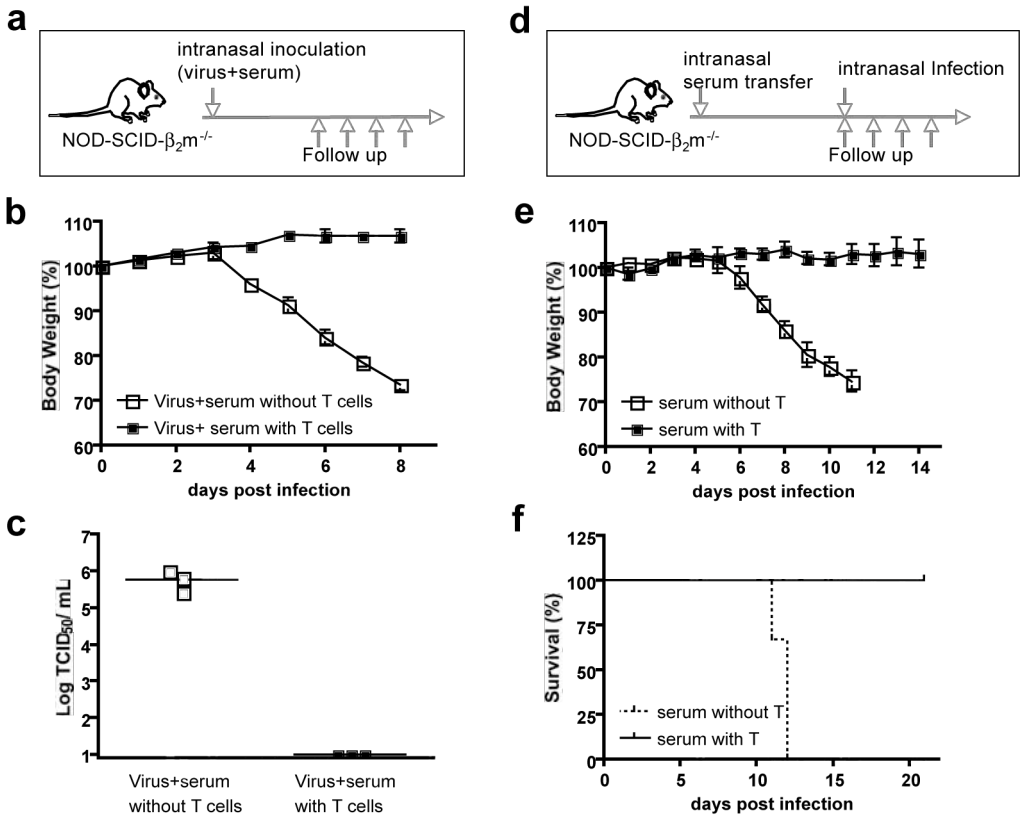

Figure 17. Serum of vaccinated mice prevents infection *in vivo* in passive protection experiments. (a) NOD-SCID-$\beta_2m^{-/-}$ mice were inoculated intranasally with 10^2 pfu of PR8 virus that was treated with serum from vaccinated humanized mice (with or without T cells; see Figure 16a and b). (b) After inoculation, the body weights were taken daily to monitor the disease burden (n=3 per group; abscissa: days post infection; ordinate: % of body weight). (c) The lungs were harvested at 8 days post inoculation to measure total viral load by $TCID_{50}$ using human NCI-H2405 lung cell line (abscissa: treatment groups; ordinate: log $TCID_{50}$/ ml). (d) NOD-SCID-$\beta_2m^{-/-}$ mice were transferred intranasally with 50 µl of serum from vaccinated humanized mice (with or without T cells; see Figure 12a and b). After 30 minutes, mice were then inoculated intranasally with 10^2 pfu of PR8 virus. (e) The body weights and survival (f) were followed daily (abscissa: days post infection; ordinate: % of survival).

and by unaltered survival (Fig. 17e and f). Thus, humanized mice vaccinated with influenza antigen-loaded *ex vivo* generated DCs produce influenza-specific human antibody that can passively protect mice from influenza virus infection.

Mice Vaccinated with Influenza Vaccine Generate Influenza Virus-Specific Humoral Immunity

The next question was the capacity of endogenous human DCs in presenting MHC class II antigens to $CD4^+$ T cells and the role of $CD4^+$ T cells in the induction of influenza-virus specific antibody response. We approached the MHC class II presentation of endogenous DCs to $CD4^+$ T cells by measuring the specific antibody production in humanized mice upon vaccination with LAIV. The quality of $CD4^+$ T cells help could influence the antibody response. Through vaccinating humanized mice with different subsets of $CD4^+$ T cells, we could dissect the $CD4^+$ T cells compartments to understand better how $CD4^+$ T cells help the antibody response.

Specific Antibody Response in Humanized Mice Vaccinated with LAIV

At 8-12 weeks post $CD34^+$ HPCs transplant, humanized mice were received Flt-3L for 10 days to mobilize DCs and followed by i.p. reconstitution of $10x10^6$ purified total $CD4^+$ T cells. Humanized mice were then vaccinated with 100 μl of LAIV either delivered i.p./ i.v. with or without additional intranasal delivery. At day 14 post vaccination, humanized mice demonstrated serum titers of PR8 virus binding IgM (Fig. 18). Of note, this is a cross-reactive antibody as 2006-2007 season contains New Caledonia H1N1 virus and the ELISA measures antibody against PR8 virus.

Central Memory $CD4^+$ T Cells in the Generation of Specific Antibody Response

Humanized mice were reconstituted with either total $CD4^+$ T cells or with their sorted subsets, i.e. central memory $CD4^+CD27^+CD45RA^-$ T cells or effector memory $CD4^+CD27^-CD45RA^-$ T cells (Fig 19a). In contrast to effector memory $CD4^+$ T cells, central memory $CD4^+$ T cells included a population of cells expressing CXCR5, a

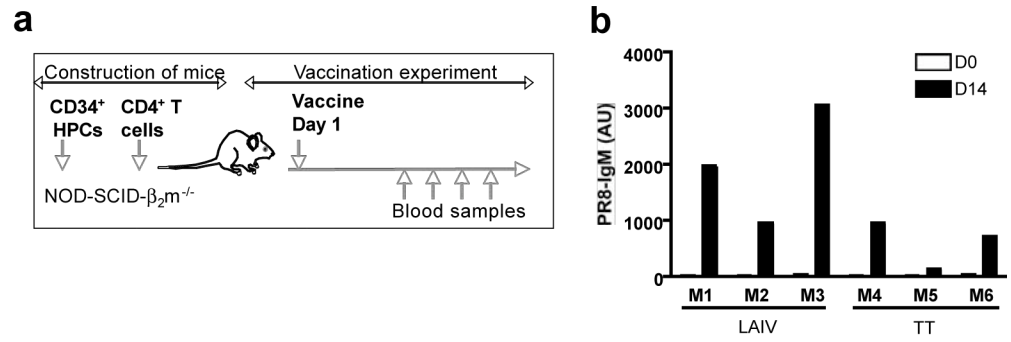

Figure 18. Mice vaccinated with LAIV generate influenza virus-specific IgM in the serum. (a) Mice were adoptively transferred with total $CD4^+$ T cells and then vaccinated with LAIV i.p./ i.v. or TT i.p. at day 1. (b) Influenza virus-specific IgM in the serum at day 14 post vaccination was measured by ELISA using PR8 virus. Each bar represents specific IgM (AU) at indicated time point post vaccination from one mouse (abscissa: treatment groups; ordinate: PR8-specific IgM).

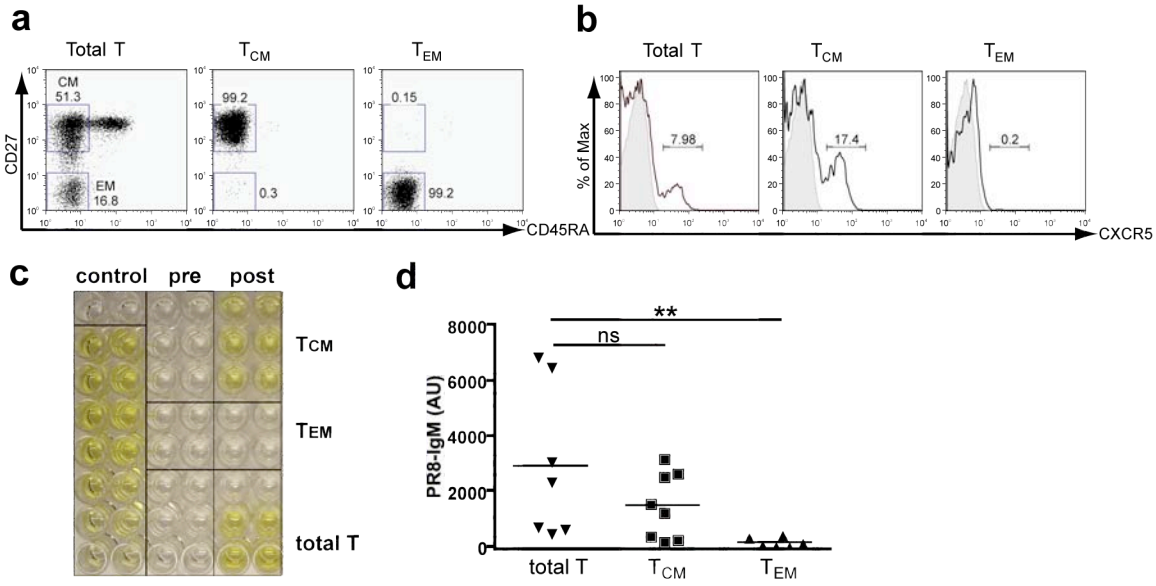

Figure 19. The generation of influenza virus-specific IgM in LAIV vaccinated mice is dependent on central memory $CD4^+$ T cells. (a) Total $CD4^+$ T cells were purified, and central memory (T_{CM}) and effector memory (T_{EM}) $CD4^+$ T cells were furthered FACS sorted based on the expression of CD45RA and CD27. (b) Subsets of $CD4^+$ T cell were analyzed for CXCR5 expression (grey: isotypic antibody; black: CXCR5 antibody). (c) Mice were adoptively transferred with total or subsets of $CD4^+$ T cells and then vaccinated with LAIV i.p./ i.v. at day 1. Influenza virus-specific IgM in the sera at pre- and post-vaccination was measured by ELISA using PR8 virus. (d) Data were from three independent experiments with three different donors (abscissa: T cell types; ordinate: PR8-specific IgM; Kruskal-Wallis test, **: $p<0.01$; ns: not significant).

chemokine receptor for CXCL13 (Fig 19b). The analysis of serum antibodies at day 14 post vaccination showed the presence of PR8 virus binding IgM in mice reconstituted with total $CD4^+$ T cells (mean ± SEM = 2921±1029) and with central memory $CD4^+$ T cells (mean ± SEM = 1503±416) while no antibody was detected in mice reconstituted with effector memory $CD4^+$ T cells (mean ± SEM = 144 ± 68; Fig. 19c and d). Antibody generation was associated with plasma cell differentiation in the spleen (Fig. 20).

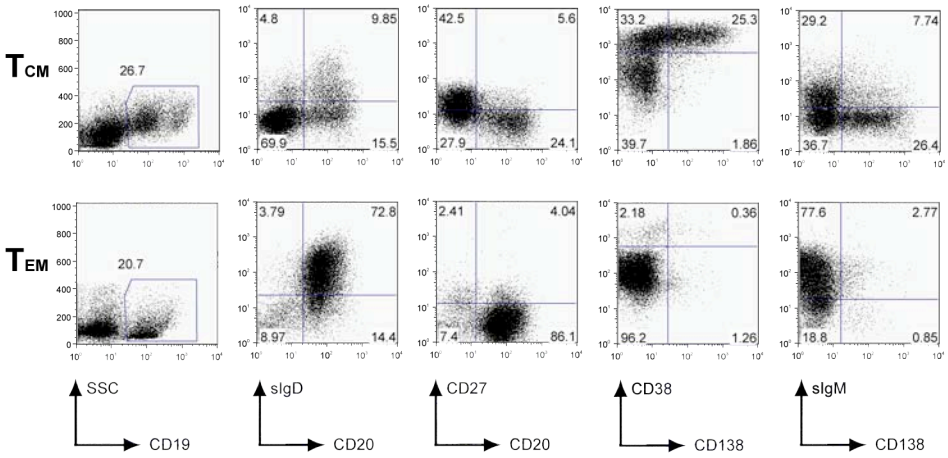

Figure 20. Plasma cell differentiation in LAIV vaccinated mice is dependent on central memory $CD4^+$ T cells. Single cell suspensions from spleen of mice with T_{CM} or T_{EM} were analyzed by flow cytometry. B cells were gated based on CD19 expression and further analyzed for the expression of CD20, CD27, CD38, CD138, sIgD and sIgM.

Single cell suspensions prepared from spleens of humanized mice reconstituted with effector memory T cells showed a population of $CD19^+$ B cells nearly all of which were $sIgD^+sIgM^+CD20^+CD27^-CD38^{low}CD138^-$. In contrast, mice reconstituted with central memory $CD4^+$ T cells showed loss of CD20, sIgD and sIgM expression and the acquisition of CD27, $CD38^{high}$ and CD138 expression consistent with plasma cell phenotype (Fig. 20). This was not due to the lack of $CD4^+$ T cells since they were recovered from the spleen at two weeks post vaccination (data not shown). Furthermore,

the lack of plasma cell differentiation also reflected on the amount of total antibody present in the serum. Mice reconstituted with effector memory T cells have limited production of different Ig subclasses (data not shown). These results demonstrate that humanized mice permit the differentiation of human plasma cells and the *in vivo* analysis of human T cell subsets. The role of $CXCR5^{+}CD4^{+}$ T cells in the humoral response will require experiments to further verified.

Mice Vaccinated with Ex Vivo-Generated DCs Expand Antigen-Specific $CD8^{+}$ T Cells

Generation of Primary and Recall $CD8^{+}$ T Cell Immunity upon Vaccination with Ex Vivo-Generated DCs

Next, we analyzed whether humanized mice could expand specific $CD8^{+}$ T cells upon vaccination with *ex vivo*-generated DCs. Here, we used the HLA-A*0201 tetramer to enumerate $CD8^{+}$ T cells recognizing a specific peptide epitope. We used melan A/MART-1_{27-35} (AAGIGILTV) peptide epitope identified in HLA-A*0201 melanoma patients (Kawakami and others 1994) to exam the priming of specific $CD8^{+}$ T cells in humanized mice. To demonstrate $CD8^{+}$ T cells response to influenza virus, we used the dominant epitope of influenza A virus $M1_{58-66}$ (GILGFVFTL) identified in HLA-A*0201 donors (Gotch and others 1987). This allowed us to exam a memory $CD8^{+}$ T cell response commonly seen upon influenza virus infection. *Ex-vivo* DCs were generated from adherent monocytes cultured with GM-CSF and IFN-α for three days. Immature DCs were then matured with 10 ng/mL of LPS for 14 hours and loaded with 10 μM of MART-1 or FluM1 peptides for another 16 hours before harvest for vaccination. Humanized mice were first reconstituted at 4-8 weeks post-transplant with $20x10^{6}$

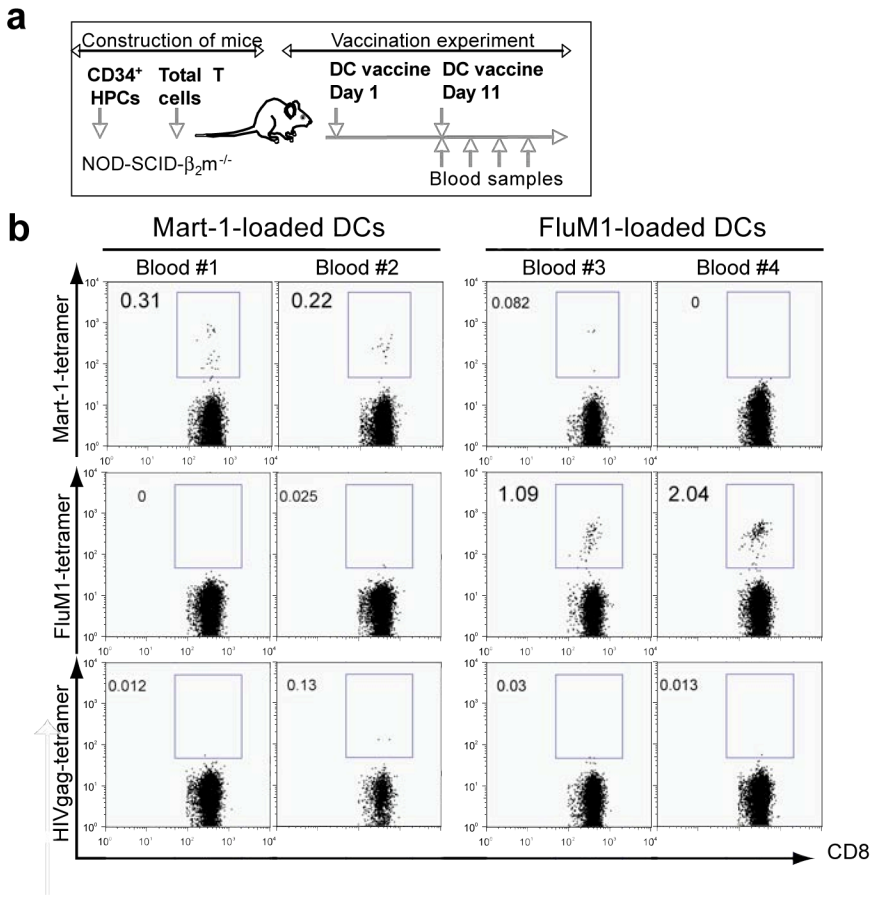

Figure 21. Mice vaccinated with peptide-pulsed *ex vivo*-generated DCs can mount primary and recall $CD8^+$ T cells immunity. (a) Ex-vivo DCs were generated from adherent monocytes cultured with GM-CSF and IFN-α for three days, matured with 10 ng/mL of LPS for 14 hours and loaded with 10 μM of MART-1 or FluM1 peptides for another 16 hours. Mice were vaccinated with either MART-1-loaded or FluM1-loaded DCs s.c. at day 1 and day 11. Blood was sampled at different time points for the analysis of specific $CD8^+$ T cells expansion by tetramer staining. (b) $CD8^+$ T cells specific to MART-1, FluM1and HIVgag were measured in the blood by tetramer staining at day 5 post boost.

purified (>95%) autologous total T cells s.c. and then vaccinated with $2x10^6$ peptide-pulsed *ex vivo*-generated DCs s.c. and boosted at day 11 (Fig. 21a). $CD8^+$ T cells specific to MART-1 and FluM1 were determined in the blood by tetramer staining at day 5 post boost (Fig. 21b). Humanized mice vaccinated with MART-1 peptide-loaded DCs expanded MART-1-specific $CD8^+$ T cells (0.31% and 0.22%) but not FluM1-specific $CD8^+$ T cells (0% and 0.025%), whereas mice vaccinated with FluM1 peptide-loaded

DCs expanded FluM1-spcific $CD8^+$ T cells (1.09% and 2.04%) but not MART-1 specific $CD8^+$ T cells (0.082% and 0%). This experiment demonstrated that tetramer-binding $CD8^+$ T cells expanded specifically in response to the antigen presented by *ex-vivo* DCs. Furthermore, it demonstrated the generation of primary T cell response in humanized mice.

We next analyzed the distribution of specific $CD8^+$ T cells in humanized mice. After 11 days post vaccination with FluM1-loaded DCs, three out of three mice in one representative experiment shown here had high frequency of FluM1-tetramer positive $CD8^+$ T cells (2.84%, 3.11% and 1.56%) in the blood (Fig. 22a). The draining LNs,

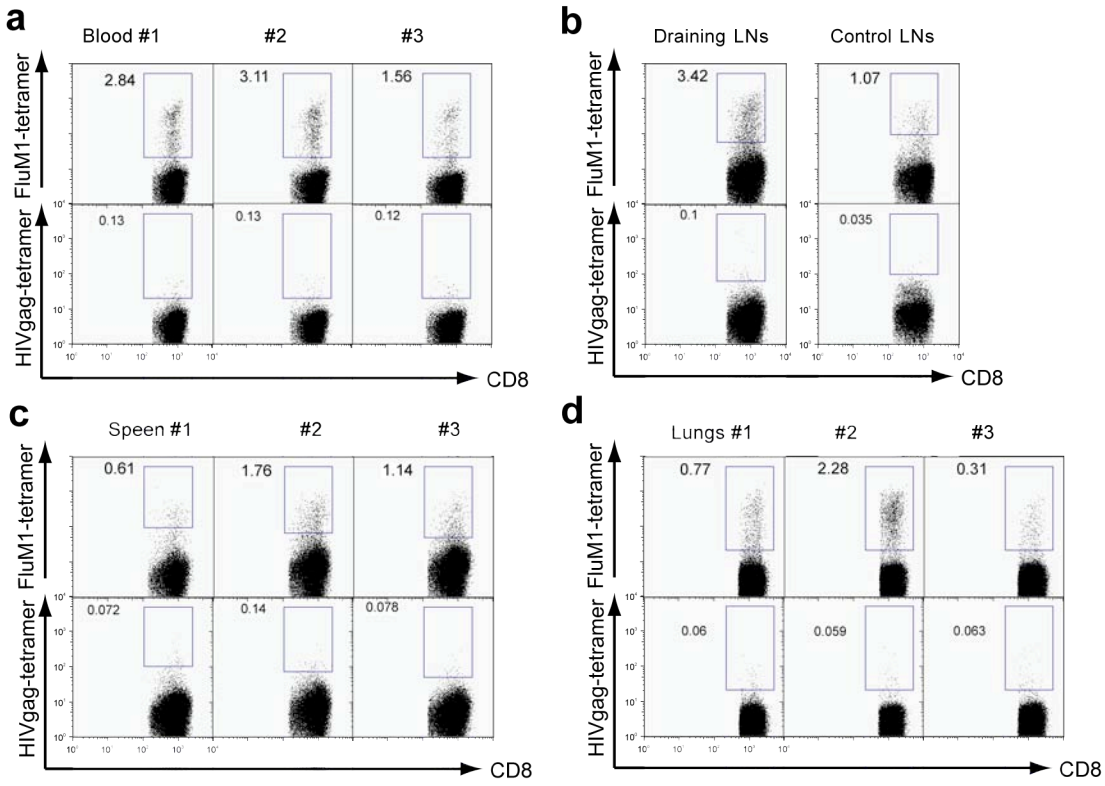

Figure 22. Expanded antigen-specific $CD8^+$ T cells can be found in lymphoid and peripheral tissues. (a) Mice were vaccinated with FluM1 peptide-pulsed *ex vivo*-generated DCs s.c.. After 11 days post DC vaccination, the frequency of FluM1-tetramer binding $CD8^+$ T cells were analyzed in the blood, (b) draining LNs, control LNs, (c) spleen, and (e) lungs of three mice. Each plot indicates one mouse analyzed except the draining and control LNs, which include cells pooled from three mice.

pooled of auxiliary and inguinal LNs, and the control lymph nodes, pooled of salivary, mesenteric and mediastinal LNs, were analyzed for FluM1-tetramer binding $CD8^+$ T cells. There were more of FluM1-specific CD8 T cells in the draining LNs (3.42%) than the control LNs (1.07%) by tetramer staining (Fig. 22b). Tetramer positive T cells could be also be detected in the spleen (0.61%, 1.76% and 1.14%; Fig. 22c) and in peripheral tissue like lungs (0.77%, 2.28%, 0.31%; Fig. 22d). In summary, specific $CD8^+$ T cells could expand upon vaccination with *ex-vivo* peptide-pulsed DCs and specific $CD8^+$ T cells could be found in blood circulation, and in both lymphoid and non-lymphoid tissues of humanized mice.

Generation of Specific $CD8^+$ T Cell Immunity by Ex-Vivo DCs Loaded with Influenza Virus

Next, we addressed whether *ex vivo*-generated DCs loaded with HI-PR8 virus could elicit specific $CD8^+$ T cell response in humanized mice. DCs were generated from adherent monocytes cultured with GM-CSF and IFNα for three days. Immature DCs were loaded with HI-PR8 virus and matured with 200 ng/mL of CD40L. Mice were vaccinated with DCs loaded with HI-PR8 virus or unloaded s.c. and boosted at day 11. $CD8^+$ T cells specific to FluM1 epitope were detected in the blood of mice vaccinated with HI-PR8 virus-loaded DCs (1.48%, 1.37%, and 0.54%; Fig. 23a and b) but not in mice vaccinated with unloaded DCs (0.043%, 0.041%, and 0.071%; Fig. 23a and b) by tetramer staining. Total $CD8^+$ T cells were sorted out from the blood of vaccinated mice to evaluate their capacity to kill PR8 virus infected target cells using chromium release assay. HLA-$A2^+$ human lung adenocarcinoma cells, NCI-H2405, were infected by PR8 virus as determined by intracellular FluNP expression (Fig. 24a). $CD8^+$ T cells from

mice vaccinated with HI-PR8-loaded DCs killed PR8-infected cells demonstrating a functional differentiation of specific $CD8^+$ T cells into cytotoxic T cells *in vivo* (Fig. 24b).

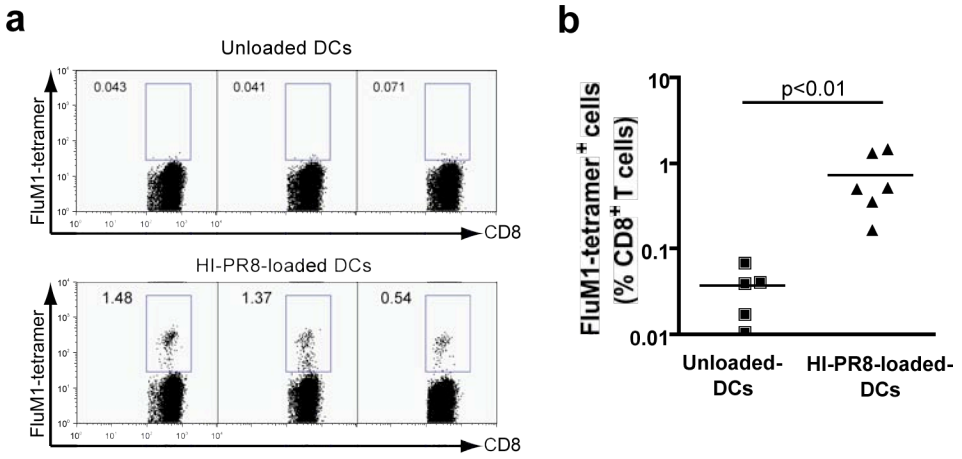

Figure 23. Antigen-specific $CD8^+$ T cell responses elicited by *ex-vivo* DCs loaded with HI-PR8 virus. (a) Mice were injected with DCs loaded with HI-PR8 virus subcutaneously on day 1 and day 11. The percentages of $CD8^+$ T cells specific to FluM1 were determined by tetramer staining at 4 days post boost in the blood. (b) The frequency of FluM1-tetramer binding $CD8^+$ T cells in the blood were from two independent experiments with two different donors (abscissa: types of DC vaccine; ordinate: % of FluM1-tetramer$^+$ cells in $CD8^+$ T cells; Mann Whitney test).

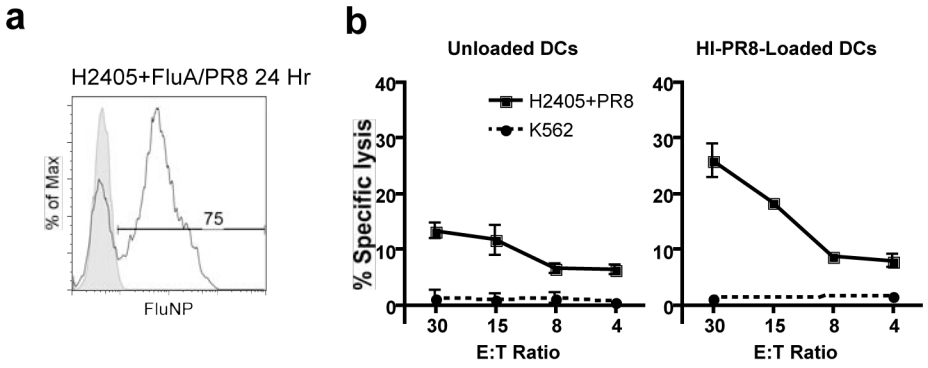

Figure 24. Antigen-specific $CD8^+$ T cells elicited by *ex-vivo* DCs loaded with HI-PR8 virus *in vivo* acquired cytotoxic function. (a) Human lung cell line, NCI-H2405, were treated by PR8 virus and the infection were confirmed by FluNP staining (gray: uninfected; black: PR8 virus treated). (d) Mice were vaccinated with DCs loaded with HI-PR8 virus s.c. on day 1 and day 11. $CD8^+$ T cells were sorted out from the blood of vaccinated mice at 5 days post boost. The cytolytic effector function of $CD8^+$ T cells against PR8 virus infected lung cell line (closed square; solid line) or K562 (closed circle; dashed line) was determined using chromium release assay (abscissa: E: T ratio; ordinate: % specific lysis).

The Kinetics of Specific CD8$^+$ T Cells upon DCs Vaccination

We next followed the frequency of specific CD8$^+$ T cells in the blood over time using tetramer staining. Humanized mice were vaccinated with DCs loaded with HI-PR8 virus and boosted at 11. Blood was sampled every three days to follow the kinetic of FluM1-specific CD8$^+$ T cells. The frequency of FluM1-specific CD8$^+$ T cells reached the peak at day 11 post primary DCs vaccination and the response dissolved at day 27 (Fig. 25a). One mouse received a boosting vaccination with HI-PR8 loaded DCs at day 27 and FluM1-specific CD8$^+$ T cells were detected in the blood at day 14 post the boosting vaccination (Data not shown). During the peak of specific CD8$^+$ T cell response, the percentage of CD8$^+$ T cells to total T cells ratio increased as well (Fig 25b). The kinetic of FluM1-specific CD8$^+$ T cells matched the kinetic of total CD8$^+$ T cell percentage suggesting a global CD8$^+$ T cells expansion upon DCs vaccination.

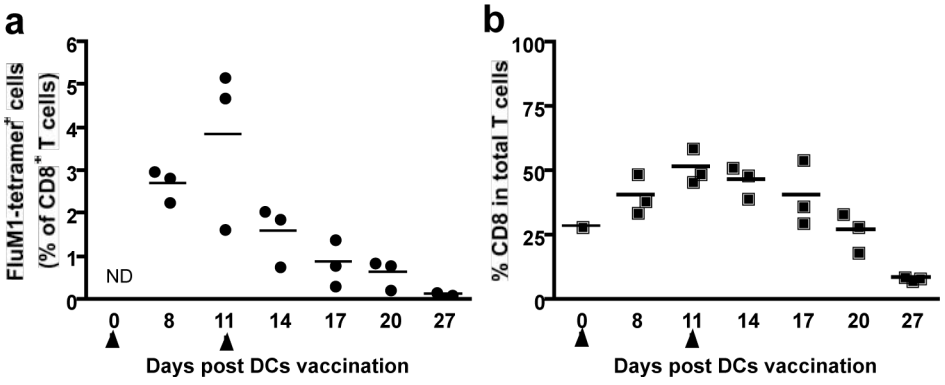

Figure 25. The kinetics of CD8$^+$ T cells response elicited by vaccination with ex-vivo DCs. (a) Mice were vaccinated with DCs loaded with HI-PR8 virus s.c. and boosted day 11. Blood was sampled at different time points for the specific CD8$^+$ T cells expansion by tetramer staining. The frequency of FluM1-specific CD8$^+$ T cells after vaccination was from a group of three mice (abscissa: days post DCs vaccination; ordinate: % of FluM1-tetramer$^+$ cells in CD8$^+$ T cells). (b) The percentage of CD8$^+$ T cells to total T cells was analyzed at different time points post vaccination from a group of three mice (abscissa: days post DCs vaccination; ordinate: % of CD8$^+$ T cells in total T cell).

Live Attenuated Trivalent Influenza Vaccine Expands FluM1-Specific CD8$^+$ T Cells in Blood and Tissues

Humanized mice received 20x10^6 autologous T cells i.p. at 4-8 weeks post CD34$^+$ HPCs transplantation. Trivalent influenza vaccine used was live attenuated influenza vaccine (LAIV) composed of H1N1 (A/New Caledonia/20/1999), H3N2 (A/Wisconsin/67/2005) and Influenza B (B/Malaysia/2506/2004) viruses (2006-2007 season) at equal hemagglutinin ratio. Mice were vaccinated once with a total of 100 μl vaccine (1/5 of human dose) delivered i.p. and i.v. (Fig. 26a). In some experiments, mice were vaccinated i.n. (Table 3). The induction of influenza-specific CD8$^+$ T cell response was assessed by FluM1-tetramer staining in the blood and tissues. Humanized mice vaccinated with LAIV demonstrated, at day 12 post vaccination, circulating FluM1-tetramer binding CD8$^+$ T cells with frequencies of 0.22%, 0.37% and 0.5% of CD8$^+$ T cells (Fig. 26b). These results were reproducible in four independent cohorts of humanized mice generated using cells from five healthy donors (Table 3). Altogether 14/16 mice vaccinated with LAIV showed expansion of FluM1-specific CD8$^+$ T cells (median = 0.19%; mean± SEM = 0.33± 0.10%, n=16; Fig. 26c and Table 3). Control mice received Tetanus Toxoid (TT) vaccine at 1/10 dose used for the human (50 μl) did not show expansion of FluM1-specific CD8$^+$ T cells (median = 0.03%; mean± SEM = 0.03%± 0.01%, n=7; Fig. 26c and Table 3).

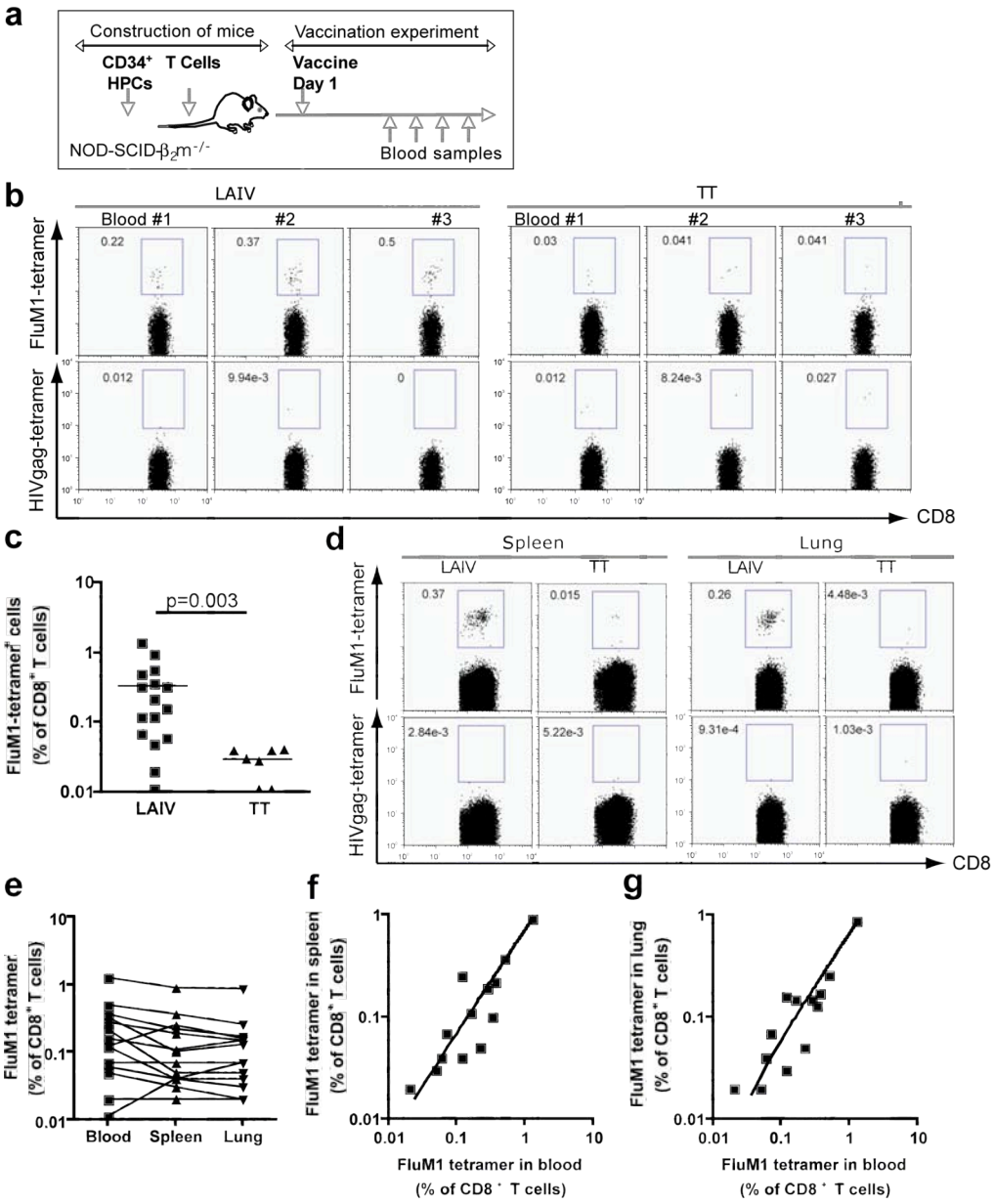

Figure 26. Mice vaccinated with trivalent live attenuated influenza vaccine (LAIV) expand FluM1-specific $CD8^+$ T cells. (a) Mice were vaccinated i.p./ i.v. with LAIV or TT. Blood was sampled for FluM1-specific $CD8^+$ T cells at different time points post vaccination. (b) At day 12 post vaccination, blood was measured for the frequency of specific $CD8^+$ T cells by FluM1-tetramer staining. HIVgag-tetramer was used as the negative control. One experiment with three mice vaccinated with LAIV or TT was illustrated here. (c) The frequency of FluM1-specific $CD8^+$ T cells in the blood at day 12 post vaccination were from four experiments with four different donors (Mann Whitney test, p= 0.0051). (d) At day 14 post vaccination, the frequencies of FluM1-tetramer binding $CD8^+$ T cells were analyzed in the spleen and lungs. (e) Each line represents the frequencies of FluM1-$tetramer^+$ cells in the blood, spleen and lungs of each TIV-vaccinated mouse. Data were from four independent experiments. (f) The frequency of FluM1-$tetramer^+$ cells in the blood correlates with the frequency in the spleen (Spearman, r=0.84 and p=0.0002) and (g) in the lung (Spearman, r=0.79 and p=0.0008).

Table 3. The frequency of FluM1-specific $CD8^+$ T cells in humanized mice vaccinated with LAIV.

Exp	Donor.	Mouse No	Vaccine (route)	% of FluM1-specific $CD8^+$ T cells			
				Tetramer			IFNγ
				Blood	Spleen	Lung	Spleen
I	A	1	PBS (i.p., i.v., i.n.)	0.05	0.09	0.04	ND
		2	LAIV (i.p., i.v., i.n.)	0.06	0.04	0.04	ND
		3	LAIV (i.p., i.v., i.n.)	0.16	0.11	0.15	ND
		4	LAIV (i.p., i.v., i.n.)	0.12	0.25	0.16	ND
		5	LAIV (i.p., i.v., i.n.)	0.05	0.03	0.02	ND
		6	LAIV (i.p., i.v., i.n.)	0.12	0.04	0.03	ND
		7	LAIV (i.p., i.v., i.n.)	0.33	0.10	0.13	ND
II	B	1	TT (i.p.)	0.03	0.03	0.01	0.08
		2	TT (i.p.)	0.04	0.02	0.00	0.00
		3	TT (i.p.)	0.04	0.02	0.01	0.10
		4	LAIV (i.p., i.v.)	0.22	0.05	0.05	0.2
		5	LAIV (i.p., i.v.)	0.37	0.22	0.17	0.43
		6	LAIV (i.p., i.v.)	0.50	0.37	0.26	0.89
III	C	1	TT (i.p.)	0.00	0.02	0.02	ND
		2	TT (i.p.)	0.00	0.02	0.02	0.02
		3	LAIV (i.p., i.v.)	0.00	0.04	0.07	0.02
		4	LAIV (i.p., i.v.)	0.07	0.07	0.07	0.03
		5	LAIV (i.p., i.v.)	0.02	0.02	0.02	0.02
IV	D	1	TT (i.p.)	0.02	0.04	0.05	0.03
		2	TT (i.p.)	0.01	0.04	0.03	0.01
		3	LAIV (i.p., i.v.)	0.28	0.19	0.15	0.13
		4	LAIV (i.p., i.v.)	1.27	0.91	0.87	0.88
V	E	1	LAIV (i.p., i.v.)	1.42	2.41	1.89	0.530
		2	LAIV (i.p., i.v.)	0.33	0.12	0.11	0.056
		3	LAIV (i.n.)	0.12	0.21	0.20	0.069
		4	LAIV (i.n.)	0.02	0.02	0.03	0.046
		5	LAIV (i.n.)	0.23	0.57	0.36	0.237
		6	LAIV (i.n.)	0.29	0.67	0.40	0.134

ND, not done.

Inactivated Trivalent Influenza Virus Vaccine Expands FluM1-Specific $CD8^+$ T Cells via Cross-presentation

The induction of immune responses after LAIV vaccination could happen through either cross-presentation or direct presentation of viral antigens by infected human cells (Williams and Bevan 2007). To determine whether human APCs in humanized mice actually cross-present processed peptides to T cells *in vivo*, we have analyzed mice vaccinated with trivalent inactivated influenza vaccine (TIV). There, viruses are

formalin-fixed, purified and chemically disrupted to generate a "split virus". At day 12 post single vaccination circulating FluM1-specific $CD8^+$ T cells could be detected in 4/4 mice: 0.88%, 0.49%, 1.2% and 0.44% (Fig. 27a). These results were reproduced in five independent cohorts of humanized mice generated using cells from four healthy donors (Fig. 27b and Table 4). Altogether 15/17 vaccinated mice showed expansion of FluM1-specifc $CD8^+$ T cells (median = 0.25%; mean± SEM = 0.50± 0.12%, n=17; Fig. 27b and Table 4). FluM1-specific $CD8^+$ T cells with high intensity of tetramer staining could also

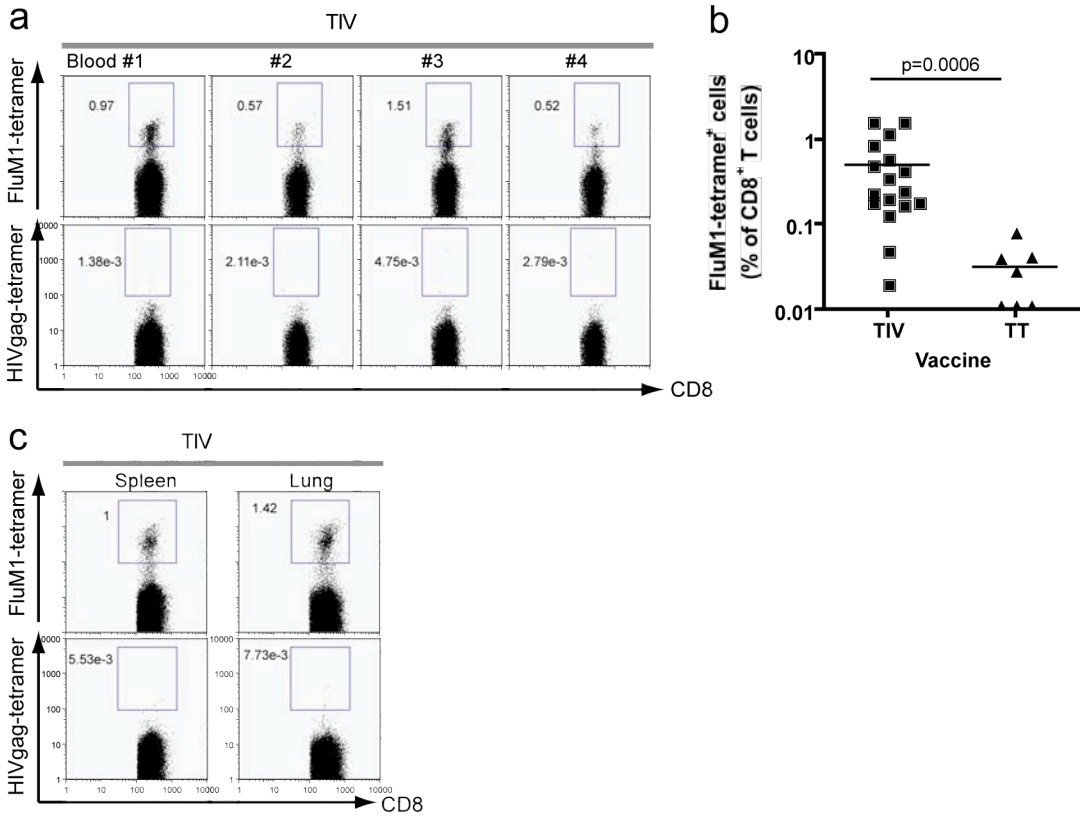

Figure 27. Mice vaccinated with trivalent split influenza vaccine (TIV) expand FluM1-specific $CD8^+$ T cells. (a) Mice were vaccinated i.p./ i.v. with TIV or TT. At day 12 post vaccination, blood was measured for the frequency of specific $CD8^+$ T cells by FluM1-tetramer staining. HIVgag-tetramer was used as the negative control. One experiment with four mice vaccinated with TIV was illustrated here. (b) The frequency of FluM1-specific $CD8^+$ T cells in the blood at day 12 post vaccination was from four independent experiments with three different donors (Mann Whitney test, p= 0.0006). (c) At day 14 post vaccination, the frequencies of FluM1-tetramer binding $CD8^+$ T cells were analyzed in the spleens and lungs.

Table 4. The frequency of FluM1-specific $CD8^+$ T cells in mice vaccinated with TIV.

Exp	Donor.	Mouse No	Vaccine (route)	% of FluM1-specific $CD8^+$ T cells			
				Tetramer			IFNγ
				Blood	Spleen	Lung	Spleen
I	A	1	PBS (i.p., i.v., i.n.)	0.05	ND	ND	ND
		8	TIV (i.p., i.v., i.n.)	0.20	ND	ND	ND
		9	TIV (i.p., i.v., i.n.)	0.18	ND	ND	ND
II	C	1	TT (i.p.)	0.00	0.02	0.02	ND
		2	TT (i.p.)	0.00	0.02	0.02	0.02
		6	TIV (i.p., i.v.)	0.17	0.12	0.12	0.10
		7	TIV (i.p., i.v.)	0.02	0.02	0.02	0.02
		8	TIV (i.p., i.v.)	0.05	0.08	0.07	0.03
III	F	1	TT (i.p.)	0.00	0.09	0.08	0.07
		2	TT (i.p.)	0.08	0.29	0.54	0.06
		3	TT (i.p.)	0.04	0.14	0.06	0.07
		4	TIV (i.p., i.v.)	0.35	ND	ND	ND
		5	TIV (i.p., i.v.)	0.60	ND	ND	ND
		6	TIV (i.p., i.v.)	0.18	ND	ND	ND
		7	TIV (i.p., i.v.)	0.88	0.49	0.55	0.63
		8	TIV (i.p., i.v.)	0.49	0.37	0.48	0.47
		9	TIV (i.p., i.v.)	1.20	1.00	1.42	0.78
		10	TIV (i.p., i.v.)	0.44	0.65	0.84	0.25
IV	F	11	PBS (i.p., i.v.)	0.10	ND	ND	ND
		12	PBS (i.p., i.v.)	0.05	ND	ND	ND
		13	TIV (i.p., i.v.)	0.13	0.12	0.12	0.10
		14	TIV (i.p., i.v.)	0.23	0.22	0.19	0.14
		15	TIV (i.p., i.v.)	0.25	0.24	0.25	0.08
V	D	1	TT (i.p.)	0.02	0.04	0.05	0.03
		2	TT (i.p.)	0.01	0.04	0.03	0.01
		5	TIV (i.p., i.v.)	0.65	0.43	0.31	0.39
		6	TIV (i.p., i.v.)	0.83	0.49	0.53	0.32

ND, not done.

be detected in tissues such as spleen and lung (Fig. 27c). These results suggested that antigens of inactivated vaccine were cross-presented *in vivo* to antigen-specific $CD8^+$ T cells thereby leading to their expansion.

To further prove this point, TIV vaccine was delivered to NOD-SCID-$\beta_2m^{-/-}$ mice that were not transplanted with $CD34^+$ HPCs but received the adoptive transfer of T and B cells. Control humanized mice were adoptively transferred with sorted human T cells (Fig. 28a). Thus, the key difference between NOD-SCID-$\beta_2m^{-/-}$ mice and humanized

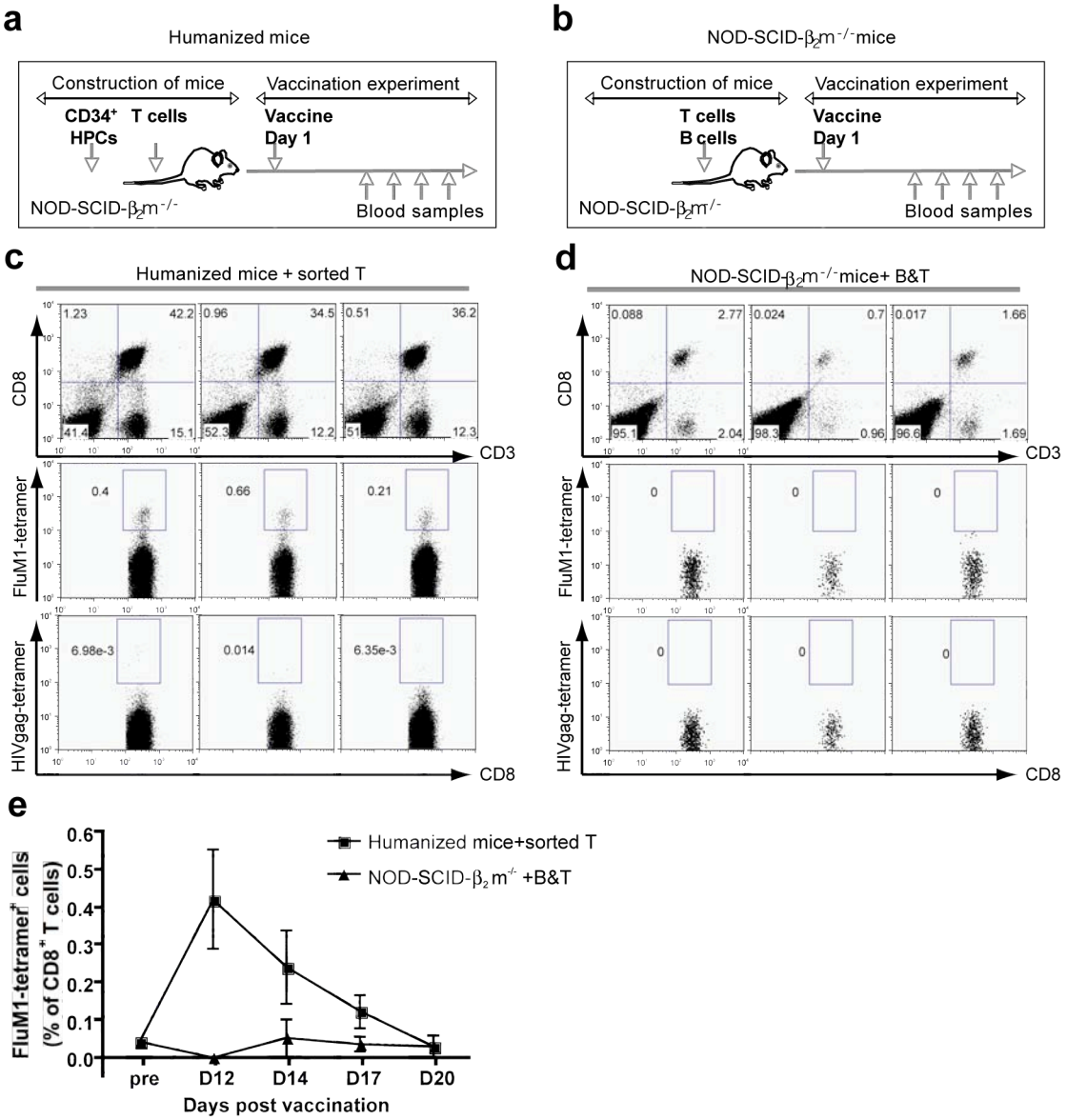

Figure 28. Cross-presentation of FluM1 to $CD8^+$ T cells by myeloid APCs in humanized mice. (a) Humanized mice were reconstituted with $20x10^6$ total T cells (purity more than 99%) and vaccinated i.p./ i.v. with TIV. Blood was sampled at different time points to monitor human T cells. (b) NOD-SCID-$\beta_2m^{-/-}$ mice were reconstituted with $30x10^6$ T cells and B cells (purity more than 99%) and vaccinated i.p./ i.v. with TIV. (c) At day 12 post vaccination, 100 μl of blood was stained for the frequency of FluM1-specific $CD8^+$ T cells in humanized mice or (d) in NOD-SCID-β2$m^{-/-}$ mice. (e) The frequencies of FluM1-tetramer binding $CD8^+$ T cells were measured at different time points post vaccination (mean ± SEM, n=3; abscissa: days post vaccination; ordinate: % of FluM1-$tetramer^+$ cells in $CD8^+$ T cells).

mice in this experiment was the presence of human DCs and myeloid cells in the latter mice (Fig. 28a and b). As shown in Figure 28c, 3/3 control humanized mice reconstituted with FACS-sorted autologous T cells demonstrated FluM1-specific $CD8^+$ T cells at day 12 post-vaccination with TIV. In contrast, NOD-SCID-$\beta_2m^{-/-}$ mice adoptively transferred with autologous T and B cells did not display FluM1-specific $CD8^+$ T cells upon vaccination with TIV (Fig. 28d). This could not be explained by the mere absence of human T cells since they could be detected albeit at lower frequency than in humanized mice. Kinetics analysis of vaccinated NOD-SCID-$\beta_2m^{-/-}$ mice showed that the lack of specific $CD8^+$ T cells at day 12 was not due to delayed response as they were still absent at day 20 (Fig. 28e). The kinetics experiments in humanized mice showed a peak response at day 12 followed by a gradual disappearance of FluM1-specific $CD8^+$ T cells from the blood by day 20. It remains to be determined whether this disappearance represents a contraction of effector T cell population or their migration to tissues. Thus, human antigen presenting cells other than B cells, most likely DCs, are able to cross-present influenza antigens *in vivo* to $CD8^+$ T cells and launch recall $CD8^+$ T cell immunity.

Live Attenuated and Inactivated Trivalent Influenza Vaccines Expand $CD8^+$ T Cells with Different Specificities

To determine the breadth of elicited influenza specific responses, human $CD8^+$ T cells from spleen suspensions at day 14 post vaccination were analyzed after 8 hours exposure to either the control HIV $gag_{77\text{-}85}$ peptide (SLYNTVATL) or three HLA-A*0201 peptides derived from influenza antigens in the presence of anti-CD28 and anti-CD49d. Influenza peptides were matrix protein 1 ($M1_{58\text{-}66}$ GILGFVFTL), nonstructural

protein 1 ($NS1_{122-130}$ AIMDKNIIL) and nuclear protein ($NP_{383-391}$ SRYWAIRTR). $CD8^+$ T cell differentiation was assessed by the expression of IFN-γ measured by intracellular staining using flow cytometry. Following vaccination with LAIV, there were up to 1% of $CD8^+$ T cells in the spleen secreting IFN-γ in response to the mixture of the four influenza peptides (Fig 29a). Single peptide analysis showed $CD8^+$ T cell responses to FluM1 (0.8% of $CD8^+$ T cells in the spleen, Fig. 29a) thus confirming tetramer-binding data shown above. $CD8^+$ T cell responses to FluNS1 peptide were also detected (0.3% of $CD8^+$ T cells in the spleen, Fig. 29a). Among the three influenza derived peptides analyzed, the FluM1 and FluNS1 peptides had the highest binding affinity to HLA-A*0201 (Fig. 29b) possibly explaining the lack of detection of T cells specific to peptide derived from FluNP. Only 0.07% $CD8^+$ T cells expressed IFN-γ upon exposure to HIV gag peptide, consistent with tetramer binding data, further demonstrating specificity of responses. Thus, mice vaccinated with LAIV vaccine generate recall $CD8^+$ T cell immunity to at least two of influenza virus antigens. $CD8^+$ T cells with both specificities have been detected in spleens from three independent mice as well as in the lungs pooled from these three mice (Fig. 29c). The presence of responses to peptide derived from non-structural protein further confirms *in vivo* infection of cells by the LAIV vaccine.

Mice vaccinated with TIV also showed the expansion of FluM1-specifc IFN-γ-secreting $CD8^+$ T cells (0.75% $CD8^+$ T cells, Fig. 29d). However, in contrast to mice vaccinated with LAIV, those vaccinated with TIV did not display $CD8^+$ T cells specific to NS1 peptide (Fig. 29d). These findings were reproduced in several mice within a cohort as well as in an independent cohort of mice constructed with cells from another healthy volunteer (Fig. 29e). The pattern of NS1-specifc $CD8^+$ T cell differentiation was

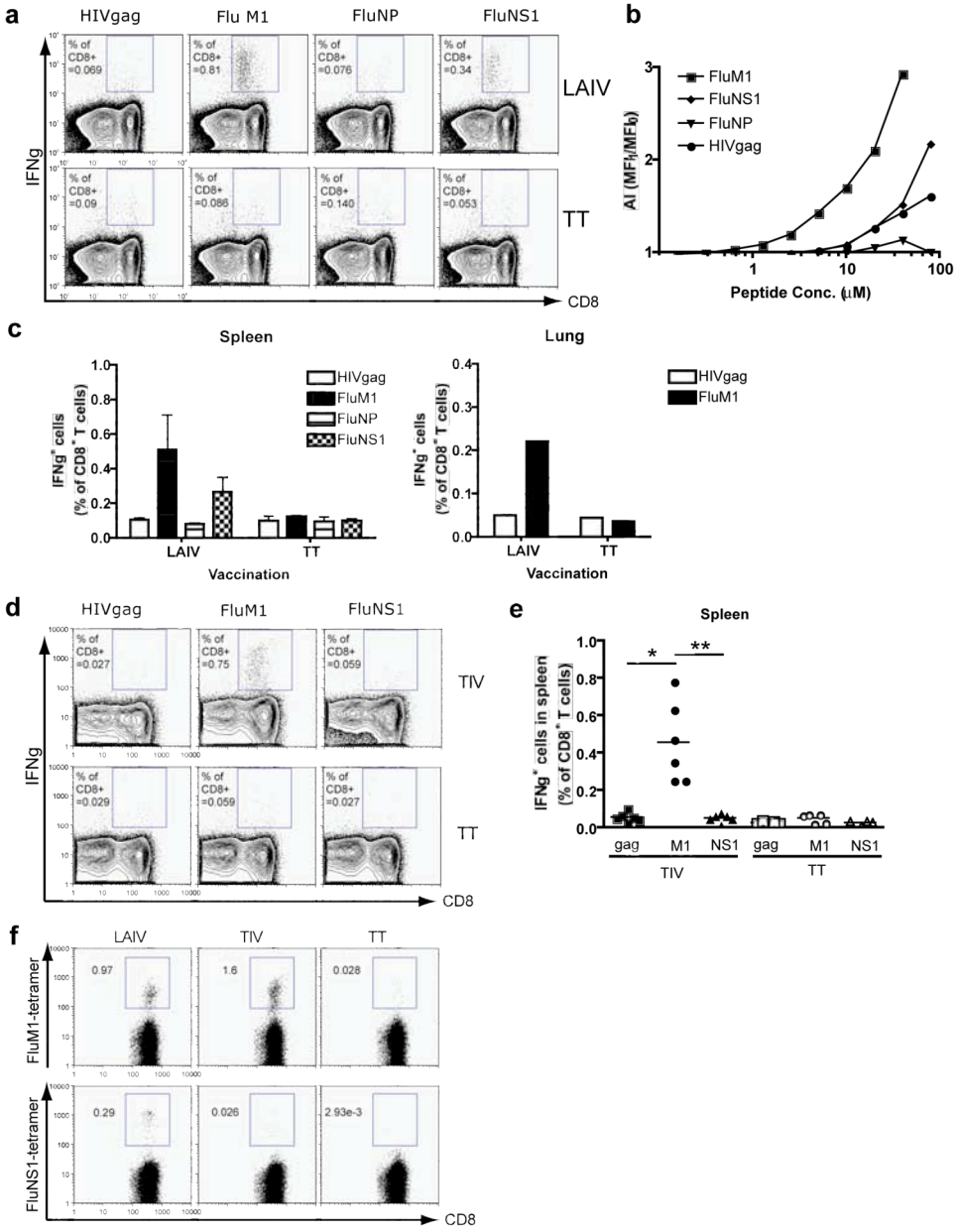

Figure 29. The breadth of $CD8^+$ T cells in mice vaccinated with influenza vaccines. (a) Mice were vaccinated with LAIV or TT. Single cell suspensions from spleen at day 14 post vaccination were stimulated with selected peptides and antibodies against CD28 and CD49d for intracellular cytokine staining. Total T cells were analyzed for the frequency of IFNγ-secreting $CD8^+$ T cells. (b) The binding affinity of selected peptides to HLA-A*0201 on T2 cells were measured by the increase surface expression of HLA-A*0201. The affinity index of each peptide is as follows: [(MFI of T2 cells loaded with peptide)/ (MFI of T2 cells without peptides)]. (c) The frequency of IFNγ-secreting $CD8^+$ T cells in the spleen (mean ±SEM, n=3) and lungs (pooled of three mice) were measured with different peptides. (d) Mice were vaccinated with TIV or TT. Total T cells were analyzed for frequencies of IFNγ-secreting $CD8^+$ T cells to different peptides and (e) illustrated in a scatter plot (mean, n=6; Kruskal-Wallis test). (f) Mice were vaccinated with LAIV, TIV or TT and the blood was measured for the frequency of specific $CD8^+$ T cells recognizing FluNS1-tetramer.

further confirmed, in an independent cohort of mice, by demonstrating the presence of NS1-tetramer binding $CD8^+$ T cells in the blood following vaccination with LAIV but not with TIV (Fig. 29f).

Live Attenuated and Inactivated Trivalent Influenza Vaccines Expand $CD8^+$ T Cells with Effector Phenotypes

An important parameter of vaccine efficacy is the differentiation of antigen-specific $CD8^+$ T cells to acquire the effector phenotype. Experiments discussed above demonstrated IFN-γ expression by influenza antigen-specific $CD8^+$ T cells. To further establish effector cell differentiation, we analyzed cytokine profiles by multicolor flow cytometry and surface expression of CD107a, a marker of lytic granule serving as a surrogate marker of CTL differentiation (Betts and others 2003). Multiparameter flow cytometry was used to analyze cells pooled from blood of three mice from a cohort vaccinated with TIV. Cells were stimulated 8 hours with either the control HIV gag or FluM1 peptides in the presence of anti-CD28 and anti-CD49d, FITC conjugated CD107a and monensin were included in the culture for the last 7 hours. After stimulation, human $CD8^+$ T cells were stained intracellularly for different cytokine expressions including IFN-γ, IL-2, and TNF-α. Together with the surface expression of CD107a, human $CD8^+$ T cells were analyzed using Boolean gating strategy for cells expressing different combination of effector markers (Fig 30a). Thus, in the blood, the two major $CD8^+$ T cell populations are $CD107a^+$ IFN-γ^+ (67%) and $CD107a^+$ (25%) demonstrating an effector phenotype (Fig. 30a). Meanwhile, only a small fraction of $CD8^+$ T cells expressing TNF-α or IL-2 could be detected in the blood (Fig. 30a). This again was confirmed in TIV vaccinated mice where the phenotype of CTLs prevailed (Fig. 30b).

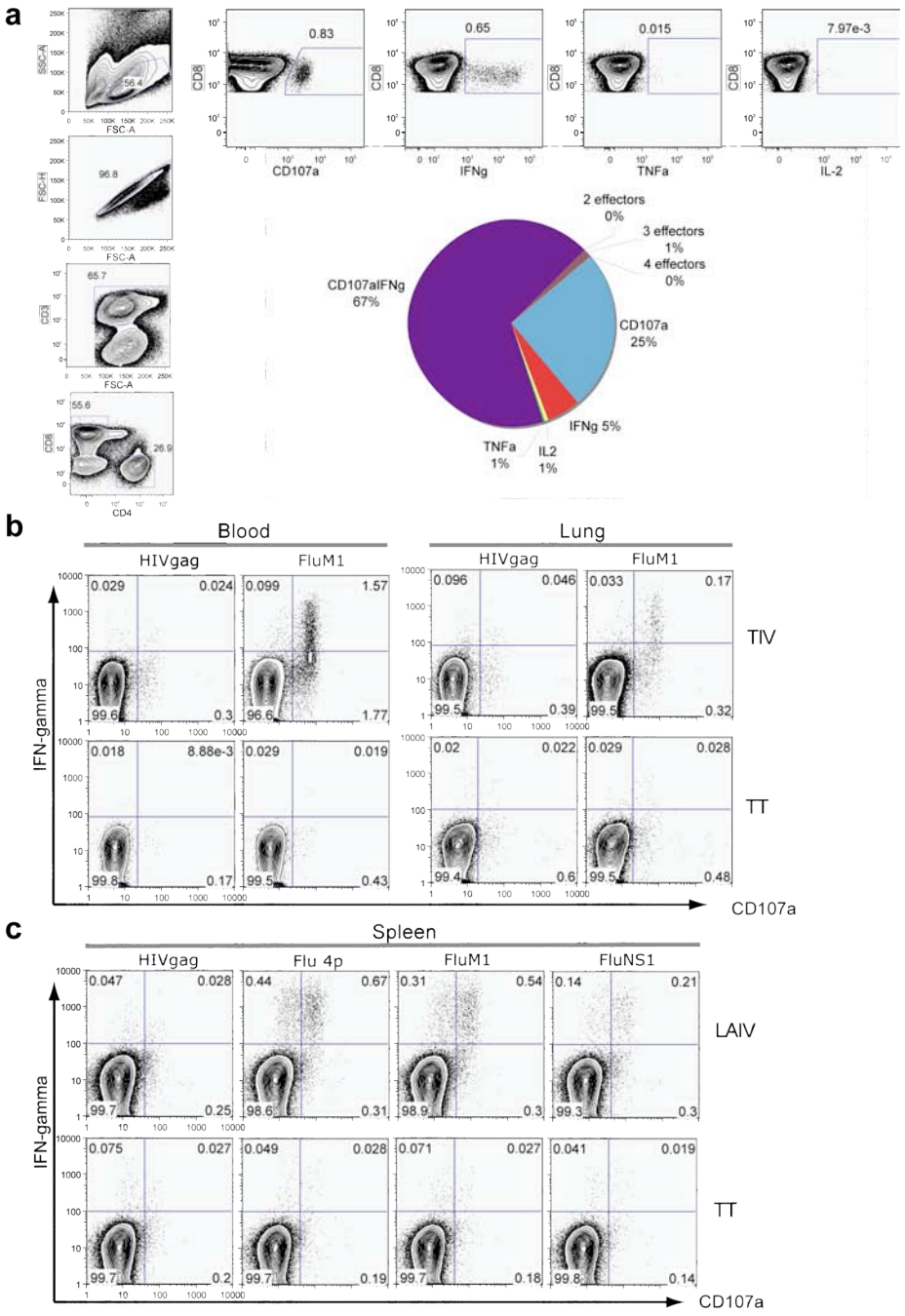

Figure 30. Cytokine production and effector cell differentiation of $CD8^+$ T cells after vaccination. (a) $CD8^+$ T cells in the blood at day 14 post TIV vaccination were stimulated for 8 hours with FluM1 peptide and antibodies against CD28 and CD49d. $CD8^+$ T cells were analyzed for CD107a, IFN-γ, IL-2, and TNF-α expression. Responding $CD8^+$ T cells expressing different combination of effector molecules were calculated using Boolean-gating strategy and plotted in a pie chart. Each pie represents the fraction of total FluM1-responding $CD8^+$ T cells secreting each combination of cytokine. (b) $CD8^+$ T cells from the blood and lungs of TIV- or TT-vaccinated mice were analyzed for IFN-γ and CD107a expression in response to HIVgag or FluM1 peptides. (c) $CD8^+$ T cells from the spleen of LAIV- or TT-vaccinated humanized mice were analyzed for IFN-γ and CD107a expression in response to different peptides.

The profile of antigen-specific $CD8^+$ T cells in TIV vaccinated mice was different in some of LAIV vaccinated mice. There, two subsets of influenza-specific IFN-γ^+ $CD8^+$ T cells could be distinguished by the expression of surface CD107a, i.e., single IFN-γ^+ $CD107a^{neg}$ and double IFN-γ^+ $CD107a^+$ $CD8^+$ T cells (Fig. 30c). Thus, humanized mice vaccinated with influenza viruses generate FluM1-specific effector $CD8^+$ T cells. Furthermore, different types of vaccines could generate $CD8^+$ T cells with different phenotype.

Taken altogether these experiments yielded important conclusions.

(1) Humanized mice vaccinated with LAIV vaccine show an expansion of IFN-γ-secreting $CD8^+$ T cells specific to at least two vaccine antigens, matrix protein and non-structural protein. This demonstrates the capacity of human APCs to process and present multiple vaccine antigens *in vivo*.

(2) TIV vaccinated mice show FluM1-specific response but lack NS1-specific response. This demonstrates the lack of infection in TIV vaccinated mice and further confirms the cross-presentation of FluM1 by human APCs.

In vivo Targeting of Human Dendritic Cells to Generate Influenza Virus-Specific Immune Responses

From these experiments, we have demonstrated the adaptive human immune responses in humanized mice model with $CD34^+$ HPCs and adoptive T cells transfer. The ultimate goal for these studies is to use these mice for the screening of novel vaccine designed to target human DCs. Through directly targeting antigen to DCs, we anticipate to induce a better immune response mediated by DCs but not other APCs and lower the amount of antigen for the induction of immune response. Here, we designed proof-of-

principle experiments using anti-DC receptor mAb and antigen fusion proteins. This would allow us to conclude the efficacy of targeting vaccine *in vivo*.

Generation of Specific $CD8^+$ T Cells in Humanized Mice Vaccinated with Anti-DC mAb and Antigen Fusion Proteins

To test the novel targeting vaccine, we first evaluated the MHC class I presentation of recombinant FluM1 protein either delivered in the form of recombinant protein (FluM1) or fusion protein conjugated to anti-DCIR mAb (DCIR-FluM1). DCIR is a C-type lectin receptor expressed on DCs (Bates and others 1999). Humanized mice were reconstituted with total human T cells at the age of 4-8 weeks post $CD34^+$ HPCs transplant. Mice were then vaccinated with 30, 10 and 1 μg of DCIR-FluM1 or FluM1, corresponding to the amount of antigen in the fusion protein. Vaccines were delivered through both i.v. and i.p. with 50 μg of poly I:C, a TLR3 agonist, as the adjuvant. The expansion of FluM1-specific $CD8^+$ T cells was measured at day 12 post vaccination in the blood. Humanized mice vaccinated with recombinant FluM1 protein had expansion of FluM1-tetramer binding $CD8^+$ T cells with the dose of 30 μg, but not 10 μg or 1μg (Fig. 31a). In contrast, mice vaccinated with DCIR-FluM1 fusion protein had expansion of FluM1-specific $CD8^+$ T cells at the dose of both 30 μg and 10 μg and less expansion at 1 μg. The expansion of FluM1-specific $CD8^+$ T cells was obtained from one experiment with three mice per dose (Fig 31b). This demonstrated that using DCIR-FluM1 fusion protein could allow at least 3 fold less of antigen to reach the same expansion of specific $CD8^+$ T cell.

Next, the phenotype and function of FluM1-specific $CD8^+$ T cells upon vaccination with DCIR-FluM1 were evaluated. Humanized mice vaccinated with 10 μg

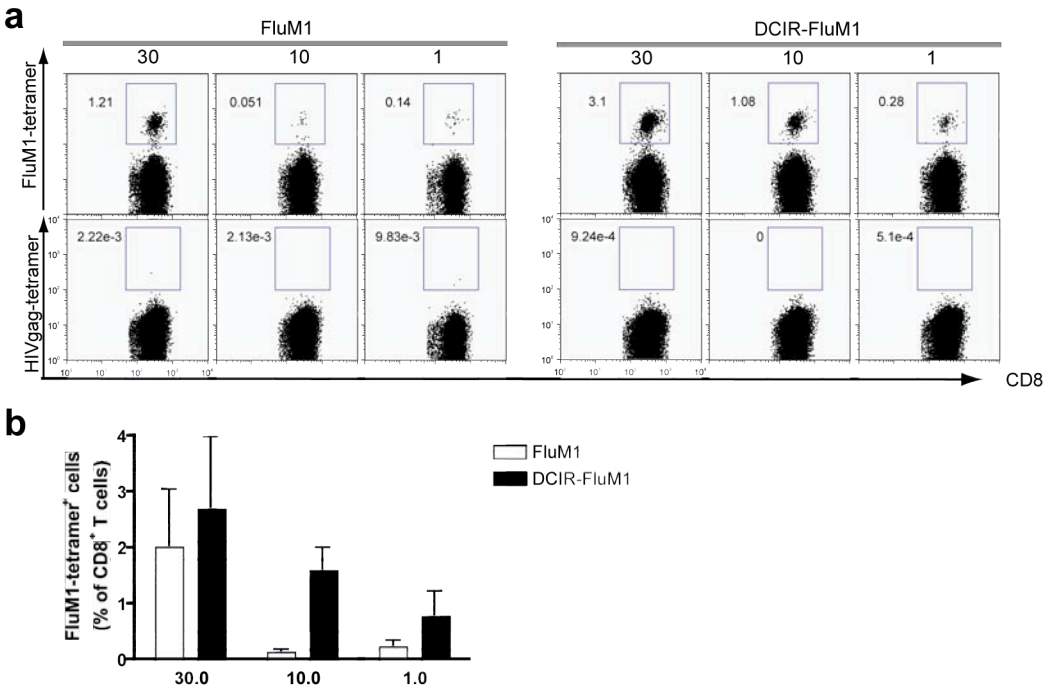

Figure 31. *In vivo* DC targeting. (a) Mice were vaccinated with DCIR-FluM1 fusion protein at different doses including 30, 10, and 1 μg, or corresponding amount of FluM1 recombinant protein. Antigens were delivered i.v./ i.p. with 50 μg poly I:C as adjuvant. Blood was sampled at day 12 post vaccination to analyze the frequency of FluM1-tetramer binding $CD8^+$ T cells. (b) Each bar represents the frequencies of FluM1-tetramer$^+$ $CD8^+$ T cells from one experiment with three mice per group (mean ±SEM).

of DCIR-FluM1 or corresponding amount of FluM1 were analyzed at day 14 post vaccination. Consistent with the result from Figure 31, mice vaccinated with DCIR-FluM1 showed expansion of FluM1-specific $CD8^+$ T cells in the spleen (0.98, 2.33 and 0.93%) in contrast to mice vaccinated with FluM1 recombinant protein (0.06, 0.11 and 0.011%; Fig. 32a). When analyzed FluM1-tetramer binding $CD8^+$ T cells, majority of specific $CD8^+$ T cells down-regulated or lost the expression of CD28. To further evaluate the function of specific $CD8^+$ T cells, cells were stimulated for 8 hours with peptides and antibodies against CD28 and CD49d and were subjected for intracellular cytokine staining. $CD8^+$ T cells were analyzed for CD107a and IFN-γ expression in

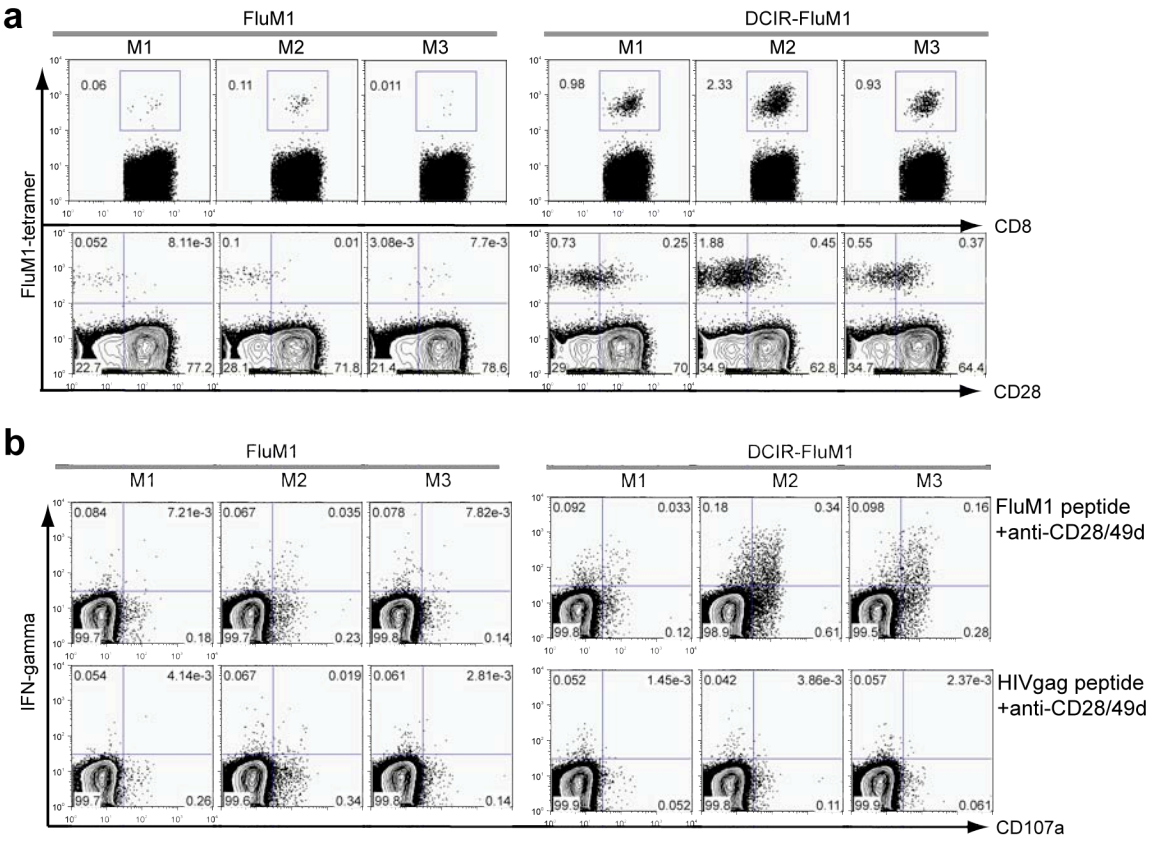

Figure 32. Mice vaccinated with DCIR-FluM1 fusion protein expand FluM1-specific effector $CD8^+$ T cells. (a) Mice were vaccinated with 10 μg of DCIR-FluM1 fusion protein or corresponding amount of FluM1 recombinant protein with 50 μg of poly I:C as adjuvant. At day 14 post vaccination, single cell suspension from spleen was analyzed for FluM1-specific $CD8^+$ T cells by flow cytometry. (b) After stimulation for 8 hours with FluM1 or HIVgag peptides and antibodies against CD28 and CD49d, cells were subjected for intracellular cytokine staining. $CD8^+$ T cells were analyzed for CD107a and IFN-γ expression.

response to FluM1. HIVgag peptides were used as a control. 50% of $CD8^+$ T cells responding to FluM1 peptide were $CD107a^+$ IFN-γ^- and the other 50% were IFN-γ^+ either with or without the expression of CD107a (Fig 32b). The loss of CD28 and the expression of CD107a suggested an effector cell differentiation. Overall, vaccination with DCIR-FluM1 fusion protein with poly I:C delivered FluM1 antigen efficiently and induced a robust expansion FluM1-specific $CD8^+$ T cells with effector phenotype in humanized mice.

CHAPTER FIVE

Discussion

The overall goal of my studies was to determine the capacity of human DCs to generate adaptive immune responses in humanized mice. That would permit to establish these mice as a model for testing human vaccines *in vivo*. I have used influenza viruses and influenza vaccines to measure the capacity of DCs to generate primary B cell responses, antibody production, and recall T cell immunity in these mice. In the initial phase of studies, I found that, upon intranasal infection with live PR8 virus, human DCs could be activated and could accumulate in mediastinal lymph nodes. These experiments assessed very basic functions of DCs *in vivo* and indicated that humanized mice could actually be used to study human DC physiology. I then moved to test influenza vaccines starting with *ex vivo*-generated DCs. This was an important step in our strategy as it permitted us to analyze the B cell compartment while controlling the DCs and the T cells. These experiments demonstrated that adaptive immune response could be generated upon vaccination via DCs. Indeed, vaccinated mice developed protective humoral immunity as well as expanded effector $CD8^+$ T cells. Importantly, preliminary experiments showed the capacity of humanized mice in generating primary T cell responses. In the next step, using seasonal influenza vaccines, both live attenuated virus and inactivated virus, I was able to show cross-presentation of viral antigens *in vivo* leading to the expansion of antigen-specific $CD8^+$ T cells. Finally, experiments with fusion proteins further proved antigen capture and cross-presentation *in vivo* via DCs.

In humanized mice, mature human DCs seemed to accumulate at three days post influenza infection in the mediastinal lymph nodes. This suggested that human DCs could migrate *in vivo* through blood and lymphatics, and utilize murine adhesion molecules. The accumulation of DCs in the lymph nodes was delayed as compared to the study in mouse where the first wave of DC migration into the draining lymph node was seen as early as 6 hours post influenza virus inoculation and increased within the first 24 hours (Legge and Braciale 2003). Sealy and others (2003) have reported a transient detection of influenza antigen in draining lymph node at 3 days post infection. The transient influenza virus antigen in draining lymph nodes might represent the influx of infected DCs migrated from infected area or the *in situ* infection in the lymph node. It is possible that we detect predominantly the accumulation of inflammatory DCs coming from the blood circulation, and that the migration through lymphatics is not faithfully reproduced. Consistent with this is the fact that we have found little evidence of local turnover of myeloid DCs in the lung in the course of infection with PR8 virus.

Humanized mice vaccinated with *ex vivo*-generated inactivated virus-pulsed DCs or with seasonal influenza vaccines generated specific antibody responses. The antibody was protective *in vitro* and could offer passive protection *in vivo*. The antibody is IgM and its generation is dependent on $CD4^+$ T cells, in particular their subset, i.e. central memory $CD4^+$ T cells. The generation of influenza virus-specific antibody was accompanied by the differentiation of human B cells into plasmablasts and plasma cells. These results showed the functionality of human B cells that have developed endogenously. The limiting factor remained the isotype switch as only low titers of human IgG could be detected and influenza-specific IgG could be detected sporadically.

Two waves of plasma cells differentiation in response to a T cell-dependent antigens have been described (Liu and Arpin 1997; MacLennan and others 2003). The first wave of antibody production comes from extrafollicular plasma cells, which are driven by high-density antigen and high affinity B cell receptor (BCR) recognition. This response is composed mainly of IgM and some IgG (Paus and others 2006). Low affinity B cells travel into the germinal center and undergo somatic hypermutation. These germinal center B cells become plasma cells, which secretes high affinity antibody and constitutes the second wave (Paus and others 2006; Phan and others 2006)). Since in our model we do not find formal germinal center structure in secondary lymphoid organ including spleen and lymph nodes, it is possible that these influenza virus-specific antibodies are secreted by extrafollicular plasma cells. This is also supported by the observation that these plasma cells appear short-lived. It will be interesting to determine plasma cell differentiation in dose response experiments and upon vaccination with low antigen dose.

The question whether these B cells responsible for neutralizing antibody have undergone somatic mutation remains to be addressed. Somatic mutation occurred on antibody binding site of Ig and is important for the generation of high affinity antibody (Manser and others 1998). We have analyzed the variable region of Ig with both IgM and IgG in humanized mice vaccinated with *ex vivo*-generated DCs pulsed with influenza virus. There are some degrees of point mutation found in the IgM and less in IgG (data not shown), suggesting a possibility of somatic mutation occurring ectopically. This preliminary observation needs further confirmation.

In contrast to T cells, B cells recognize unprocessed antigens. Antigens are available for B cells activation either through direct diffusion into B cells follicles (Pape and others 2007) or through the aid of DCs (Pape and others 2007; Qi and others 2006). DCs can present unprocessed antigens and activate antigen-specific extrafollicular B cells. As a bridge, DCs present unprocessed antigen to B cells and peptide antigen to T cells and serve as a platform facilitating the activation of T cells-dependent B cells. Here, we have illustrated this through the generation of specific antibody to influenza virus by ex-vivo DCs loaded with influenza virus antigen.

We found that only the mice reconstituted with central memory $CD4^+$ T cells, but not those reconstituted with effector memory T cells, showed B cell differentiation and the antibody secretion. CD40L ligation via activated T is important in the differentiation of B cells and drives naïve B cells into memory B cells but not plasma cells (Arpin and others 1995). However, CD40L does not provide the explanation since its is rapidly expressed on both central memory and effector memory $CD4^+$ T cells upon the engagement with antigen (Koguchi and others 2007; Stubbe and others 2006). Human central memory $CD4^+$ T cells are composed of cells committed into Th1, Th2 and uncommitted $CXCR5^+$ follicular B helper T (T_{FH}) cells (Lanzavecchia and Sallusto 2005; Moser and others 2002; Schaerli and others 2000). CXCR5 is a follicular homing receptor for CXCL13, a molecule present in B cell follicles. Human tonsillar T_{FH} cells produce CXCL13 and IL-21, a potent cytokine for B cells differentiation into plasma cells (Breitfeld and others 2000; Bryant and others 2007; Chtanova and others 2004). Our analysis of T cells prior adoptive transfer showed that $CXCR5^+$ $CD4^+$ T cells are almost exclusively confined to central memory population. Thus, $CXCR5^+$ T_{FH} cells in

the central memory compartment but not effector memory compartment could be responsible for the T cell-dependent antibody response. Experiments aimed to determine the role of $CXCR5^+$ T cells in the generation of antibody response are ongoing.

In our model, T cells were purposely isolated from PBMCs autologous to $CD34^+$ HPCs that were used to transplant the mice. In this scenerio, human T cells repertoire is not biased as in the case of the current humanized mouse model with endogenous T cells, where T cells are selected on murine thymic epithelial cells and only partially on human DCs that might migrate to the thymus (Legrand and others 2006). In our model, we also benefited from the presence of memory T cells and could thus use recall responses to measure the function of antigen presenting cells. Our humanized mice were able to generate memory $CD8^+$ T cells response as well as primary $CD8^+$ T cells response as in the case of MART-1 specific $CD8^+$ T cells. This is fundamental in the vaccine design since the goals are to reinforce existing memory compartment and to generate new memory compartment from naïve compartment against chronic viral infection and cancer (Yewdell and Haeryfar 2005).

Our studies on the kinetics of specific $CD8^+$ T cells showed a transient expansion of antigen-specific $CD8^+$ T cells in humanized mice. These specific $CD8^+$ T cells circulated in the blood, and were detected for at least two weeks. As to whether these specific $CD8^+$ T cells simply die or emigrant into tissue remains to be determined. It will be interesting to see if a memory T cells response could be established in these humanized mice when vaccinated with a primary antigens like HIV antigens or tumor antigens.

Mice vaccinated with inactivated virus showed the expansion of $CD8^+$ T cells, thereby illustrating the capacity of human DCs to cross-present vaccine antigens. Antigen cross-presentation was further confirmed by experiments in which mice were vaccinated with the anti-DCIR and FluM1 fusion protein.

Mice vaccinated with inactivated virus showed FluM1-specific response but lack NS1-specific response. This is consistent with the lack of NS1 protein in inactivated virus (Birch-Machin and others 1997; Dimmock 1969). Indeed, in animal studies of antibody responses to natural infection and to vaccination with inactivated influenza virus, antibodies against NS1 are used as DIVA, i.e., differentiating infected from vaccinated animals (Birch-Machin and others 1997). There, infected animals develop antibodies to NS1 while vaccinated animals not because there is no NS1 in the vaccine. In our model of $CD8^+$ T cell immunity, this observation further demonstrated the specificity of observed responses in vaccinated mice. In the absence of the NS1 antigen in inactivated virus, no expansion of $CD8^+$ T cells specific to this antigen were detected.

It would be desirable to increase memory CTLs that could recognize different types of influenza virus and could provide the second line of protection against influenza virus infection. Our results confirmed the studies in human that the repertoire of memory CTL was broad toward structural and nonstructural proteins of influenza viruses (Boon and others 2002; Gianfrani and others 2000; Jameson and others 1998). The administration of live attenuated virus could allow the enhancement of CTLs response to non-structural protein, i.e. NS1, as illustrated here. However, when we looked at the expansion of FluM1-specific $CD8^+$ T cells, inactivated virus expanded specific $CD8^+$ T

cells more efficiently than live attenuated virus. The mechanism of this remains to be determined.

The patterns of antigen-specific $CD8^+$ T cell immunity elicited by live-attenuated and inactivated vaccines in humans are just recently being studied. In one such analysis, the mean percentages of IFN-γ-secreting influenza antigen-specific T cells (both $CD4^+$ and $CD8^+$) increased significantly after attenuated virus but not after inactivated virus immunization in children aged 5 to 9 years (He and others 2006). Although such differences are not necessarily confirmed in other age groups (He and others 2006), classically, inactivated virus vaccine is considered more efficient in the generation of humoral rather than $CD8^+$ T cell responses (Palese and Garcia-Sastre 2002). However, this might be related to the standard intramuscular route of vaccination. Herein, both vaccines were delivered via the same routes, i.e. i.v. and i.p., since our objective was to utilize responses to these vaccines as a measurement of *in vivo* antigen presenting cell function. Thus, these results demonstrate the value of humanized mice in testing immunogenic efficacy of vaccines.

We found predominant CTL phenotype in inactivated virus-vaccinated mice while live attenuated virus-vaccinated mice showed the presence of two separate populations, i.e. CTLs and cytokine (IFN-γ)-producing $CD8^+$ T cells. The mechanism(s) leading to the polarization of effector phenotype to CTLs in mice vaccinated with inactivated virus remains to be determined. Nevertheless, the expansion of FluM1-specific memory $CD8^+$ T cells with different phenotypes might reflect the plasticity of virus-specific memory T cell compartment (Selin and Welsh 2004). Indeed, memory T cells are heterogeneous and can yield different functional phenotypes. In our model, this

might be combined with the presentation of influenza vaccine antigens by distinct APCs. This point needs to be established.

In fact, our model goes beyond influenza vaccines. We showed here that humanized mice could be vaccinated with *ex vivo*-generated DCs to analyze primary response to tumor-associated antigen. Therefore, this model can be used in the design of DCs-based immunotherapy used for cancer patients. Although the active immunotherapy using *ex vivo*-generated DCs pulsed with antigens is now in clinical trials, the induction of effector $CD8^+$ T cells with high avidity is still suboptimal (Palucka and others 2007). The improvements could be done via improving antigen preparation or DCs maturation. Using humanized mice, we can fine-tune the parameters to select the best combination of antigens and DCs for the better $CD8^+$ T cells response before costly and resource demanding clinical trials.

CHAPTER SIX

Conclusions

- Our results using seasonal influenza vaccines demonstrate the value of humanized mice in testing the quality of vaccine elicited immune responses.

- Our results using anti-DC and FluM1 fusion protein demonstrate *in vivo* DC targeting, thereby further proving the value of humanized mice to study the physiology of human DCs as well as novel vaccination strategies.

DCs play a central role in vaccination as illustrated in Figure 34. Traditional influenza vaccines delivered intramuscularly induce an immune response through random targeting antigen to different DC subset, i.e. interstitial DCs, Langerhans cells or pDCs. To ensure a direct delivery of antigen to a desired DC subset, vaccination with antigen-pulsed *ex vivo*-generated DCs can ensure the right delivery. However, using DCs as vectors for preventing influenza virus infection may be impractical despite therapeutic DCs vaccines are used in clinical trials on cancer patients (Palucka and others 2006). The novel vaccines based on antibody recognition to specific receptor on DCs will allow the delivery of antigen carried by antibody into a desired DCs subset and endocytic compartment for antigen presentation. Since this targeting vaccine is based on antibody recognition, an *in vivo* system with human immune system will be preferable. Hence, humanized mice are valuable in testing novel vaccine based on targeting human DCs.

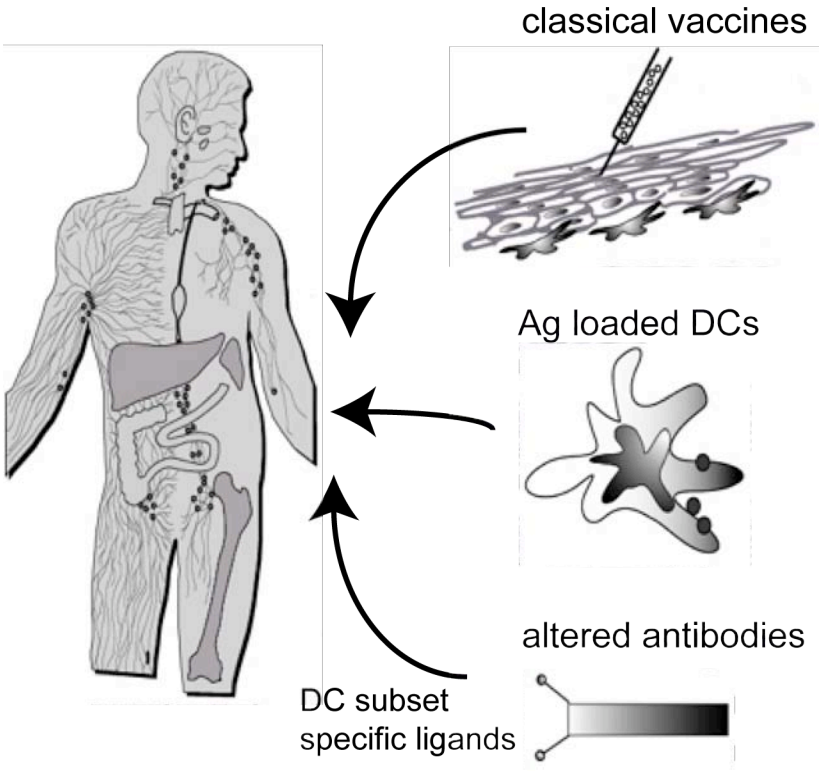

Figure 33. DCs play a central role in vaccination. The design of novel vaccines is evolving from random targeting of human DCs by classical vaccine to specifically targeting antigen into a particular DC subset. Antigen-pulsed DC vaccination serves as an intermediate necessary to establish the optimal antigens loading and DC activation strategy.

APPENDIX

APPENDIX

List of Current and Future Publications

Original Publications

1. **Yu CI,** Gallegos M, Marches F, Zurawski Z, Ramilo O, Zurawski S, García-Sastre A, Banchereau J and Palucka AK. Cross-presentation of attenuated and inactivated influenza virus vaccine antigens to $CD8^+$ T cells in humanized mice (in preparation).

2. Matsui T, Connolly JE, Michnevitz M, Chaussabel D, **Yu CI**, Glaser C, Tindle S, Pypaert M, Freitas H, Piqueras B, Banchereau J and Palucka AK. CD2 distinguishes two subsets of human plasmacytoid dendritic cells with distinct phenotype and functions (submitted).

3. Klechevsky E, **Yu CI**, Flamar A, Snipes L, Marches F, Cao Y, Liu M, Li XH, Gallegos M, Agouna-Deciat O, Reiter Y, Zurawski S, Zurawski G, Palucka AK, Banchereau J. Cross-priming human CD8+ T cells through targeting antigens to myeloid and plasmacytoid dendritic cells via DCIR, a C-type lectin containing an immunoreceptor tyrosine-based inhibitory motif (in preparation).

4. **Yu CI,** Marches F, Gallegos M, Oh S, Zurawski S, Ramilo O, Solorzano A, García-Sastre A, Zurawski G, Banchereau J and Palucka AK. Humanized mice generate antibody responses to influenza virus vaccines (in preparation).

5. **Yu CI**, Marches F, Pedroza-Gonzales A, Gallegos M, Banchereau J and Palucka AK. Humanized mice to test the immune efficacy of *ex vivo* generated DC vaccine (in preparation).

6. **Yu CI,** Marches F, Gallegos M, Ramilo O, García-Sastre A, Zurawski S, Zurawski G Banchereau J and Palucka AK. Humanized mice to study pathophysiology of human DCs in the lung (in preparation).

Review

Aspord C, **Yu CI**, Banchereau J and Palucka AK. 2007. Humanized mice for the development and testing of human vaccines. Expert Opin Drug Discov 2(7):949-960.

BIBLIOGRAPHY

Ackerman AL, Kyritsis C, Tampe R, Cresswell P. 2003. Early phagosomes in dendritic cells form a cellular compartment sufficient for cross presentation of exogenous antigens. Proc Natl Acad Sci U S A 100(22):12889-94.

Ackerman AL, Kyritsis C, Tampe R, Cresswell P. 2005. Access of soluble antigens to the endoplasmic reticulum can explain cross-presentation by dendritic cells. Nat Immunol 6(1):107-13.

Akbari O, Freeman GJ, Meyer EH, Greenfield EA, Chang TT, Sharpe AH, Berry G, DeKruyff RH, Umetsu DT. 2002. Antigen-specific regulatory T cells develop via the ICOS-ICOS-ligand pathway and inhibit allergen-induced airway hyperreactivity. Nat Med 8(9):1024-32.

Albert ML, Sauter B, Bhardwaj N. 1998. Dendritic cells acquire antigen from apoptotic cells and induce class I-restricted CTLs. Nature 392(6671):86-9.

Allan RS, Waithman J, Bedoui S, Jones CM, Villadangos JA, Zhan Y, Lew AM, Shortman K, Heath WR, Carbone FR. 2006. Migratory dendritic cells transfer antigen to a lymph node-resident dendritic cell population for efficient CTL priming. Immunity 25(1):153-62.

Arndt U, Wennemuth G, Barth P, Nain M, Al-Abed Y, Meinhardt A, Gemsa D, Bacher M. 2002. Release of macrophage migration inhibitory factor and CXCL8/interleukin-8 from lung epithelial cells rendered necrotic by influenza A virus infection. J Virol 76(18):9298-306.

Arpin C, Dechanet J, Van Kooten C, Merville P, Grouard G, Briere F, Banchereau J, Liu YJ. 1995. Generation of memory B cells and plasma cells in vitro. Science 268(5211):720-2.

Baenziger S, Tussiwand R, Schlaepfer E, Mazzucchelli L, Heikenwalder M, Kurrer MO, Behnke S, Frey J, Oxenius A, Joller H and others. 2006. Disseminated and sustained HIV infection in CD34+ cord blood cell-transplanted Rag2-/-gamma c-/- mice. Proc Natl Acad Sci U S A 103(43):15951-6.

Banchereau J, Steinman RM. 1998. Dendritic cells and the control of immunity. Nature 392(6673):245-52.

Barton GM, Kagan JC, Medzhitov R. 2006. Intracellular localization of Toll-like receptor 9 prevents recognition of self DNA but facilitates access to viral DNA. Nat Immunol 7(1):49-56.

Bates EE, Fournier N, Garcia E, Valladeau J, Durand I, Pin JJ, Zurawski SM, Patel S, Abrams JS, Lebecque S and others. 1999. APCs express DCIR, a novel C-type lectin surface receptor containing an immunoreceptor tyrosine-based inhibitory motif. J Immunol 163(4):1973-83.

Beigel JH, Farrar J, Han AM, Hayden FG, Hyer R, de Jong MD, Lochindarat S, Nguyen TK, Nguyen TH, Tran TH and others. 2005. Avian influenza A (H5N1) infection in humans. N Engl J Med 353(13):1374-85.

Belz GT, Behrens GM, Smith CM, Miller JF, Jones C, Lejon K, Fathman CG, Mueller SN, Shortman K, Carbone FR and others. 2002. The CD8alpha(+) dendritic cell is responsible for inducing peripheral self-tolerance to tissue-associated antigens. J Exp Med 196(8):1099-104.

Belz GT, Smith CM, Eichner D, Shortman K, Karupiah G, Carbone FR, Heath WR. 2004a. Cutting edge: conventional CD8 alpha+ dendritic cells are generally involved in priming CTL immunity to viruses. J Immunol 172(4):1996-2000.

Belz GT, Smith CM, Kleinert L, Reading P, Brooks A, Shortman K, Carbone FR, Heath WR. 2004b. Distinct migrating and nonmigrating dendritic cell populations are involved in MHC class I-restricted antigen presentation after lung infection with virus. Proc Natl Acad Sci U S A 101(23):8670-5.

Belz GT, Xie W, Doherty PC. 2001. Diversity of epitope and cytokine profiles for primary and secondary influenza a virus-specific CD8+ T cell responses. J Immunol 166(7):4627-33.

Bender A, Albert M, Reddy A, Feldman M, Sauter B, Kaplan G, Hellman W, Bhardwaj N. 1998. The distinctive features of influenza virus infection of dendritic cells. Immunobiology 198(5):552-67.

Bennett SR, Carbone FR, Karamalis F, Miller JF, Heath WR. 1997. Induction of a CD8+ cytotoxic T lymphocyte response by cross-priming requires cognate CD4+ T cell help. J Exp Med 186(1):65-70.

Bettelli E, Korn T, Kuchroo VK. 2007. Th17: the third member of the effector T cell trilogy. Curr Opin Immunol 19(6):652-7.

Betts MR, Brenchley JM, Price DA, De Rosa SC, Douek DC, Roederer M, Koup RA. 2003. Sensitive and viable identification of antigen-specific CD8+ T cells by a flow cytometric assay for degranulation. J Immunol Methods 281(1-2):65-78.

Beyer WE, Palache AM, de Jong JC, Osterhaus AD. 2002. Cold-adapted live influenza vaccine versus inactivated vaccine: systemic vaccine reactions, local and systemic antibody response, and vaccine efficacy. A meta-analysis. Vaccine 20(9-10):1340-53.

Bhatia M, Bonnet D, Murdoch B, Gan OI, Dick JE. 1998. A newly discovered class of human hematopoietic cells with SCID-repopulating activity. Nat Med 4(9):1038-45.

Bhatia M, Wang JC, Kapp U, Bonnet D, Dick JE. 1997. Purification of primitive human hematopoietic cells capable of repopulating immune-deficient mice. Proc Natl Acad Sci U S A 94(10):5320-5.

Birch-Machin I, Rowan A, Pick J, Mumford J, Binns M. 1997. Expression of the nonstructural protein NS1 of equine influenza A virus: detection of anti-NS1 antibody in post infection equine sera. J Virol Methods 65(2):255-63.

Blander JM, Medzhitov R. 2006. Toll-dependent selection of microbial antigens for presentation by dendritic cells. Nature 440(7085):808-12.

Bonifaz L, Bonnyay D, Mahnke K, Rivera M, Nussenzweig MC, Steinman RM. 2002. Efficient targeting of protein antigen to the dendritic cell receptor DEC-205 in the steady state leads to antigen presentation on major histocompatibility complex class I products and peripheral CD8+ T cell tolerance. J Exp Med 196(12):1627-38.

Bonifaz LC, Bonnyay DP, Charalambous A, Darguste DI, Fujii S, Soares H, Brimnes MK, Moltedo B, Moran TM, Steinman RM. 2004. In vivo targeting of antigens to maturing dendritic cells via the DEC-205 receptor improves T cell vaccination. J Exp Med 199(6):815-24.

Boon AC, de Mutsert G, Graus YM, Fouchier RA, Sintnicolaas K, Osterhaus AD, Rimmelzwaan GF. 2002. The magnitude and specificity of influenza A virus-specific cytotoxic T-lymphocyte responses in humans is related to HLA-A and -B phenotype. J Virol 76(2):582-90.

Bosma GC, Custer RP, Bosma MJ. 1983. A severe combined immunodeficiency mutation in the mouse. Nature 301(5900):527-30.

Boyle J, Eastman D, Millar C, Camuglia S, Cox J, Pearse M, Good J, Drane D. 2007. The utility of ISCOMATRIX adjuvant for dose reduction of antigen for vaccines requiring antibody responses. Vaccine 25(14):2541-4.

Breitfeld D, Ohl L, Kremmer E, Ellwart J, Sallusto F, Lipp M, Forster R. 2000. Follicular B helper T cells express CXC chemokine receptor 5, localize to B cell follicles, and support immunoglobulin production. J Exp Med 192(11):1545-52.

Brokstad KA, Eriksson JC, Cox RJ, Tynning T, Olofsson J, Jonsson R, Davidsson A. 2002. Parenteral vaccination against influenza does not induce a local antigen-specific immune response in the nasal mucosa. J Infect Dis 185(7):878-84.

Bryant VL, Ma CS, Avery DT, Li Y, Good KL, Corcoran LM, de Waal Malefyt R, Tangye SG. 2007. Cytokine-mediated regulation of human B cell differentiation into Ig-secreting cells: predominant role of IL-21 produced by CXCR5+ T follicular helper cells. J Immunol 179(12):8180-90.

Bukczynski J, Wen T, Ellefsen K, Gauldie J, Watts TH. 2004. Costimulatory ligand 4-1BBL (CD137L) as an efficient adjuvant for human antiviral cytotoxic T cell responses. Proc Natl Acad Sci U S A 101(5):1291-6.

Burgdorf S, Kautz A, Bohnert V, Knolle PA, Kurts C. 2007. Distinct pathways of antigen uptake and intracellular routing in CD4 and CD8 T cell activation. Science 316(5824):612-6.

Bush RM, Bender CA, Subbarao K, Cox NJ, Fitch WM. 1999. Predicting the evolution of human influenza A. Science 286:1921-1925.

Cao X, Shores EW, Hu-Li J, Anver MR, Kelsall BL, Russell SM, Drago J, Noguchi M, Grinberg A, Bloom ET and others. 1995. Defective lymphoid development in mice lacking expression of the common cytokine receptor gamma chain. Immunity 2(3):223-38.

Carballido JM, Namikawa R, Carballido-Perrig N, Antonenko S, Roncarolo MG, de Vries JE. 2000. Generation of primary antigen-specific human T- and B-cell responses in immunocompetent SCID-hu mice. Nat Med 6(1):103-6.

Carballido JM, Schols D, Namikawa R, Zurawski S, Zurawski G, Roncarolo MG, de Vries JE. 1995. IL-4 induces human B cell maturation and IgE synthesis in SCID-hu mice. Inhibition of ongoing IgE production by in vivo treatment with an IL-4/IL-13 receptor antagonist. J Immunol 155(9):4162-70.

Cashman J, Bockhold K, Hogge DE, Eaves AC, Eaves CJ. 1997a. Sustained proliferation, multi-lineage differentiation and maintenance of primitive human haemopoietic cells in NOD/SCID mice transplanted with human cord blood. Br J Haematol 98(4):1026-36.

Cashman JD, Lapidot T, Wang JC, Doedens M, Shultz LD, Lansdorp P, Dick JE, Eaves CJ. 1997b. Kinetic evidence of the regeneration of multilineage hematopoiesis from primitive cells in normal human bone marrow transplanted into immunodeficient mice. Blood 89(12):4307-16.

Caux C, Massacrier C, Vanbervliet B, Dubois B, Durand I, Cella M, Lanzavecchia A, Banchereau J. 1997. CD34+ hematopoietic progenitors from human cord blood differentiate along two independent dendritic cell pathways in response to granulocyte-macrophage colony-stimulating factor plus tumor necrosis factor alpha: II. Functional analysis. Blood 90(4):1458-70.

Caux C, Massacrier C, Vanbervliet B, Dubois B, Van Kooten C, Durand I, Banchereau J. 1994. Activation of human dendritic cells through CD40 cross-linking. J Exp Med 180(4):1263-72.

Caux C, Vanbervliet B, Massacrier C, Dezutter-Dambuyant C, de Saint-Vis B, Jacquet C, Yoneda K, Imamura S, Schmitt D, Banchereau J. 1996. CD34+ hematopoietic progenitors from human cord blood differentiate along two independent dendritic cell pathways in response to GM-CSF+TNF alpha. J Exp Med 184(2):695-706.

Cella M, Facchetti F, Lanzavecchia A, Colonna M. 2000. Plasmacytoid dendritic cells activated by influenza virus and CD40L drive a potent TH1 polarization. Nat Immunol 1(4):305-10.

Cerwenka A, Morgan TM, Dutton RW. 1999a. Naive, effector, and memory CD8 T cells in protection against pulmonary influenza virus infection: homing properties rather than initial frequencies are crucial. J Immunol 163(10):5535-43.

Cerwenka A, Morgan TM, Harmsen AG, Dutton RW. 1999b. Migration kinetics and final destination of type 1 and type 2 CD8 effector cells predict protection against pulmonary virus infection. J Exp Med 189(2):423-34.

Chen W, Antonenko S, Sederstrom JM, Liang X, Chan AS, Kanzler H, Blom B, Blazar BR, Liu YJ. 2004. Thrombopoietin cooperates with FLT3-ligand in the generation of plasmacytoid dendritic cell precursors from human hematopoietic progenitors. Blood 103(7):2547-53.

Chtanova T, Tangye SG, Newton R, Frank N, Hodge MR, Rolph MS, Mackay CR. 2004. T Follicular Helper Cells Express a Distinctive Transcriptional Profile, Reflecting Their Role as Non-Th1/Th2 Effector Cells That Provide Help for B Cells. J Immunol 173(1):68-78.

Cottey R, Rowe C, Bender B. 2001. Influenza virus. Current Protocols in Immunology. Hoboken, NJ: John Wiley & Sons, Inc. p 19.11.4-31.

Cresswell P, Ackerman AL, Giodini A, Peaper DR, Wearsch PA. 2005. Mechanisms of MHC class I-restricted antigen processing and cross-presentation. Immunol Rev 207:145-57.

Crowe SR, Turner SJ, Miller SC, Roberts AD, Rappolo RA, Doherty PC, Ely KH, Woodland DL. 2003. Differential antigen presentation regulates the changing patterns of CD8+ T cell immunodominance in primary and secondary influenza virus infections. J Exp Med 198(3):399-410.

Day CL, Kaufmann DE, Kiepiela P, Brown JA, Moodley ES, Reddy S, Mackey EW, Miller JD, Leslie AJ, DePierres C and others. 2006. PD-1 expression on HIV-specific T cells is associated with T-cell exhaustion and disease progression. Nature 443(7109):350-4.

de Jong MD, Bach VC, Phan TQ, Vo MH, Tran TT, Nguyen BH, Beld M, Le TP, Truong HK, Nguyen VV and others. 2005. Fatal avian influenza A (H5N1) in a child presenting with diarrhea followed by coma. N Engl J Med 352(7):686-91.

Delneste Y. 2004. Scavenger receptors and heat-shock protein-mediated antigen cross-presentation. Biochem Soc Trans 32(Pt 4):633-5.

Delneste Y, Magistrelli G, Gauchat J, Haeuw J, Aubry J, Nakamura K, Kawakami-Honda N, Goetsch L, Sawamura T, Bonnefoy J and others. 2002. Involvement of LOX-1 in dendritic cell-mediated antigen cross-presentation. Immunity 17(3):353-62.

Dhodapkar MV, Steinman RM. 2002. Antigen-bearing immature dendritic cells induce peptide-specific CD8(+) regulatory T cells in vivo in humans. Blood 100(1):174-7.

Diebold SS, Kaisho T, Hemmi H, Akira S, Reis e Sousa C. 2004. Innate antiviral responses by means of TLR7-mediated recognition of single-stranded RNA. Science 303:1529-1531.

Dimmock NJ. 1969. New virus-specific antigens in cells infected with influenza virus. Virology 39(2):224-34.

Dubsky P, Saito H, Leogier M, Dantin C, Connolly JE, Banchereau J, Palucka AK. 2007. IL-15-induced human DC efficiently prime melanoma-specific naive CD8+ T cells to differentiate into CTL. Eur J Immunol 37(6):1678-90.

Ferguson NM, Galvani AP, Bush RM. 2003. Ecological and immunological determinants of influenza evolution. Nature 422:428-433.

Ferko B, Stasakova J, Romanova J, Kittel C, Sereinig S, Katinger H, Egorov A. 2004. Immunogenicity and protection efficacy of replication-deficient influenza A viruses with altered NS1 genes. J Virol 78(23):13037-45.

Flynn KJ, Belz GT, Altman JD, Ahmed R, Woodland DL, Doherty PC. 1998. Virus-specific CD8+ T cells in primary and secondary influenza pneumonia. Immunity 8(6):683-91.

Fodor E, Devenish L, Engelhardt OG, Palese P, Brownlee GG, Garcia-Sastre A. 1999. Rescue of influenza A virus from recombinant DNA. J Virol 73(11):9679-82.

Fonteneau JF, Gilliet M, Larsson M, Dasilva I, Munz C, Liu YJ, Bhardwaj N. 2003. Activation of influenza virus-specific CD4+ and CD8+ T cells: a new role for plasmacytoid dendritic cells in adaptive immunity. Blood 101(9):3520-6.

Fraser CC, Kaneshima H, Hansteen G, Kilpatrick M, Hoffman R, Chen BP. 1995. Human allogeneic stem cell maintenance and differentiation in a long-term multilineage SCID-hu graft. Blood 86(5):1680-93.

Freeman GJ, Long AJ, Iwai Y, Bourque K, Chernova T, Nishimura H, Fitz LJ, Malenkovich N, Okazaki T, Byrne MC and others. 2000. Engagement of the PD-1 immunoinhibitory receptor by a novel B7 family member leads to negative regulation of lymphocyte activation. J Exp Med 192(7):1027-34.

Fukaura H, Kent SC, Pietrusewicz MJ, Khoury SJ, Weiner HL, Hafler DA. 1996. Induction of circulating myelin basic protein and proteolipid protein-specific transforming grwoth factor-b1-secreting Th3 cells by oral administration of myelin in multiple sclerosis patients. J. Clin. Invest. 98(1):70-77.

Gay NJ, Gangloff M. 2007. Structure and function of Toll receptors and their ligands. Annu Rev Biochem 76:141-65.

Geijtenbeek TB, van Vliet SJ, Engering A, t Hart BA, van Kooyk Y. 2004. Self- and nonself-recognition by C-type lectins on dendritic cells. Annu Rev Immunol 22:33-54.

Gerhard W. 2001. The role of the antibody response in influenza virus infection. Curr Top Microbiol Immunol 260:171-90.

Gething MJ, Bye J, Skehel J, Waterfield M. 1980. Cloning and DNA sequence of double-stranded copies of haemagglutinin genes from H2 and H3 strains elucidates antigenic shift and drift in human influenza virus. Nature 287(5780):301-6.

Gianfrani C, Oseroff C, Sidney J, Chesnut RW, Sette A. 2000. Human memory CTL response specific for influenza A virus is broad and multispecific. Hum Immunol 61(5):438-52.

Gimeno R, Weijer K, Voordouw A, Uittenbogaart CH, Legrand N, Alves NL, Wijnands E, Blom B, Spits H. 2004. Monitoring the effect of gene silencing by RNA interference in human CD34+ cells injected into newborn RAG2-/- gammac-/- mice: functional inactivation of p53 in developing T cells. Blood 104(13):3886-93.

Gitlin L, Barchet W, Gilfillan S, Cella M, Beutler B, Flavell RA, Diamond MS, Colonna M. 2006. Essential role of mda-5 in type I IFN responses to polyriboinosinic:polyribocytidylic acid and encephalomyocarditis picornavirus. Proc Natl Acad Sci U S A 103(22):8459-64.

Gomez-Puertas P, Albo C, Perez-Pastrana E, Vivo A, Portela A. 2000. Influenza virus matrix protein is the major driving force in virus budding. J Virol 74(24):11538-47.

Gordon PR, Leimig T, Babarin-Dorner A, Houston J, Holladay M, Mueller I, Geiger T, Handgretinger R. 2003. Large-scale isolation of CD133+ progenitor cells from G-CSF mobilized peripheral blood stem cells. Bone Marrow Transplant 31(1):17-22.

Gotch F, Rothbard J, Howland K, Townsend A, McMichael A. 1987. Cytotoxic T lymphocytes recognize a fragment of influenza virus matrix protein in association with HLA-A2. Nature 326(6116):881-2.

Greenwald RJ, Freeman GJ, Sharpe AH. 2005. The B7 family revisited. Annu Rev Immunol 23:515-48.

Groux H, O'Garra A, Bigler M, Rouleau M, Antonenko S, de Vries JE, Roncarolo MG. 1997. A CD4+ T-cell subset inhibits antigen-specific T-cell responses and prevent colitis. Nature 389:737-742.

Guermonprez P, Saveanu L, Kleijmeer M, Davoust J, Van Endert P, Amigorena S. 2003. ER-phagosome fusion defines an MHC class I cross-presentation compartment in dendritic cells. Nature 425(6956):397-402.

Habib T, Senadheera S, Weinberg K, Kaushansky K. 2002. The common gamma chain (gamma c) is a required signaling component of the IL-21 receptor and supports IL-21-induced cell proliferation via JAK3. Biochemistry 41(27):8725-31.

Harada Y, Muramatsu M, Shibata T, Honjo T, Kuroda K. 2003. Unmutated immunoglobulin M can protect mice from death by influenza virus infection. J Exp Med 197(12):1779-85.

Hazenberg MD, Borghans JA, de Boer RJ, Miedema F. 2003. Thymic output: a bad TREC record. Nat Immunol 4(2):97-9.

He XS, Holmes TH, Zhang C, Mahmood K, Kemble GW, Lewis DB, Dekker CL, Greenberg HB, Arvin AM. 2006. Cellular immune responses in children and adults receiving inactivated or live attenuated influenza vaccines. J Virol 80(23):11756-66.

Hendriks J, Gravestein LA, Tesselaar K, van Lier RA, Schumacher TN, Borst J. 2000. CD27 is required for generation and long-term maintenance of T cell immunity. Nat Immunol 1(5):433-40.

Heufler C, Koch F, Stanzl U, Topar G, Wysocka M, Trinchieri G, Enk A, Steinman RM, Romani N, Schuler G. 1996. Interleukin-12 is produced by dendritic cells and mediates T helper 1 development as well as interferon-gamma production by T helper 1 cells. Eur J Immunol 26(3):659-68.

Hiramatsu H, Nishikomori R, Heike T, Ito M, Kobayashi K, Katamura K, Nakahata T. 2003. Complete reconstitution of human lymphocytes from cord blood CD34+ cells using the NOD/SCID/gammacnull mice model. Blood 102(3):873-80.

Horisberger MA. 1995. Interferons, Mx genes, and resistance to influenza virus. Am J Respir Crit Care Med 152(4 Pt 2):S67-71.

Houde M, Bertholet S, Gagnon E, Brunet S, Goyette G, Laplante A, Princiotta MF, Thibault P, Sacks D, Desjardins M. 2003. Phagosomes are competent organelles for antiggen cross-presentation. Nature 425:402-406.

Hutloff A, Dittrich AM, Beier KC, Eljaschewitsch B, Kraft R, Anagnostopoulos I, Kroczek RA. 1999. ICOS is an inducible T-cell co-stimulator structurally and functionally related to CD28. Nature 397(6716):263-6.

Ifversen P, Borrebaeck CA. 1996. SCID-hu-PBL: a model for making human antibodies? Semin Immunol 8(4):243-8.

Ishikawa F, Yasukawa M, Lyons B, Yoshida S, Miyamoto T, Yoshimoto G, Watanabe T, Akashi K, Shultz LD, Harada M. 2005. Development of functional human blood and immune systems in NOD/SCID/IL2 receptor {gamma} chain(null) mice. Blood 106(5):1565-73.

Ito T, Wang YH, Duramad O, Hanabuchi S, Perng OA, Gilliet M, Qin FX, Liu YJ. 2006. OX40 ligand shuts down IL-10-producing regulatory T cells. Proc Natl Acad Sci U S A 103(35):13138-43.

Ito T, Yang M, Wang YH, Lande R, Gregorio J, Perng OA, Qin XF, Liu YJ, Gilliet M. 2007. Plasmacytoid dendritic cells prime IL-10-producing T regulatory cells by inducible costimulator ligand. J Exp Med 204(1):105-15.

Itoh M, Takahashi T, Sakaguchi N, Kuniyasu Y, Shimizu J, Otsuka F, Sakaguchi S. 1999. Thymus and autoimmunity: production of CD25+CD4+ naturally anergic and suppressive T cells as a key function of the thymus in maintaining immunologic self-tolerance. J. Immunol. 162:5317-5326.

Jameson J, Cruz J, Ennis FA. 1998. Human cytotoxic T-lymphocyte repertoire to influenza A viruses. J Virol 72(11):8682-9.

Jarrossay D, Napolitani G, Colonna M, Sallusto F, Lanzavecchia A. 2001. Specialization and complementarity in microbial molecule recognition by human myeloid and plasmacytoid dendritic cells. Eur. J. Immunol. 31:3388-3393.

Jensen PE. 2007. Recent advances in antigen processing and presentation. Nat Immunol 8(10):1041-8.

Johnson BJ, Costelloe EO, Fitzpatrick DR, Haanen JB, Schumacher TN, Brown LE, Kelso A. 2003. Single-cell perforin and granzyme expression reveals the anatomical localization of effector CD8+ T cells in influenza virus-infected mice. Proc Natl Acad Sci U S A 100(5):2657-62.

Kadowaki N, Antonenko S, Lau JY, Liu YJ. 2000. Natural interferon alpha/beta-producing cells link innate and adaptive immunity. J Exp Med 192(2):219-26.

Kadowaki N, Ho S, Antonenko S, Malefyt RW, Kastelein RA, Bazan F, Liu YJ. 2001. Subsets of human dendritic cell precursors express different toll-like receptors and respond to different microbial antigens. J Exp Med 194(6):863-9.

Kamel-Reid S, Dick JE. 1988. Engraftment of immune-deficient mice with human hematopoietic stem cells. Science 242(4886):1706-9.

Kang DC, Gopalkrishnan RV, Wu Q, Jankowsky E, Pyle AM, Fisher PB. 2002. mda-5: An interferon-inducible putative RNA helicase with double-stranded RNA-dependent ATPase activity and melanoma growth-suppressive properties. Proc Natl Acad Sci U S A 99(2):637-42.

Kapsenberg M. 2003. Dendritic-cell control of pathogen-driven T-cell polarization. Nature Rev. Immunol. 3:984-993.

Karsunky H, Merad M, Cozzio A, Weissman IL, Manz MG. 2003. Flt3 ligand regulates dendritic cell development from Flt3+ lymphoid and myeloid-committed progenitors to Flt3+ dendritic cells in vivo. J Exp Med 198(2):305-13.

Kastelein RA, Hunter CA, Cua DJ. 2007. Discovery and biology of IL-23 and IL-27: related but functionally distinct regulators of inflammation. Annu Rev Immunol 25:221-42.

Kato H, Sato S, Yoneyama M, Yamamoto M, Uematsu S, Matsui K, Tsujimura T, Takeda K, Fujita T, Takeuchi O and others. 2005. Cell type-specific involvement of RIG-I in antiviral response. Immunity 23(1):19-28.

Kawakami Y, Eliyahu S, Sakaguchi K, Robbins PF, Rivoltini L, Yannelli JR, Appella E, Rosenberg SA. 1994. Identification of the immunodominant peptides of the MART-1 human melanoma antigen recognized by the majority of HLA-A2-restricted tumor infiltrating lymphocytes. J Exp Med 180(1):347-52.

Kawaoka Y, Krauss S, Webster RG. 1989. Avian-to-human transmission of the PB1 gene of influenza A viruses in the 1957 and 1968 pandemics. J Virol 63(11):4603-8.

Koguchi Y, Thauland TJ, Slifka MK, Parker DC. 2007. Preformed CD40 ligand exists in secretory lysosomes in effector and memory CD4+ T cells and is quickly expressed on the cell surface in an antigen-specific manner. Blood 110(7):2520-7.

Kogure T, Suzuki T, Takahashi T, Miyamoto D, Hidari KI, Guo CT, Ito T, Kawaoka Y, Suzuki Y. 2006. Human trachea primary epithelial cells express both sialyl(alpha2-3)Gal receptor for human parainfluenza virus type 1 and avian influenza viruses, and sialyl(alpha2-6)Gal receptor for human influenza viruses. Glycoconj J 23(1-2):101-6.

Kolb E, Laine E, Strehler D, Staeheli P. 1992. Resistance to influenza virus infection of Mx transgenic mice expressing Mx protein under the control of two constitutive promoters. J Virol 66(3):1709-16.

Kollet O, Peled A, Byk T, Ben-Hur H, Greiner D, Shultz L, Lapidot T. 2000. beta2 microglobulin-deficient (B2m(null)) NOD/SCID mice are excellent recipients for studying human stem cell function. Blood 95(10):3102-5.

Kopf M, Brombacher F, Bachmann MF. 2002. Role of IgM antibodies versus B cells in influenza virus-specific immunity. Eur J Immunol 32(8):2229-36.

Kuci S, Wessels JT, Buhring HJ, Schilbach K, Schumm M, Seitz G, Loffler J, Bader P, Schlegel PG, Niethammer D and others. 2003. Identification of a novel class of human adherent CD34- stem cells that give rise to SCID-repopulating cells. Blood 101(3):869-76.

Kurts C, Kosaka H, Carbone FR, Miller JF, Heath WR. 1997. Class I-restricted cross-presentation of exogenous self-antigens leads to deletion of autoreactive CD8(+) T cells. J Exp Med 186(2):239-45.

Kuruvilla JG, Troyer RM, Devi S, Akkina R. 2007. Dengue virus infection and immune response in humanized RAG2(-/-)gamma(c)(-/-) (RAG-hu) mice. Virology 369(1):143-52.

Kyoizumi S, Baum CM, Kaneshima H, McCune JM, Yee EJ, Namikawa R. 1992. Implantation and maintenance of functional human bone marrow in SCID-hu mice. Blood 79(7):1704-11.

Lamb RA, Krug RM. 1996. Orthomyxoviridae: the viruses and their replication. In: Fields BN, Knipe DM, Howley PM, editors. Fundamental Virolgoy. 3 ed. Philadelphia: Lippincott-Raven Publishers. p 605-647.

Lambkin R, McLain L, Jones SE, Aldridge SL, Dimmock NJ. 1994. Neutralization escape mutants of type A influenza virus are readily selected by antisera from mice immunized with whole virus: a possible mechanism for antigenic drift. Journal of General Virology 75(12):3493-3502.

Lan P, Tonomura N, Shimizu A, Wang S, Yang YG. 2006. Reconstitution of a functional human immune system in immunodeficient mice through combined human fetal thymus/liver and CD34+ cell transplantation. Blood 108(2):487-92.

Lanzavecchia A, Sallusto F. 2001. Regulation of T cell immunity by dendritic cells. Cell 106(3):263-6.

Lanzavecchia A, Sallusto F. 2005. Understanding the generation and function of memory T cell subsets. Curr Opin Immunol 17(3):326-32.

Lapidot T, Kollet O. 2002. The essential roles of the chemokine SDF-1 and its receptor CXCR4 in human stem cell homing and repopulation of transplanted immune-deficient NOD/SCID and NOD/SCID/B2m(null) mice. Leukemia 16(10):1992-2003.

Lapidot T, Pflumio F, Doedens M, Murdoch B, Williams DE, Dick JE. 1992. Cytokine stimulation of multilineage hematopoiesis from immature human cells engrafted in SCID mice. Science 255(5048):1137-41.

Le Goffic R, Pothlichet J, Vitour D, Fujita T, Meurs E, Chignard M, Si-Tahar M. 2007. Cutting Edge: Influenza A virus activates TLR3-dependent inflammatory and RIG-I-dependent antiviral responses in human lung epithelial cells. J Immunol 178(6):3368-72.

Legge KL, Braciale TJ. 2003. Accelerated migration of respiratory dendritic cells to the regional lymph nodes is limited to the early phase of pulmonary infection. Immunity 18(2):265-77.

Legrand N, Weijer K, Spits H. 2006. Experimental models to study development and function of the human immune system in vivo. J Immunol 176(4):2053-8.

Leroux-Roels I, Borkowski A, Vanwolleghem T, Drame M, Clement F, Hons E, Devaster JM, Leroux-Roels G. 2007. Antigen sparing and cross-reactive immunity with an adjuvanted rH5N1 prototype pandemic influenza vaccine: a randomised controlled trial. Lancet 370(9587):580-9.

Li P, Gregg JL, Wang N, Zhou D, O'Donnell P, Blum JS, Crotzer VL. 2005. Compartmentalization of class II antigen presentation: contribution of cytoplasmic and endosomal processing. Immunol Rev 207:206-17.

Litinskiy MB, Nardelli B, Hilbert DM, He B, Schaffer A, Casali P, Cerutti A. 2002. DCs induce CD40-independent immunoglobulin class switching through BLyS and APRIL. Nat Immunol 3(9):822-9.

Liu C, Eichelberger MC, Compans RW, Air GM. 1995. Influenza type A virus neuraminidase does not play a role in viral entry, replication, assembly, or budding. J Virol 69(2):1099-106.

Liu YJ, Arpin C. 1997. Germinal center development. Immunol Rev 156:111-26.

Lowry PA, Shultz LD, Greiner DL, Hesselton RM, Kittler EL, Tiarks CY, Rao SS, Reilly J, Leif JH, Ramshaw H and others. 1996. Improved engraftment of human cord blood stem cells in NOD/LtSz-scid/scid mice after irradiation or multiple-day injections into unirradiated recipients. Biol Blood Marrow Transplant 2(1):15-23.

Macatonia SE, Hosken NA, Litton M, Vieira P, Hsieh CS, Culpepper JA, Wysocka M, Trinchieri G, Murphy KM, O'Garra A. 1995. Dendritic cells produce IL-12 and direct the development of Th1 cells from naive CD4+ T cells. J Immunol 154(10):5071-9.

MacLennan IC, Toellner KM, Cunningham AF, Serre K, Sze DM, Zuniga E, Cook MC, Vinuesa CG. 2003. Extrafollicular antibody responses. Immunol Rev 194:8-18.

Manser T, Tumas-Brundage KM, Casson LP, Giusti AM, Hande S, Notidis E, Vora KA. 1998. The roles of antibody variable region hypermutation and selection in the development of the memory B-cell compartment. Immunol Rev 162:183-96.

Maraskovsky E, Brasel K, Teepe M, Roux ER, Lyman SD, Shortman K, McKenna HJ. 1996. Dramatic increase in the numbers of functionally mature dendritic cells in Flt3 ligand-treated mice: multiple dendritic cell subpopulations identified. J Exp Med 184(5):1953-62.

Mariathasan S, Monack DM. 2007. Inflammasome adaptors and sensors: intracellular regulators of infection and inflammation. Nat Rev Immunol 7(1):31-40.

Marshall D, Sealy R, Sangster M, Coleclough C. 1999. TH cells primed during influenza virus infection provide help for qualitatively distinct antibody responses to subsequent immunization. J Immunol 163(9):4673-82.

MartIn-Fontecha A, Sebastiani S, Hopken UE, Uguccioni M, Lipp M, Lanzavecchia A, Sallusto F. 2003. Regulation of dendritic cell migration to the draining lymph node: impact on T lymphocyte traffic and priming. J Exp Med 198(4):615-21.

Martln-Fontecha A, Sebastiani S, Hopken UE, Uguccioni M, Lipp M, Lanzavecchia A, Sallusto F. 2003. Regulation of dendritic cell migration to the draining lymph node: impact on T lymphocyte traffic and priming. J. Exp. Med. 198(4):615-621.

Matsumura T, Kametani Y, Ando K, Hirano Y, Katano I, Ito R, Shiina M, Tsukamoto H, Saito Y, Tokuda Y and others. 2003. Functional CD5+ B cells develop predominantly in the spleen of NOD/SCID/gammac(null) (NOG) mice transplanted either with human umbilical cord blood, bone marrow, or mobilized peripheral blood CD34+ cells. Exp Hematol 31(9):789-97.

McCune JM. 1996. Development and applications of the SCID-hu mouse model. Semin Immunol 8(4):187-96.

McCune JM, Namikawa R, Kaneshima H, Shultz LD, Lieberman M, Weissman IL. 1988. The SCID-hu mouse: murine model for the analysis of human hematolymphoid differentiation and function. Science 241(4873):1632-9.

McGettrick AF, O'Neill LA. 2004. The expanding family of MyD88-like adaptors in Toll-like receptor signal transduction. Mol Immunol 41(6-7):577-82.

Medzhitov R, Preston-Hurlburt P, Janeway CA, Jr. 1997. A human homologue of the Drosophila Toll protein signals activation of adaptive immunity. Nature 388(6640):394-7.

Melkus MW, Estes JD, Padgett-Thomas A, Gatlin J, Denton PW, Othieno FA, Wege AK, Haase AT, Garcia JV. 2006. Humanized mice mount specific adaptive and innate immune responses to EBV and TSST-1. Nat Med 12(11):1316-22.

Mestas J, Hughes CC. 2004. Of mice and not men: differences between mouse and human immunology. J Immunol 172(5):2731-8.

Meyer-Wentrup F, Benitez-Ribas D, Tacken PJ, Punt CJ, Figdor CG, de Vries IJ, Adema GJ. 2008. Targeting DCIR on human plasmacytoid dendritic cells results in antigen presentation and inhibits IFN-{alpha} production. Blood.

Mirshahidi S, Huang CT, Sadegh-Nasseri S. 2001. Anergy in peripheral memory CD4(+) T cells induced by low avidity engagement of T cell receptor. J Exp Med 194(6):719-31.

Mombaerts P, Iacomini J, Johnson RS, Herrup K, Tonegawa S, Papaioannou VE. 1992. RAG-1-deficient mice have no mature B and T lymphocytes. Cell 68(5):869-77.

Moser B, Schaerli P, Loetscher P. 2002. CXCR5(+) T cells: follicular homing takes center stage in T-helper-cell responses. Trends Immunol 23(5):250-4.

Mosier DE, Gulizia RJ, Baird SM, Wilson DB. 1988. Transfer of a functional human immune system to mice with severe combined immunodeficiency. Nature 335(6187):256-9.

Mozdzanowska K, Furchner M, Washko G, Mozdzanowski J, Gerhard W. 1997. A pulmonary influenza virus infection in SCID mice can be cured by treatment with hemagglutinin-specific antibodies that display very low virus-neutralizing activity in vitro. J Virol 71(6):4347-55.

Mozdzanowska K, Furchner M, Zharikova D, Feng J, Gerhard W. 2005. Roles of CD4+ T-cell-independent and -dependent antibody responses in the control of influenza virus infection: evidence for noncognate CD4+ T-cell activities that enhance the therapeutic activity of antiviral antibodies. J Virol 79(10):5943-51.

Muller M, Brenig B, Winnacker EL, Brem G. 1992. Transgenic pigs carrying cDNA copies encoding the murine Mx1 protein which confers resistance to influenza virus infection. Gene 121(2):263-70.

Murphy WJ, Taub DD, Longo DL. 1996. The huPBL-SCID mouse as a means to examine human immune function in vivo. Semin Immunol 8(4):233-41.

Namikawa R, Weilbaecher KN, Kaneshima H, Yee EJ, McCune JM. 1990. Long-term human hematopoiesis in the SCID-hu mouse. J Exp Med 172(4):1055-63.

Neumann G, Watanabe T, Ito H, Watanabe S, Goto H, Gao P, Hughes M, Perez DR, Donis R, Hoffmann E and others. 1999. Generation of influenza A viruses entirely from cloned cDNAs. Proc Natl Acad Sci U S A 96(16):9345-50.

Ohmura-Hoshino M, Matsuki Y, Aoki M, Goto E, Mito M, Uematsu M, Kakiuchi T, Hotta H, Ishido S. 2006. Inhibition of MHC class II expression and immune responses by c-MIR. J Immunol 177(1):341-54.

Palese P, Garcia-Sastre A. 2002. Influenza vaccines: present and future. J Clin Invest 110(1):9-13.

Palese P, Schulman JL. 1976. RNA pattern of 'swine' influenza virus isolated from man is similar to those of other swine influenza viruses. Nature 263(5577):528-530.

Palese P, Tobita K, Ueda M, Compans RW. 1974. Characterization of temperature sensitive influenza virus mutants defective in neuraminidase. Virology 61(2):397-410.

Palucka AK, Blanck JP, Bennett L, Pascual V, Banchereau J. 2005a. Cross-regulation of TNF and IFN-alpha in autoimmune diseases. Proc Natl Acad Sci U S A 102(9):3372-7.

Palucka AK, Gatlin J, Blanck JP, Melkus MW, Clayton S, Ueno H, Kraus ET, Cravens P, Bennett L, Padgett-Thomas A and others. 2003. Human dendritic cell subsets in NOD/SCID mice engrafted with CD34+ hematopoietic progenitors. Blood 102(9):3302-10.

Palucka AK, Laupeze B, Aspord C, Saito H, Jego G, Fay J, Paczesny S, Pascual V, Banchereau J. 2005b. Immunotherapy via dendritic cells. Adv Exp Med Biol 560:105-14.

Palucka AK, Ueno H, Connolly J, Kerneis-Norvell F, Blanck JP, Johnston DA, Fay J, Banchereau J. 2006. Dendritic cells loaded with killed allogeneic melanoma cells can induce objective clinical responses and MART-1 specific CD8+ T-cell immunity. J Immunother 29(5):545-57.

Palucka AK, Ueno H, Fay JW, Banchereau J. 2007. Taming cancer by inducing immunity via dendritic cells. Immunol Rev 220(1):129-50.

Palucka K, Banchereau J. 2002. How dendritic cells and microbes interact to elicit or subvert protective immune responses. Curr Opin Immunol 14(4):420-31.

Pape KA, Catron DM, Itano AA, Jenkins MK. 2007. The humoral immune response is initiated in lymph nodes by B cells that acquire soluble antigen directly in the follicles. Immunity 26(4):491-502.

Paus D, Phan TG, Chan TD, Gardam S, Basten A, Brink R. 2006. Antigen recognition strength regulates the choice between extrafollicular plasma cell and germinal center B cell differentiation. J Exp Med 203(4):1081-91.

Pavlovic J, Haller O, Staeheli P. 1992. Human and mouse Mx proteins inhibit different steps of the influenza virus multiplication cycle. J Virol 66(4):2564-9.

Peiris M, Yuen KY, Leung CW, Chan KH, Ip PL, Lai RW, Orr WK, Shortridge KF. 1999. Human infection with influenza H9N2. Lancet 354(9182):916-7.

Peled A, Petit I, Kollet O, Magid M, Ponomaryov T, Byk T, Nagler A, Ben-Hur H, Many A, Shultz L and others. 1999. Dependence of human stem cell engraftment and repopulation of NOD/SCID mice on CXCR4. Science 283(5403):845-8.

Phan TG, Paus D, Chan TD, Turner ML, Nutt SL, Basten A, Brink R. 2006. High affinity germinal center B cells are actively selected into the plasma cell compartment. J Exp Med 203(11):2419-24.

Pichlmair A, Schulz O, Tan CP, Naslund TI, Liljestrom P, Weber F, Reis e Sousa C. 2006. RIG-I-mediated antiviral responses to single-stranded RNA bearing 5'-phosphates. Science 314(5801):997-1001.

Piqueras B, Connolly J, Freitas H, Palucka AK, Banchereau J. 2006. Upon viral exposure, myeloid and plasmacytoid dendritic cells produce 3 waves of distinct chemokines to recruit immune effectors. Blood 107(7):2613-8.

Prochazka M, Gaskins HR, Shultz LD, Leiter EH. 1992. The nonobese diabetic scid mouse: model for spontaneous thymomagenesis associated with immunodeficiency. Proc Natl Acad Sci U S A 89(8):3290-4.

Pulendran B, Banchereau J, Burkeholder S, Kraus E, Guinet E, Chalouni C, Caron D, Maliszewski C, Davoust J, Fay J and others. 2000. Flt3-ligand and granulocyte colony-stimulating factor mobilize distinct human dendritic cell subsets in vivo. J Immunol 165(1):566-72.

Pulendran B, Palucka K, Banchereau J. 2001. Sensing pathogens and tuning immune responses. Science 293(5528):253-6.

Pulendran B, Smith JL, Caspary G, Brasel K, Pettit D, Maraskovsky E, Maliszewski CR. 1999. Distinct dendritic cell subsets differentially regulate the class of immune response in vivo. Proc Natl Acad Sci U S A 96(3):1036-41.

Qi H, Egen JG, Huang AY, Germain RN. 2006. Extrafollicular activation of lymph node B cells by antigen-bearing dendritic cells. Science 312(5780):1672-6.

Renegar KB, Small PA, Jr., Boykins LG, Wright PF. 2004. Role of IgA versus IgG in the control of influenza viral infection in the murine respiratory tract. J Immunol 173(3):1978-86.

Rissoan MC, Soumelis V, Kadowaki N, Grouard G, Briere F, de Waal Malefyt R, Liu YJ. 1999. Reciprocal control of T helper cell and dendritic cell differentiation. Science 283(5405):1183-6.

Roncarolo MG, Battaglia M. 2007. Regulatory T-cell immunotherapy for tolerance to self antigens and alloantigens in humans. Nat Rev Immunol 7(8):585-98.

Rouleau M, Namikawa R, Antonenko S, Carballido-Perrig N, Roncarolo MG. 1996. Antigen-specific cytotoxic T cells mediate human fetal pancreas allograft rejection in SCID-hu mice. J Immunol 157(12):5710-20.

Saeki H, Moore AM, Brown MJ, Hwang ST. 1999. Secondary lymphoid-tissue chemokine (SLC) and CC chemokine receptor 7 (CCR7) participate in the emigration pathway of mature dendritic cells from the skin to regional lymph nodes. J. Immunol. 162:2472-2475.

Sakaguchi S. 2006. Regulatory T cells. Springer Semin Immunopathol 28(1):1-2.

Sallusto F, Palermo B, Lenig D, Miettinen M, Matikainen S, Julkunen I, Forster R, Burgstahler R, Lipp M, Lanzavecchia A. 1999. Distinct patterns and kinetics of chemokine production regulate dendritic cell function. Eur. J. Immunol. 29:1617-1625.

Schaerli P, Willimann K, Lang AB, Lipp M, Loetscher P, Moser B. 2000. CXC chemokine receptor 5 expression defines follicular homing T cells with B cell helper function. J Exp Med 192(11):1553-62.

Schmid D, Pypaert M, Munz C. 2007. Antigen-loading compartments for major histocompatibility complex class II molecules continuously receive input from autophagosomes. Immunity 26(1):79-92.

Schneider P, MacKay F, Steiner V, Hofmann K, Bodmer JL, Holler N, Ambrose C, Lawton P, Bixler S, Acha-Orbea H and others. 1999. BAFF, a novel ligand of the tumor necrosis factor family, stimulates B cell growth. J Exp Med 189(11):1747-56.

Sealy R, Surman S, Hurwitz JL, Coleclough C. 2003. Antibody response to influenza infection of mice: different patterns for glycoprotein and nucleocapsid antigens. Immunology 108(4):431-9.

Selin LK, Welsh RM. 2004. Plasticity of T cell memory responses to viruses. Immunity 20(1):5-16.

Shevach EM. 2006. From vanilla to 28 flavors: multiple varieties of T regulatory cells. Immunity 25(2):195-201.

Shin JS, Ebersold M, Pypaert M, Delamarre L, Hartley A, Mellman I. 2006. Surface expression of MHC class II in dendritic cells is controlled by regulated ubiquitination. Nature 444(7115):115-8.

Shinkai Y, Rathbun G, Lam KP, Oltz EM, Stewart V, Mendelsohn M, Charron J, Datta M, Young F, Stall AM and others. 1992. RAG-2-deficient mice lack mature lymphocytes owing to inability to initiate V(D)J rearrangement. Cell 68(5):855-67.

Shu LL, LIn YP, Wright SM, Shortridge KF, Webster RG. 1994. Evidence for interspecies transmission and reassortment of influenza A viruses in pigs in southern China. Virology 202:825-833.

Shultz LD, Banuelos S, Lyons B, Samuels R, Burzenski L, Gott B, Lang P, Leif J, Appel M, Rossini A and others. 2003. NOD/LtSz-Rag1nullPfpnull mice: a new model system with increased levels of human peripheral leukocyte and hematopoietic stem-cell engraftment. Transplantation 76(7):1036-42.

Shultz LD, Lyons BL, Burzenski LM, Gott B, Chen X, Chaleff S, Kotb M, Gillies SD, King M, Mangada J and others. 2005. Human lymphoid and myeloid cell development in NOD/LtSz-scid IL2R gamma null mice engrafted with mobilized human hemopoietic stem cells. J Immunol 174(10):6477-89.

Shultz LD, Schweitzer PA, Christianson SW, Gott B, Schweitzer IB, Tennent B, McKenna S, Mobraaten L, Rajan TV, Greiner DL and others. 1995. Multiple defects in innate and adaptive immunologic function in NOD/LtSz-scid mice. J Immunol 154(1):180-91.

Smith CM, Wilson NS, Waithman J, Villadangos JA, Carbone FR, Heath WR, Belz GT. 2004. Cognate CD4(+) T cell licensing of dendritic cells in CD8(+) T cell immunity. Nat Immunol 5(11):1143-8.

Smits HH, van Beelen AJ, Hessle C, Westland R, de Jong E, Soeteman E, Wold A, Wierenga EA, Kapsenberg ML. 2004. Commensal Gram-negative bacteria prime human dendritic cells for enhanced IL-23 and IL-27 expression and enhanced Th1 development. Eur J Immunol 34(5):1371-80.

Soumelis V, Reche PA, Kanzler H, Yuan W, Edward G, Homey B, Gilliet M, Ho S, Antonenko S, Lauerma A and others. 2002. Human epithelial cells trigger dendritic cell mediated allergic inflammation by producing TSLP. Nat Immunol 3(7):673-80.

Sprenger H, Meyer RG, Kaufmann A, Bussfeld D, Rischkowsky E, Gemsa D. 1996. Selective induction of monocyte and not neutrophil-attracting chemokines after influenza A virus infection. J Exp Med 184(3):1191-6.

Steinhauer DA. 2002. Genetics of influenza viruses. Annual Review of Genetics 36:305-332.

Steinman RM, Banchereau J. 2007. Taking dendritic cells into medicine. Nature 449(7161):419-26.

Steinman RM, Hawiger D, Liu K, Bonifaz L, Bonnyay D, Mahnke K, Iyoda T, Ravetch J, Dhodapkar M, Inaba K and others. 2003. Dendritic cell function in vivo during the steady state: a role in peripheral tolerance. Ann N Y Acad Sci 987:15-25.

Stubbe M, Vanderheyde N, Goldman M, Marchant A. 2006. Antigen-specific central memory CD4+ T lymphocytes produce multiple cytokines and proliferate in vivo in humans. J Immunol 177(11):8185-90.

Subbarao K, Klimov A, Katz J, Regnery H, Lim W, Hall H, Perdue M, Swayne D, Bender C, Huang J and others. 1998. Characterization of an avian influenza A (H5N1) virus isolated from a child with a fatal respiratory illness. Science 279(5349):393-6.

Takeda K, Kaisho T, Akira S. 2003. Toll-like receptors. Annu Rev Immunol 21:335-76.

Taraban VY, Rowley TF, Al-Shamkhani A. 2004. Cutting edge: a critical role for CD70 in CD8 T cell priming by CD40-licensed APCs. J Immunol 173(11):6542-6.

Tary-Lehmann M, Lehmann PV, Schols D, Roncarolo MG, Saxon A. 1994. Anti-SCID mouse reactivity shapes the human CD4+ T cell repertoire in hu-PBL-SCID chimeras. J Exp Med 180(5):1817-27.

Thompson WW, Shay DK, Weintraub E, Brammer L, Bridges CB, Cox NJ, Fukuda K. 2004. Influenza-associated hospitalizations in the United States. Jama 292(11):1333-40.

Thompson WW, Shay DK, Weintraub E, Brammer L, Cox N, Anderson LJ, Fukuda K. 2003. Mortality associated with influenza and respiratory syncytial virus in the United States. Jama 289(2):179-86.

Thornton AM, Shevach EM. 1998. CD4+CD25+ immunoregulatory T cells suppress polyclonal T cell activation in vitro by inhibiting interleukin 2 production. J Exp Med 188(2):287-96.

Ting JP, Kastner DL, Hoffman HM. 2006. CATERPILLERs, pyrin and hereditary immunological disorders. Nat Rev Immunol 6(3):183-95.

Traggiai E, Chicha L, Mazzucchelli L, Bronz L, Piffaretti JC, Lanzavecchia A, Manz MG. 2004. Development of a human adaptive immune system in cord blood cell-transplanted mice. Science 304(5667):104-7.

Trautmann L, Janbazian L, Chomont N, Said EA, Gimmig S, Bessette B, Boulassel MR, Delwart E, Sepulveda H, Balderas RS and others. 2006. Upregulation of PD-1 expression on HIV-specific CD8+ T cells leads to reversible immune dysfunction. Nat Med 12(10):1198-202.

Tripp RA, Sarawar SR, Doherty PC. 1995. Characteristics of the influenza virus-specific CD8+ T cell response in mice homozygous for disruption of the H-2lAb gene. J Immunol 155(6):2955-9.

Uhlig HH, McKenzie BS, Hue S, Thompson C, Joyce-Shaikh B, Stepankova R, Robinson N, Buonocore S, Tlaskalova-Hogenova H, Cua DJ and others. 2006. Differential activity of IL-12 and IL-23 in mucosal and systemic innate immune pathology. Immunity 25(2):309-18.

Ungchusak K, Auewarakul P, Dowell SF, Kitphati R, Auwanit W, Puthavathana P, Uiprasertkul M, Boonnak K, Pittayawonganon C, Cox NJ and others. 2005. Probable person-to-person transmission of avian influenza A (H5N1). N Engl J Med 352(4):333-40.

Valladeau J, Ravel O, Dezutter-Dambuyant C, Moore K, Kleijmeer M, Liu Y, Duvert-Frances V, Vincent C, Schmitt D, Davoust J and others. 2000. Langerin, a novel C-type lectin specific to Langerhans cells, is an endocytic receptor that induces the formation of Birbeck granules. Immunity 12:71-81.

van Niel G, Wubbolts R, Ten Broeke T, Buschow SI, Ossendorp FA, Melief CJ, Raposo G, van Balkom BW, Stoorvogel W. 2006. Dendritic cells regulate exposure of MHC class II at their plasma membrane by oligoubiquitination. Immunity 25(6):885-94.

Vandekerckhove BA, Baccala R, Jones D, Kono DH, Theofilopoulos AN, Roncarolo MG. 1992. Thymic selection of the human T cell receptor V beta repertoire in SCID-hu mice. J Exp Med 176(6):1619-24.

Vandekerckhove BA, Jones D, Punnonen J, Schols D, Lin HC, Duncan B, Bacchetta R, de Vries JE, Roncarolo MG. 1993. Human Ig production and isotype switching in severe combined immunodeficient-human mice. J Immunol 151(1):128-37.

Veckman V, Osterlund P, Fagerlund R, Melen K, Matikainen S, Julkunen I. 2006. TNF-alpha and IFN-alpha enhance influenza-A-virus-induced chemokine gene expression in human A549 lung epithelial cells. Virology 345(1):96-104.

Verhoeyen M, Fang R, Jou WM, Devos R, Huylebroeck D, Saman E, Fiers W. 1980. Antigenic drift between the haemagglutinin of the Hong Kong influenza strains A/Aichi/2/68 and A/Victoria/3/75. Nature 286(5775):771-6.

Wang YH, Ito T, Wang YH, Homey B, Watanabe N, Martin R, Barnes CJ, McIntyre BW, Gilliet M, Kumar R and others. 2006. Maintenance and polarization of human TH2 central memory T cells by thymic stromal lymphopoietin-activated dendritic cells. Immunity 24(6):827-38.

Watanabe N, Hanabuchi S, Marloie-Provost MA, Antonenko S, Liu YJ, Soumelis V. 2005. Human TSLP promotes CD40 ligand-induced IL-12 production by myeloid dendritic cells but maintains their Th2 priming potential. Blood 105(12):4749-51.

Watanabe S, Terashima K, Ohta S, Horibata S, Yajima M, Shiozawa Y, Dewan MZ, Yu Z, Ito M, Morio T and others. 2007. Hematopoietic stem cell-engrafted NOD/SCID/IL2Rgamma null mice develop human lymphoid systems and induce long-lasting HIV-1 infection with specific humoral immune responses. Blood 109(1):212-8.

Weaver CT, Murphy KM. 2007. T-cell subsets: the more the merrier. Curr Biol 17(2):R61-3.

Williams MA, Bevan MJ. 2007. Effector and memory CTL differentiation. Annu. Rev. Immunol. 25:171-192.

Yahata T, Ando K, Nakamura Y, Ueyama Y, Shimamura K, Tamaoki N, Kato S, Hotta T. 2002. Functional human T lymphocyte development from cord blood CD34+ cells in nonobese diabetic/Shi-scid, IL-2 receptor gamma null mice. J Immunol 169(1):204-9.

Yanagihara S, Komura E, Nagafune J, Watarai H, Yamaguchi Y. 1998. EBI1/CCR7 is a new member of dendritic cell chemokine receptor that is up-regulated upon maturation. J. Immunol. 161:3096-3101.

Yewdell JW, Haeryfar SM. 2005. Understanding presentation of viral antigens to CD8+ T cells in vivo: the key to rational vaccine design. Annu Rev Immunol 23:651-82.

Yoshino H, Ueda T, Kawahata M, Kobayashi K, Ebihara Y, Manabe A, Tanaka R, Ito M, Asano S, Nakahata T and others. 2000. Natural killer cell depletion by anti-asialo GM1 antiserum treatment enhances human hematopoietic stem cell engraftment in NOD/Shi-scid mice. Bone Marrow Transplant 26(11):1211-6.